SCATTERING AND RADIATION OF GRAVITY WAVES BY AN ELLIPTICAL CYLINDER

by

Hsuan Shan Chen

and

Chiang C. Mei

RALPH M. PARSONS LABORATORY
for
WATER RESOURCES AND HYDRODYNAMICS

Report No. 140

Prepared Under the Support of:
Fluid Dynamics Branch, Office of Naval Research
Department of the Navy
Conract No. N00014-67-A-0204-0036

August 1971

MIT

DEPARTMENT
OF
CIVIL
ENGINEERING

SCHOOL OF ENGINEERING
MASSACHUSETTS INSTITUTE OF TECHNOLOGY
Cambridge, Massachusetts 02139

R71-29

SCATTERING AND RADIATION OF GRAVITY WAVES BY AN ELLIPTICAL CYLINDER

by

Hsuan Shan Chen

and

Chiang C. Mei

Report No. 140

RALPH M. PARSONS LABORATORY
FOR WATER RESOURCES AND HYDRODYNAMICS
Department of Civil Engineering
Massachusetts Institute of Technology

Prepared Under the Support of:
Fluid Dynamics Branch, Office of Naval Research
Department of the Navy
Contract No. N00014-67-A-0204-0036

August 1971

Security Classification

DOCUMENT CONTROL DATA - R & D

(Security classification of title, body of abstract and indexing annotation must be entered when the overall report is classified)

1. ORIGINATING ACTIVITY *(Corporate author)*
Parsons Laboratory for Water Resources and Hydrodynamics
Department of Civil Engineering
Massachusetts Institute of Technology

2a. REPORT SECURITY CLASSIFICATION
Unclassified

2b. GROUP

3. REPORT TITLE

SCATTERING AND RADIATION OF GRAVITY WAVES BY AN ELLIPTICAL CYLINDER

4. DESCRIPTIVE NOTES *(Type of report and inclusive dates)*
Final Report (1970-1971)

5. AUTHOR(S) *(First name, middle initial, last name)*

Hsuan S. Chen and Chiang C. Mei

6. REPORT DATE	7a. TOTAL NO. OF PAGES	7b. NO. OF REFS
August 1971	149	36

8a. CONTRACT OR GRANT NO.	9a. ORIGINATOR'S REPORT NUMBER(S)
N00014-67-A-0204-0036	R71-29
b. PROJECT NO. R.M. Parsons Laboratory for Water Resources and Hydrodynamics, DSR 71972	
c.	9b. OTHER REPORT NO(S) *(Any other numbers that may be assigned this report)*
d.	Parsons Laboratory Tech. Report No. 140

10. DISTRIBUTION STATEMENT

This document has been approved for public release and sale; its distribution is unlimited

11. SUPPLEMENTARY NOTES	12. SPONSORING MILITARY ACTIVITY
	Fluid Dynamics Branch, Office of Naval Research, Department of the Navy

13. ABSTRACT

Theoretical results of scattering and radiation of simple-harmonic gravity waves by a vertical cylinder of elliptical cross-section are worked out in this report. The cylinder extends from the free surface to the bottom of the sea of constant depth. Linearized theory for small amplitude waves is adopted. The question of flow separation is not treated. The mathematical solution follows the usual pattern of separation of variables in elliptical polar coordinates, leading to Mathieu's equations. The recent computer program for Mathieu functions by Clemm is then used. Physical quantities calculated include the wave forces and moments in various directions on, and the scattering amplitude around, a stationary cylinder due to a plane incident wavetrain. Also calculated are the damping coefficients representing radiation energy losses due to various modes of oscillation of a cylinder in the absence of incident waves. All these data are essential in a complete study of wave-body interactions. By the method of images the scattering of plane incident wave by a semi-elliptical peninsula is similarly studied. Extensive numerical results are presented for various degrees of ellipticity (from a thin plate to a near-circle), angles of incidence and for wave-lengths ranging from very long to comparable to the horizontal dimensions of the cylinder. These results should provide useful information for the design of large ocean structures.

DD FORM 1 NOV 65 1473 (PAGE 1)
S/N 0102-014-6700

Security Classification

D-23822

14 KEY WORDS	LINK A		LINK B		LINK C	
	ROLE	WT	ROLE	WT	ROLE	WT
Surface Wave Scattering Wave forces on an object Diffraction by an Elliptical Cylinder						

ABSTRACT

Theoretical results of scattering and radiation of simple-harmonic gravity waves by a vertical cylinder of elliptical cross-section are worked out in this report.

The cylinder extends from the free surface to the bottom of the sea of constant depth. Linearized theory for small amplitude waves is adopted. The question of flow separation is not treated.

The mathematical solution follows the usual pattern of separation of variables in elliptical polar coordinates, leading to Mathieu's equations. The recent computer program for Mathieu functions by Clemm is then used.

Physical quantities calculated include the wave forces and moments in various directions on, and the scattering amplitude around, a stationary cylinder due to a plane incident wavetrain. Also calculated are the damping coefficients representing radiation energy losses due to various modes of oscillation of a cylinder in the absence of incident waves. All these data are essential in a complete study of wave-body interactions.

By the method of images the scattering of plane incident wave by a semi-elliptical peninsula is similarly studied.

Extensive numerical results are presented for various degrees of ellipticity (from a thin plate to a near-circle), angles of incidence and for wave-lengths ranging from very long

to comparable to the horizontal dimensions of the cylinder. These results should provide useful information for the design of large ocean structures.

This report was submitted as the thesis by H.S. Chen to the Department of Civil Engineering, Massachusetts Institute of Technology, for the degrees of Master of Science and of Civil Engineer. Chiang C. Mei was the thesis supervisor.

ACKNOWLEDGMENT

The present investigation is a part of a continuing research entitled "Surface Wave Studies" sponsored by the Fluid Dynamics Branch, Office of Naval Research, under contract N00014-67-A-0204-0036. The authors wish to express their sincere appreciation for this support. As the execution of this work hinges on the numerical calculation of Mathieu Functions, we are grateful for Richard Barakat of Harvard University for important references on the existing computer programs. Assistance in drawing preparation and proof-reading by Mr. R.T. Ho is also acknowledged.

The contract is administered by the Division of Sponsored Research, Massachusetts Institute of Technology under the designation DSR 71972.

TABLE OF CONTENTS

1. INTRODUCTION

In recent years, due to the interest in the exploration of minerals (especially oil) , food, and other resources located in and beneath the waters of the oceans, the activities of coastal and offshore constructions are ever-increasing and are anticipated to remain so in the future years. The success of such explorations concerning the oceans is partly based on the ability to design and to build the coastal and offshore structures safely and economically, which in turn depends on the sound understanding of the interaction of structures and natural processes in the ocean.

The interaction of gravity waves and structures is rather complicated in many aspects : such as the non-linear effects of waves, viscous and turbulent effects on the drag, irregular geometry of structures, ... etc. However, an understanding of such interaction can be developed through simplified analytical studies, experimental investigations, and even full-scale measurements. A survey of recent experimental works in this field is available in Ippen (1966)[19] .

Earlier studies in gravity waves interacting with a cylindrical structure are focused on the force system exerting upon the cylinder due to small amplitude waves.

Morison (1950-53)[26] approached this problem by considering that the total wave force on an element of a vertical circular cylinder is the sum of the drag and inertia force components : i.e.

$$dF = dF_D + dF_I = \left(\underbrace{C_D \rho \frac{U|U|}{2}}_{dF_D \,:\, \text{drag}} + \underbrace{C_M \rho \frac{\pi D^2}{4} \frac{dU}{dt}}_{dF_I \,:\, \text{inertia force}} \right) dz$$

where C_D = the drag coefficient

C_M = the inertia or mass coefficient

ρ = mass density of the water

U = instantaneous horizontal water particle velocity

D = diameter of circular cylinder

This approach appears to have a sound physical basis , and is also widely accepted in engineering practice. However , in this approach the incident wave is assumed to be unaffected by the cylindrical object. In reality the incident wave is scattered on encountering an object, more so if the object is large in some sense. Furthermore, C_D and C_M are determined from model tests and used on prototype by extrapolation. The range of D/L (the ratio of diameter of the circular cylinder to the wavelength) used in Morison's experiments is 0.009 to 0.042 , the data for C_D and C_M are pertinent to small structures such as piles. The use of these values in calculating wave forces on large

structures must be examined with caution.

MacCamy (1952)[23] assumed the fluid to be inviscid, the motion irrotational, and applied the scattering theory (or diffraction theory) to this problem. In Acoustics and in Electromagnetics the problem of scattering by a circular cylinder of infinite extent has already been solved for a long time. Havelock (1940)[17] applied this theory to the case of gravity wave acting upon a circular cylinder, but little numerical result was presented. MacCamy applied this theory to a cylinder of finite length equal to the water depth, and the results of forces were given.

The linearized scattering theory states that the total wave is the superposition of the incident wave and the scattered wave. For inviscid fluids, the forces obtained by MacCamy is analogous to Morison's inertia force components. However for large bodies such forces vary widely due to diffraction effects. The scattering theory is employed in our work.

Harleman (1955)[16] proposed a wave force theory that applied Morison's concept of separation of inertia and drag effects. The proposed procedure incorporates the scattering theory for inertia force component and utilizes a drag component which is in the form similar to Morison's but makes use of the steady state drag coefficient for cylinders. This procedure amounts to the linear superposition of viscous and

irrotational effects. MacCamy has mentioned that due to the formation of a wake on the "downstream" of the cylinder, the separation of viscous effects and inertia is not logical, and the use of a steady state drag instead of unsteady state drag is not reasonable.

In the problems of gravity wave interaction with a object, the ratio $2\pi r_o/L$ (ratio of characteristic length of object, r_o , to the wavelength, L) is an important parameter as the scattering property of the object. Another significant effect is viscosity which causes the generation of a boundary layer around the body and the formation of a wake region on the "downstream" side of the body. However, wake separation is primarily dependent upon the ratio of the orbit size of a fluid particle to the object size. For a given wavelength the ratio is reflected in the ratio , $H/2r_o$ (H wave height). Small values of $H/2r_o$ correspond to small values of relative displacement of the fluid particles, in which case the flow near the object remains attached and unseparated, and wake effects are then unimportant.

Garrison (1970)[14] used parameters $2\pi r_o/L$, and H/r_o to classify the general waves-structure interaction problem in a diagram, as in figure 1.1. and suggested the general regions of applicability of the theories. Precise values of $H/2r_o$, $2\pi r_o/L$ which separate the regions of applicability of the theories are still lacking. In particular for large-scale

structures and small-amplitude waves, scattering theory approaches are appropriate.

Theoretical studies of the problem of wave interaction with an elliptic cylinder of infinite length has also been done in Acoustics and in Electromagnetics. A collection of these works is presented by Bowman (1969)[7]. Due to computational difficulties, the numerical results are restricted to the long-wavelength range. Havelock (1940)[17] had touched on this case in water waves, but nothing was presented in his paper except the following statement: "For a vertical obstacle of infinite draft, ... , the effect of a cylinder of elliptic section would be of special interest, but the analytical solution does not lend itself to computation, when the wavelength is of the same order as the length of the axis".

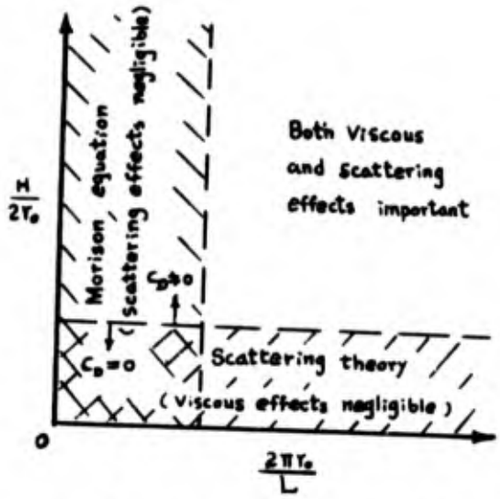

Fig. 1.1 Regions of applicability

Luigi Montefusco (1968)[25] investigated the scattering problem of gravity wave by an isolated plate which is a thin ellipse, only the wave amplitude was presented.

Because the elliptic cylinder is an obvious generalization of the circular cylinder, and the thin elliptic

cylinder may be used as a model for the plate barrier, the elliptic cylinder is important in approximating a variety of practical geometries. In this work we shall study theoretically the problems of scattering and radiation of linear gravity waves by an elliptic cylinder.

The elliptic cylindrical coordinates are employed, the horizontal part of the Laplace equation leads to ordinary differential equations of Mathieu type, and therefore Mathieu solutions. The computer program for Mathieu solutions by Clemm (1969)[11] is used for computation.

The exact solution of the problem of scattering type is carried out in Chapter 3. The force system on a fixed elliptic cylinder are obtained through direct pressure integration along the body surface. The differential scattering cross section and the total scattering cross section are also studied. The results of semi-elliptic peninsula are obtained by using the image method.

The radiation problem of a body in forced oscillation is solved in Chapter 5. As a check, the results are used to calculate forces on a stationary cylinder in incoming waves by using Haskind's theorem. The forces obtained from both scattering and radiation theories are of course the same. A further result which can be obtained is the damping factor, usually defined as the part of the reacting force which is in phase with the body velocity. The component of the reacting

force in phase with the body acceleration is related to the added mass, which requires information of the evanescent wave modes in the near field of the body, and is not computed here.

It is interesting to note that this problem of elliptic cylinders has been studied for at least many decades, but due to the complexities of Mathieu functions, the numerical results of the solution have been quite limited.

In naval architecture, the interaction of gravity waves with floating (or submerged) elliptic cylinder is of great interest. It is anticipated that the solution to this problem can be obtained by using the technique of Black and Mei (1970)[3] in treating similar problems of a circular cylinder. However difficulties might exist in computing numerical values of Mathieu solutions of imaginary arguments.

2. PROBLEM FORMULATION AND GENERAL SOLUTIONS

In this chapter we shall specify the governing equation and boundary conditions, and consider an elliptic cylinder standing vertically on the bottom of the ocean. Elliptic cylindrical coordinates is chosen. The general solutions are obtained through using the method of separation of variables.

2-1 Formulation of the Boundary Value Problems

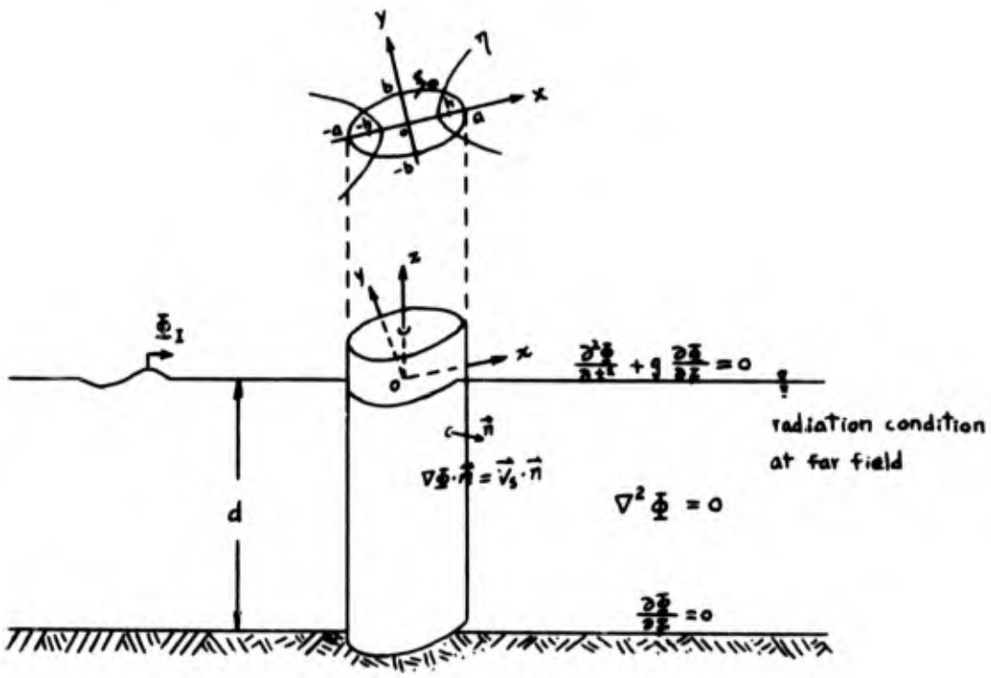

Fig. 2.1 Problem Specification

If the flow is assumed to be irrotational, the fluid velocity can be given by the gradient of the velocity potential or $\vec{V} = \nabla\Phi$. In an incompressible fluid, the

divergence of the velocity vector vanishes, therefore,

$$\nabla^2\Phi = 0 \tag{2.1}$$

Stoker (1957)[34] presents a detailed development for the linearized free surface boundary condition. Under the assumption of zero external pressure on the free surface, it takes the following form:

$$\frac{\partial^2\Phi}{\partial t^2} + g\frac{\partial\Phi}{\partial z} = 0 \qquad \text{for } z=0 \tag{2.2}$$

The boundary condition on the solid surface is such that the fluid velocity normal to the wall is equal to the normal velocity component of the wall.

$$\nabla\Phi\cdot\vec{n} = \vec{V}_s\cdot\vec{n} \tag{2.3}$$

where $\vec{V}_s$ is the velocity of the wall, n is the unit normal vector outward to the wall.

The domain refers to the fluid region extending from the edge of the obstacle to infinity in horizontal directions, and from the free surface to the bottom in the vertical direction. Furthermore, In order to have a complete formulation of the problem with a uniquely determined solution, we must add the so-called radiation condition in the far field. Thus for pure radiation problems the radiated waves must be outgoing in the farfield; for

scattering problems the scattered waves (total minus the incident) must be outgoing in the far field.

2-2 General solutions in Elliptic Cylindrical Coordinates

The velocity potential can be conveniently separated into spatial and temporal parts. In cartesian coordinates $\Phi(x,y,z,t) = \phi(x,y,z)e^{-i\omega t}$. The spatial part of boundary value problems becomes

$$\nabla^2\phi = 0 \tag{2.1'}$$

$$\frac{\partial\phi}{\partial z} - \frac{\omega^2}{g}\phi = 0 \qquad \text{for } z=0 \tag{2.2'}$$

$$\nabla\phi \cdot \vec{n} = \vec{v}_s \cdot \vec{n} \qquad \text{on solid wall} \tag{2.3'}$$

where we assume $\vec{V}_s = \vec{v}_s e^{-i\omega t}$.

Assuming that we have finite fluid depth,d, and $\phi(x,y,z) = F(x,y)Z(z)$, making use of separation of variables again, equations (2.1')-(2.3') reduce to

$$\begin{cases} \frac{d^2Z}{dz^2} - k^2Z = 0 & (2.1"a) \\ \frac{\partial^2F}{\partial x^2} + \frac{\partial^2F}{\partial y^2} + k^2F = 0 & (2.1"b) \end{cases}$$

$$\frac{dZ}{dz} - \frac{\omega^2}{g}Z = 0 \qquad \text{for } z=0 \tag{2.2"}$$

$$\frac{dZ}{dz} = 0 \qquad \text{for } z=-d \tag{2.3"a}$$

$$\nabla F \cdot \vec{n} = \vec{v}_s \cdot \vec{n} \qquad \text{on the solid body} \tag{2.3"b}$$

where k is a separation constant and will be determined

through the free surface boundary condition.

2-2-1 Vertical Component Solution

The solution of equation (2.1"a) with boundary condition (2.3"a) gives,

$$Z(z) = \text{const.}\ \cosh k(z+d)$$

substituting into the free surface boundary condition, equation (2.2"), lead to the equation

$$gk \tanh kd = \omega^2 \qquad (2.4)$$

This is the relationship between the wave number (k), the wave frequency (ω), and the water depth (d).

Equation (2.4) states that the wave velocity ($c=\frac{\omega}{k}$) is dependent on the wave length ($L=\frac{2\pi}{k}$). Wave components with different wave length will then disperse at different speeds. For this reason equation (2.4) is called the dispersion equation.

For given ω and d, Equation (2.4) has an infinite number of imaginary roots, say k_i ($i>2$), which represent the evanescent modes, and two symmetric real roots, say $\pm k_1$ ($k_1>0$) which represent the propagating modes.

We can also find out that by making use of the dispersion equation, $\cosh k_i(z+d)$ constitutes a complete set of orthogonal eigenfunctions in the interval $[-d,0]$. Such that

$$\int_{-d}^{0} \cosh k_i(z+d)\cosh k_j(z+d)dz = N_{k_i}\delta_{ij} \qquad (2.5)$$

where $N_{k_i} = \frac{d}{2}\left(\frac{\sinh 2k_i d}{2k_i d} + 1\right)$ and δ_{ij} is the Kronecker delta.

2-2-2 Horizontal Component Solution

The relationship between carterian coordinates and elliptical coordinates is given by (A.2): $x=h\cosh\xi\cos\eta$, $y=h\sinh\xi\sin\eta$. Since we are dealing with an elliptical cylinder, it is convenient to express the scalar Helmholtz equation (2.1"b) in elliptical coordinates by using the equation (A.2) and §B-1

$$\frac{\partial^2 F}{\partial \xi^2} + \frac{\partial^2 F}{\partial \eta^2} + 2q_i(\cosh 2\xi - \cos\eta)F = 0 \qquad (2.6)$$

where $q_i = (k_i h/2)^2$. By the dispersion equation, we notice that only $q_1 = (\pm k_1 h/2)^2 > 0$ and all other $q_i = (k_i h/2)^2 < 0$ $(i \geq 2)$. Again making use of separation of variables, $F(\xi,\eta) = G_1(\xi)G_2(\eta)$, and assigning a separation constant a_i, we reduce equation (2.6) to

$$\frac{d^2 G_2}{d\eta^2} + (a_i - 2q_i\cos 2\eta)G_2 = 0 \qquad (2.7)$$

$$\frac{d^2 G_1}{d\xi^2} - (a_i - 2q_i\cosh 2\xi)G_1 = 0 \qquad (2.8)$$

Mathieu (1868)[24], in solving the problem of the elliptic membrance, obtained a differential equation (2.7) and analysed many of its properties. It is evident that equation (2.8) may

be derived directly from equation (2.7) by writing $\eta = \pm i\xi$, and vice versa: § B-2 . Therefore, equations (2.7) and (2.8) are called the Mathieu and the modified Mathieu equations respectively. Equation (2.7) has periodic solutions: § B-3 – § B-7 .

$$G_2(\eta) = \begin{cases} ce_m(\eta, q_i) \\ se_m(\eta, q_i) \end{cases}$$

and equation (2.8) has the solutions

$$G_1(\xi) = \begin{cases} Mc_m^{(1)}(\xi, q_i) \\ Ms_m^{(1)}(\xi, q_i), \end{cases} \quad \begin{cases} Mc_m^{(2)}(\xi, q_i) \\ Ms_m^{(2)}(\xi, q_i), \end{cases} \quad \text{or} \begin{cases} Mc_m^{(3)}(\xi, q_i) \\ Ms_m^{(3)}(\xi, q_i) \end{cases}$$

$$(m=0,1,2,\dots)$$

where $ce_m(\eta, q_i)$ and $se_m(\eta, q_i)$, in the notations of Ince (1931)[13], are the cosine and the sine Mathieu functions. While $Mc_m^{(i)}(\xi, q_i)$ and $Ms_m^{(i)}(\xi, q_i)$ $(i=1,2,3)$, in the notations of Blanch and Clemm (1965)[5], are the modified Mathieu functions (or the radial Mathieu function) of the i-th kind. We remark that from equation (B.22).

$$Mc_m^{(3)}(\xi, q_i) = Mc_m^{(1)}(\xi, q_i) + iMc_m^{(2)}(\xi, q_i)$$
$$Ms_m^{(3)}(\xi, q_i) = Ms_m^{(1)}(\xi, q_i) + iMs_m^{(2)}(\xi, q_i)$$

For convenience of identity, we may consider the Mathieu functions $ce_m(\eta, q_i)$, $se_m(\eta, q_i)$ as corresponding to $\cos m\eta$, $\sin m\eta$, and modified Mathieu functions $Mc_m^{(j)}(\xi, q_i)$ and $Ms_m^{(j)}(\xi, q_i)$ $(j=1,2,3)$, to Bessel functions $J_m(\ )$, $Y_m(\ )$, and Hankel

function $H_m^{(j)}(\ )$ respectively. § B-9.

A solution comprising the product of any two functions which are solutions of equations (2.7), (2.8) respectively has to have the same value of a_i and q_i. The physical solution must be single-valued, therefore the periodic solutions shall be chosen and the solutions of equation (2.6) are

$$F(\xi,\eta) = \begin{cases} Mc_m^{(j)}(\xi,q_i)\,ce_m(\eta,q_i) \\ Ms_m^{(j)}(\xi,q_i)\,se_m(\eta,q_i) \end{cases} \qquad (2.9)$$

$$(j=1,2,3)$$

3. THE SCATTERING OF GRAVITY WAVE BY A STATIONARY VERTICAL ELLIPTIC CYLINDER

When a gravity wave encounters an obstacle, some of the wave is deflected from its original course. In linear problems it is usual to define the difference between the actual wave and the undisturbed wave (incident wave), which would be present if the obstacle were not there, as the scattered wave. Since the actual wave, the sum of the incident wave and the scattered wave, being a field having zero normal velocity on the surface of the obstacle, the scattered wave could be thought as the wave generated at the obstacle surface by some excitation due to the incident wave.

In this chapter, we shall separate the scattered wave from the undisturbed plane wave. We shall be interested in the forces and moments exerting upon an elliptic cylinder by the total wave, in the angular distribution of the scattered wave intensity,and in the total intensity of the scattered wave.

3-1 The Incident Wave

The velocity potential of the incident wave of amplitude a_1, travelling in the direction which makes an angle θ_1 with the x-axis, can be represented by

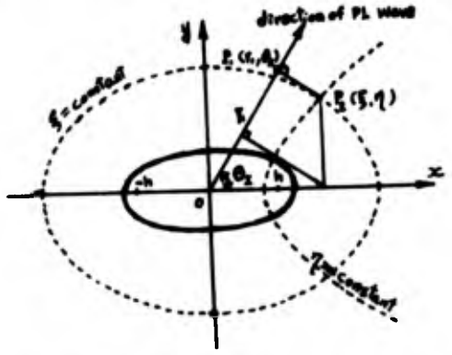

Fig. 3.1 Illustrating plane gravity wave impinging on an elliptical cylinder.

$$\Phi_I(\xi,\eta,z,t) = \phi_I(\xi,\eta,z)e^{-i\omega t} = \frac{gA_I}{\omega}\frac{\cosh k_1(z+d)}{\cosh k_1 d}e^{i(k_1 r-\omega t)} \qquad (3.1)$$

where $r = x\cos\theta_I + y\sin\theta_I = h\cosh\xi\cos\eta\cos\theta_I + h\sinh\xi\sin\eta\sin\theta_I$ (3.2)

only the real part of the equation (3.1) has physical significance.

When expressed in terms of Mathieu functions , equation (3.1) is

$$\Phi_I = \frac{2gA_I}{\omega}\frac{\cosh k_1(z+d)}{\cosh k_1 d}e^{-i\omega t}\sum_{n=0}^{\infty}$$

$$\Big\{ (-1)^n Mc^{(1)}_{2n}(\xi,q_1)ce_{2n}(\eta,q_1)ce_{2n}(\theta_I,q_1) +$$

$$+(-1)^{n+1}Ms^{(1)}_{2n+2}(\xi,q_1)se_{2n+2}(\eta,q_1)se_{2n+2}(\theta_I,q_1) +$$

$$+(-1)^n iMc^{(1)}_{2n+1}(\xi,q_1)ce_{2n+1}(\eta,q_1)ce_{2n+1}(\theta_I,q_1) +$$

$$+(-1)^n iMs^{(1)}_{2n+1}(\xi,q_1)se_{2n+1}(\eta,q_1)se_{2n+1}(\theta_I,q_1)\Big\} \qquad (3.3)$$

$$(i = (-1)^{\frac{1}{2}})$$

this is a solution of equations (2.1), (2.2), and (2.3"a), and represents the velocity potential of plane progressing wave in the absence of the cylinder in elliptical cylinder coordinates.

3-2 The Scattered Wave

In the presence of the cylinder, besides satisfying Laplace equation, and boundary conditions on free surface and the bottom, the scattered wave must satisfy the radiation condition

in the far field and the boundary condition on the cylinder.

The radiation condition requires that the scattered wave behaves like outgoing progressing waves at a sufficently great distance from the cylinder. Mathematically, this condition is necessary for a complete formulation of the problem to ensure a uniquely determined solution.

The modified Mathieu functions of the third kind obey the radiation condition for time dependence of the type $e^{-i\omega t}$ and possess the asymptotic form: (B.25),

$$\begin{matrix} Mc_m^{(3)}(\xi,q_1) \\ Ms_m^{(3)}(\xi,q_1) \end{matrix} \sim \left(\frac{2}{\pi k_1 h \cosh\xi}\right)^{\frac{1}{2}} e^{i(k_1 h\cosh\xi - \frac{m\pi}{2} - \frac{\pi}{4})}$$

Therefore the scattered wave potential that satisfies the radiation condition takes the form

$$\begin{aligned} \Phi_s(\xi,\eta,z,t) &= \phi_s(\xi,\eta,z)e^{-i\omega t} \\ &= \frac{\varrho g Q_1}{\omega}\frac{\cosh k_1(z+d)}{\cosh k_1 d}e^{-i\omega t}\sum_{n=0}^{\infty} \\ &\Big\{ c_{2n}\, Mc_{2n}^{(3)}(\xi,q_1)ce_{2n}(\eta,q_1)ce_{2n}(\theta_1,q_1) + \\ &+ c_{2n+1}Mc_{2n+1}^{(3)}(\xi,q_1)ce_{2n+1}(\eta,q_1)ce_{2n+1}(\theta_1,q_1) + \\ &+ s_{2n+1}Ms_{2n+1}^{(3)}(\xi,q_1)se_{2n+1}(\eta,q_1)se_{2n+1}(\theta_1,q_1) + \\ &+ s_{2n+2}Ms_{2n+2}^{(3)}(\xi,q_1)se_{2n+2}(\eta,q_1)se_{2n+2}(\theta_1,q_1) \Big\} \end{aligned} \tag{3.4}$$

where c_m, s_m are constant coefficients to be determined by the boundary condition on the body.

Since the surface of the cylinder is assumed to be immobile, the velocity of fluid particles normal thereto must be zero. i.e. the sum of the normal velocities of the incident and scattered waves shall vanish at $\xi=\xi_0$. and using (A.7) : $dn = l_1\, d\xi$,

$$\frac{\partial \Phi_i}{\partial n} + \frac{\partial \Phi_s}{\partial n} = 0 \qquad \text{at} \quad \xi=\xi_0$$

thus,

$$\frac{\partial \Phi_i}{\partial \xi} + \frac{\partial \Phi_s}{\partial \xi} = 0 \qquad \text{at} \quad \xi=\xi_0 \tag{3.5}$$

substituting equations (3.3),(3.4) into (3.5). Hence

$$\left.\frac{\partial \Phi_i}{\partial \xi} + \frac{\partial \Phi_s}{\partial \xi}\right|_{\xi=\xi_0} = \frac{2qa_1}{\omega}\,\frac{\cosh K_1(z+d)}{\cosh K_1 d}\, e^{-i\omega t} \sum_{n=0}^{\infty}$$

$$\Big\{\Big[(-1)^n Mc^{(1)\prime}_{2n}(\xi_0,q_1) + c_{2n}\, Mc^{(3)\prime}_{2n}(\xi_0,q_1)\Big]\, ce_{2n}(\eta,q_1)ce_{2n}(\theta_1,q_1) +$$

$$+\Big[(-1)^{n+1} Ms^{(1)\prime}_{2n+2}(\xi_0,q_1) + s_{2n+2} Ms^{(3)\prime}_{2n+2}(\xi_0,q_1)\Big]\, se_{2n+2}(\eta,q_1)se_{2n+2}(\theta_1,q_1) +$$

$$+\Big[(-1)^n i Mc^{(1)\prime}_{2n+1}(\xi_0,q_1) + c_{2n+1} Mc^{(3)\prime}_{2n+1}(\xi_0,q_1)\Big]\, ce_{2n+1}(\eta,q_1)ce_{2n+1}(\theta_1,q_1) +$$

$$+\Big[(-1)^n i Ms^{(1)\prime}_{2n+1}(\xi_0,q_1) + s_{2n+1} Ms^{(3)\prime}_{2n+1}(\xi_0,q_1)\Big]\, se_{2n+1}(\eta,q_1)se_{2n+1}(\theta_1,q_1)\Big\}$$

$$= 0 \tag{3.5a}$$

and making use of the orthogonal properties of $ce_m(\eta,q_1)$, $se_m(\eta,q_1)$ in the interval $(0,2\pi)$: (B.12), equation (3.5a) gives

$$c_{2n} = (-1)^{n+1} \frac{Mc_{2n}^{(1)'}(\xi_0,q_1)}{Mc_{2n}^{(3)'}(\xi_0,q_1)}, \qquad c_{2n+1} = (-1)^{n+1} \frac{i\,Mc_{2n+1}^{(1)'}(\xi_0,q_1)}{Mc_{2n+1}^{(3)'}(\xi_0,q_1)}$$

$$s_{2n+2} = (-1)^{n+2} \frac{Ms_{2n+2}^{(1)'}(\xi_0,q_1)}{Ms_{2n+2}^{(3)'}(\xi_0,q_1)}, \qquad s_{2n+1} = (-1)^{n+1} \frac{i\,Ms_{2n+1}^{(1)'}(\xi_0,q_1)}{Ms_{2n+1}^{(3)'}(\xi_0,q_1)} \tag{3.6}$$

Therefore the velocity potential at any point on or outside the cylinder is

$$\Phi = \Phi_I + \Phi_S = \frac{2gA_1}{\omega} \frac{\cosh k_1(z+d)}{\cosh k_1 d} e^{-i\omega t} f(\xi,\eta) \tag{3.7}$$

where we define

$$\begin{aligned} f(\xi,\eta) = \sum_{n=0}^{\infty} (-1)^n \cdot \\ \cdot \Big\{ & \left[Mc_{2n}^{(1)}(\xi,q_1) - \frac{Mc_{2n}^{(1)'}(\xi_0,q_1)}{Mc_{2n}^{(3)'}(\xi_0,q_1)} Mc_{2n}^{(3)}(\xi,q_1) \right] ce_{2n}(\eta,q_1) ce_{2n}(\theta_1,q_1) + \\ & + i \left[Mc_{2n+1}^{(1)}(\xi,q_1) - \frac{Mc_{2n+1}^{(1)'}(\xi_0,q_1)}{Mc_{2n+1}^{(3)'}(\xi_0,q_1)} Mc_{2n+1}^{(3)}(\xi,q_1) \right] ce_{2n+1}(\eta,q_1) ce_{2n+1}(\theta_1,q_1) + \\ & + i \left[Ms_{2n+1}^{(1)}(\xi,q_1) - \frac{Ms_{2n+1}^{(1)'}(\xi_0,q_1)}{Ms_{2n+1}^{(3)'}(\xi_0,q_1)} Ms_{2n+1}^{(3)}(\xi,q_1) \right] se_{2n+1}(\eta,q_1) se_{2n+1}(\theta_1,q) + \\ & - \left[Ms_{2n+2}^{(1)}(\xi,q_1) - \frac{Ms_{2n+2}^{(1)'}(\xi_0,q_1)}{Ms_{2n+2}^{(3)'}(\xi_0,q_1)} Ms_{2n+2}^{(3)}(\xi,q_1) \right] se_{2n+2}(\eta,q_1) se_{2n+2}(\theta_1,q) \Big\} \end{aligned} \tag{3.7a}$$

Equation (3.7) may be regarded as the general solution of the problem.

3-3 Forces and Moments on the Elliptic Cylinder

The wave forces are obtained by directly integrating the pressure around the cylinder. The pressure exerted on the

cylinder is computed from Bernoulli's equation. Because we are only interested in the dynamic pressure and considering only the linearized problem, the pressure is

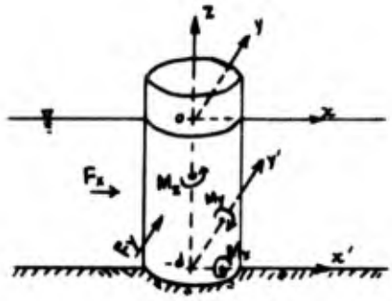

Fig. 3.2 Forces and Moments

$$P = -\rho\frac{\partial\Phi}{\partial t}$$

$$= 2\rho g a_I i \frac{\cosh k_1(z+d)}{\cosh k_1 d} e^{-i\omega t} f(\xi,\eta) \qquad (3.8)$$

(i) Forces

Since the integral in the z-direction from z=0 to the free surface, $z=\zeta$, is of second order in ka, the total x-component of the force acting on the cylinder can be written as

$$F_x = -\int_{-d}^{0} dz \int_{\text{body surface}} P\cos(n,x)ds = -(h\sinh\xi_0)\int_{-d}^{0} dz \int_{0}^{2\pi} P\cos\eta\, d\eta\Big|_{\xi=\xi_0}$$

$$= -(2\rho g a_I i)(h\sinh\xi_0)e^{-i\omega t}\int_{-d}^{0}\frac{\cosh k_1(z+d)}{\cosh k_1 d}\,dz\int_{0}^{2\pi} f(\xi_0,\eta)\cos\eta\, d\eta$$

and

$$\int_0^{2\pi} f(\xi_0,\eta)\cos\eta\, d\eta = \sum_{n=0}^{\infty}(-1)^n \int_0^{2\pi}$$

$$\left\{\left[Mc_{2n}^{(1)}(\xi_0,q_1) - \frac{Mc_{2n}^{(1)\prime}(\xi_0,q_1)}{Mc_{2n}^{(3)\prime}(\xi_0,q_1)} Mc_{2n}^{(3)}(\xi_0,q_1)\right] ce_{2n}(\eta,q_1)ce_{2n}(\theta_1,q_1) +\right.$$

$$+i\left[Mc_{2n+1}^{(1)}(\xi_0,q_1) - \frac{Mc_{2n+1}^{(1)\prime}(\xi_0,q_1)}{Mc_{2n+1}^{(3)\prime}(\xi_0,q_1)} Mc_{2n+1}^{(3)}(\xi_0,q_1)\right] ce_{2n+1}(\eta,q_1)ce_{2n+1}(\theta_1,q_1) +$$

$$\left.+i\left[Ms_{2n+1}^{(1)}(\xi_0,q_1) - \frac{Ms_{2n+1}^{(1)\prime}(\xi_0,q_1)}{Ms_{2n+1}^{(3)\prime}(\xi_0,q_1)} Ms_{2n+1}^{(3)}(\xi_0,q)\right] se_{2n+1}(\eta,q_1)se_{2n+1}(\theta_1,q_1) +\right.$$

$$-\left[Ms^{(1)}_{2n+2}(\xi_o,q_1) - \frac{Ms^{(1)'}_{2n+2}(\xi_o,q_1)}{Ms^{(3)'}_{2n+2}(\xi_o,q_1)} Ms^{(3)}_{2n+2}(\xi_o,q_1)\right] se_{2n+2}(\eta,q_1)se_{2n+2}(\theta_2,q_1)\Big\}\cdot$$

$$\cdot\cos\eta\, d\eta$$

making use of (B.13) : i.e. $\int_o^{2\pi} ce_{2n}(\eta,q_1)\cos\eta\, d\eta = \int_o^{2\pi} se_m(\eta,q_1)\cos\eta\, d\eta = 0$, and $\int_o^{2\pi} ce_{2n+1}(\eta,q_1)\cos\eta\, d\eta = \pi A_1^{(2n+1)}$, and Wronskians (B.23) : $W\left[Mc^{(1)}_m(\xi,q_1), Mc^{(3)}_m(\xi,q_1)\right] = \frac{2i}{\pi}$.

then

$$\int_0^{2\pi} f(\xi_o,\eta)\cos\eta\, d\eta = \sum_{n=o}^{\infty}(-1)^{n+1} \frac{2A_1^{(2n+1)}}{Mc^{(3)'}_{2n+1}(\xi_o,q_1)} ce_{2n+1}(\theta_2,q_1) \qquad (3.9)$$

Hence,

$$F_x = (2\rho g a_1)(2dh\sinh\xi_o)\left(\frac{1}{d}\int_{-d}^{0}\frac{\cosh k_1(z+d)}{\cosh k_1 d}dz\right)e^{-i\omega t}$$

$$\sum_{n=o}^{\infty}(-1)^n \frac{iA_1^{(2n+1)}}{Mc^{(3)'}_{2n+1}(\xi_o,q_1)} ce_{2n+1}(\theta_2,q_1)$$

$$= (2a_1g\rho)(2dh\sinh\xi_o)\, C_{k_1d}\,|C_{Fx}|\, e^{i(\theta_{Fx}-\omega t)} \qquad (3.10)$$

where $$C_{k_1d} = \frac{1}{d}\int_{-d}^{0}\frac{\cosh k_1(z+d)}{\cosh k_1 d}\,dz = \frac{\tanh k_1 d}{k_1 d} \qquad (3.10a)$$

$$C_{Fx} = |C_{Fx}|\, e^{i\theta_{Fx}} = \sum_{n=o}^{\infty}(-1)^n \frac{iA_1^{(2n+1)}}{Mc^{(3)'}_{2n+1}(\xi_o,q_1)} ce_{2n+1}(\theta_2,q_1)$$

$$= Re\{C_{Fx}\} + iIm\{C_{Fx}\} \qquad (3.10b)$$

Re{ }, Im{ } indicate the real and the imaginary parts. We further define the amplitude and the phase of the x-force by:

$$|C_{Fx}| = \left([\mathrm{Re}\{C_{Fx}\}]^2 + [\mathrm{Im}\{C_{Fx}\}]^2 \right)^{\frac{1}{2}} \tag{3.10c}$$

$$\theta_{Fx} = \tan^{-1}\left(\frac{\mathrm{Im}\{C_{Fx}\}}{\mathrm{Re}\{C_{Fx}\}}\right) \tag{3.10d}$$

The total y-component force is

$$F_y = -\int_{-d}^{0} dz \int_{\text{body surface}} P\cos(n,y)\,ds = -(h\cosh\xi_0)\int_{-d}^{0} dz \int_{0}^{2\pi} P\sin\eta\, d\eta$$

$$= -(2\rho g a_1 i)(h\cosh\xi_0)e^{-i\omega t}\int_{-d}^{0}\frac{\cosh k_1(z+d)}{\cosh k_1 d}\,dz\int_{0}^{2\pi} f(\xi_0,\eta)\sin\eta\, d\eta$$

By using (B.14), $\int_0^{2\pi} ce_m(\eta,q_1)\sin\eta\,d\eta = \int_0^{2\pi} se_{2n+2}(\eta,q_1)\sin\eta\,d\eta = 0$, $\int_0^{2\pi} se_{2n+1}(\eta,q_1)\sin\eta\,d\eta = \pi B_1^{(2n+1)}$, and Wronskian (B.23), $W[Ms_m^{(1)}(\xi,q_1),\ Ms_m^{(3)}(\xi,q_1)] = \frac{2i}{\pi}$, we have

$$\int_0^{2\pi} f(\xi_0,\eta)\sin\eta\,d\eta = \sum_{n=0}^{\infty}(-1)^{n+1}\frac{2B_1^{(2n+1)}}{Ms_{2n+1}^{(3)\prime}(\xi_0,q_1)}\,se_{2n+1}(\theta_1,q_1) \tag{3.11}$$

Thus

$$F_y = (2\rho g a_1)(2dh\cosh\xi_0)\left(\frac{1}{d}\int_{-d}^{0}\frac{\cosh k_1(z+d)}{\cosh k_1 d}\,dz\right)e^{-i\omega t}\cdot$$

$$\cdot\sum_{n=0}^{\infty}(-1)^n\frac{iB_1^{(2n+1)}}{Ms_{2n+1}^{(3)\prime}(\xi_0,q_1)}\,se_{2n+1}(\theta_1,q_1)$$

$$= (2a_1\rho g)(2dh\cosh\xi_0)\,C_{k_1 d}\,|C_{Fy}|\,e^{i(\theta_{Fy}-\omega t)} \tag{3.12}$$

where

$$C_{Fy} = |C_{Fy}|e^{i\theta_{Fy}} = \sum_{n=0}^{\infty}(-1)^n\frac{iB_1^{(2n+1)}}{Ms_{2n+1}^{(3)\prime}(\xi_0,q_1)}\,se_{2n+1}(\theta_1,q_1) \tag{3.12a}$$

$$|C_{Fy}| = \left([\mathrm{Re}\{C_{Fy}\}]^2 + [\mathrm{Im}\{C_{Fy}\}]^2\right)^{\frac{1}{2}} \tag{3.12b}$$

$$\theta_{Fy} = \tan^{-1}\left(\frac{\mathrm{Im}\{C_{Fy}\}}{\mathrm{Re}\{C_{Fy}\}}\right) \qquad (3.12c)$$

(2) Moments

Since the pressure is given in equation (3.8), the moments about any axis can be carried out. But for practical reasons, we shall only work out x-, y-, z-moment about axes passing through x=0, y=0, z=-d.

The moment about x-axis at point z=-d is

$$M_x = -\int_{-d}^{0}(z+d)\left\{-\int_{\text{body surface}} P\cos(n,y)\,ds\right\}dz \qquad \text{for} \quad \xi=\xi_0$$

substitute equation (3.8) into the preceding equation and integrate, we have

$$\begin{aligned}
M_x &= \int_{-d}^{0}(z+d)\left\{(h\cosh\xi_0)\int_0^{2\pi} P\sin\eta\,d\eta\Big|_{\xi=\xi_0}\right\}dz \\
&= (2\rho g a_1 i)(h\cosh\xi_0)e^{-i\omega t}\int_0^{2\pi} f(\xi_0,\eta)\sin\eta\,d\eta \cdot \\
&\qquad \cdot\int_{-d}^{0}(z+d)\,\frac{\cosh k_1(z+d)}{\cosh k_1 d}\,dz \\
&= (2a_1\rho g)(2dh\cosh\xi_0)\left(\frac{\tanh k_1 d}{k_1 d}\right)e^{-i\omega t}\left\{\sum_{n=0}^{\infty}(-1)^{n+1}\frac{i B_1^{(2n+1)}}{M_{2n+1}^{(3)'}(\xi_0,q_1)}\right. \\
&\qquad \left. se_{2n+1}(\xi_0,q_1)\right\}(d)\left(1-\frac{\coth k_1 d}{k_1 d}+\frac{\operatorname{csch} k_1 d}{k_1 d}\right) \\
&= -F_y\, d\left(1-\frac{\coth k_1 d}{k_1 d}+\frac{\operatorname{csch} k_1 d}{k_1 d}\right) \\
&= -F_y\, d\, C_{k_1 xy} \qquad (3.13)
\end{aligned}$$

where $$C_{k_1 xy} = 1-\frac{\coth k_1 d}{k_1 d}+\frac{\operatorname{csch} k_1 d}{k_1 d} \qquad (3.13a)$$

Similarly, the moment about y-axis at point z=-d can be obtained to be

$$M_y = \int_{-d}^{0}(z+d)\left\{-\int_{\text{body surface}} P\cos(n,x)ds\right\}dz$$

$$= -\int_{-d}^{0}(z+d)\left\{(h\sinh\xi_o)\int_0^{2\pi} P\cos\eta\, d\eta\Big|_{\xi=\xi_o}\right\}dz$$

$$= -(2\rho g a_1 i)(h\sinh\xi_o)e^{-i\omega t}\int_{-d}^{0}(z+d)\frac{\cosh k_1(z+d)}{\cosh k_1 d}dz \cdot$$

$$\cdot \int_0^{2\pi} f(\xi_o,\eta)\cos\eta\, d\eta$$

$$= F_x\, dC_{kxy} \qquad (3.14)$$

The moment about z-axis due to horizontal forces on a small element of unit length in the η direction is $\Delta M_z = P\cos(n,x)y - P\cos(n,y)x = -\frac{h^2}{2i_1}P\sin 2\eta$, §A-3, for $\xi = \xi_o$. so the total moment about z-axis

$$M_z = \int_{-d}^{0}dz\int_{\text{body surface}}\Delta M\, ds = \int_{-d}^{0}dz\int_0^{2\pi}(-\frac{h^2}{2}P\sin 2\eta)d\eta$$

$$= -(2\rho g a_1 i)(\frac{h^2}{2})e^{-i\omega t}\int_{-d}^{0}\frac{\cosh k_1(z+d)}{\cosh k_1 d}dz\int_0^{2\pi} f(\xi_o,\eta)\sin 2\eta\, d\eta$$

$$= -(2\rho g a_1 i)(\frac{dh^2}{2})e^{-i\omega t}(\frac{1}{d}\int_{-d}^{0}\frac{\cosh k_1(z+d)}{\cosh k_1 d}dz)\int_0^{2\pi} f(\xi_o,\eta)\cdot$$

$$\cdot \sin 2\eta\, d\eta$$

And again using equation (3.7a), the Wronskian $W\left[Ms^{(1)}_{2n+2}(\xi,q_1), Ms^{(3)}_{2n+2}(\xi,q)\right] = \frac{2i}{\pi}$ and the orthogonality of sine-, cosine-functions in the interval $[0,2\pi]$; equations (B.14a,b,c), we then have

$$\int_0^{2\pi} f(\xi_0,\eta)\sin 2\eta\, d\eta = \sum_{n=0}^{\infty}(-1)^{n+1}\frac{2i\,B_2^{(2n+2)}}{Ms_{2n+2}^{(3)\prime}(\xi_0,q_1)}se_{2n+2}(\theta_1,q_1) \qquad (3.15)$$

therefore

$$M_{1z} = (2\rho g a_1)(dh^2)\left(\frac{\tanh k_1 d}{k_1 d}\right)e^{-i\omega t}\sum_{n=0}^{\infty}(-1)^{n+1}\frac{B_2^{(2n+2)}}{Ms_{2n+2}^{(3)\prime}(\xi_0,q_1)}\cdot$$

$$\cdot\, se_{2n+2}(\theta_1,q_1)$$

$$= (2\rho g a_1)(dh^2)C_{kd}\left|C_{Mz}\right| e^{i(\theta_{Mz}-\omega t)} \qquad (3.16)$$

where

$$C_{Mz} = \left|C_{Mz}\right|e^{i\theta_{Mz}} = \sum_{n=0}^{\infty}(-1)^{n+1}\frac{B_2^{(2n+2)}}{Ms_{2n+2}^{(3)\prime}(\xi_0,q_1)}se_{2n+2}(\theta_1,q_1) \qquad (3.16a)$$

and

$$\left|C_{Mz}\right| = \left(\left[Re\{C_{Mz}\}\right]^2 + \left[Im\{C_{Mz}\}\right]^2\right)^{\frac{1}{2}} \qquad (3.16b)$$

$$\theta_{Mz} = \tan^{-1}\left(\frac{Im\{C_{Mz}\}}{Re\{C_{Mz}\}}\right) \qquad (3.16c)$$

3-4 The Scattered field at large distances

Invoking Bernoulli's equation we find from (3.4) and (3.6) the elevation of the scattered waves, ζ_s,

$$\zeta_s = -\frac{1}{g}\left.\frac{\partial \Phi_s}{\partial t}\right|_{z=0} = 2a_1 i e^{-i\omega t}\sum_{n=0}^{\infty}(-1)^{n+1}\cdot$$

$$\cdot\left\{\frac{Mc_{2n}^{(1)\prime}(\xi_0,q_1)}{Mc_{2n}^{(3)\prime}(\xi_0,q_1)}Mc_{2n}^{(3)}(\xi,q_1)ce_{2n}(\eta,q_1)ce_{2n}(\theta_1,q_1) +\right.$$

$$+ i\frac{Mc_{2n+1}^{(1)\prime}(\xi_0,q_1)}{Mc_{2n+1}^{(3)\prime}(\xi_0,q_1)}Mc_{2n+1}^{(3)}(\xi,q_1)ce_{2n+1}(\eta,q_1)ce_{2n+1}(\theta_1,q_1) +$$

$$\left. + i\frac{Ms_{2n+1}^{(1)\prime}(\xi_0,q_1)}{Ms_{2n+1}^{(3)\prime}(\xi_0,q_1)}Ms_{2n+1}^{(3)}(\xi,q)se_{2n+1}(\eta,q_1)se_{2n+1}(\theta_1,q_1) -\right.$$

$$- \frac{Ms^{(1)'}_{2n+2}(\xi_0,q_1)}{Ms^{(3)'}_{2n+2}(\xi_0,q_1)} Ms^{(3)}_{2n+2}(\xi,q_1)se_{2n+2}(\eta,q_1)se_{2n+2}(\theta_I,q_1)\Big\} \tag{3.17}$$

Making use of the asympotic form of the modified Mathieu functions in the far field, $Mc^{(3)}_m(\xi,q_1)$ (or $Ms^{(3)}_m(\xi,q_1)$) $\sim\sqrt{\frac{2}{\pi K_1 h\cosh\xi}}\cdot e^{i(K_1 h\cosh\xi-\frac{2m+1}{4}\pi)}$, (B-25), we obtain ζ_s far from the cylinder

$$\zeta_{s_\infty} \sim a_I A(\eta)\sqrt{\frac{h\cosh\xi_0}{h\cosh\xi}}\, e^{i(K_1 h\cosh\xi-\omega t)} \tag{3.18}$$

where

$$A(\eta) = -2\sqrt{\frac{2}{\pi K_1 h\cosh\xi_0}}\, e^{i\frac{\pi}{4}} \sum_{n=0}^{\infty} \cdot$$

$$\Big\{ \frac{Mc^{(1)'}_{2n}(\xi_0,q_1)}{Mc^{(3)'}_{2n}(\xi_0,q_1)} ce_{2n}(\eta,q_1)ce_{2n}(\theta_I,q_1) +$$

$$+ \frac{Mc^{(1)'}_{2n+1}(\xi_0,q_1)}{Mc^{(3)'}_{2n+2}(\xi_0,q_1)} ce_{2n+1}(\eta,q_1)ce_{2n+1}(\theta_I,q_1) +$$

$$+ \frac{Ms^{(1)'}_{2n+1}(\xi_0,q_1)}{Ms^{(3)'}_{2n+1}(\xi_0,q_1)} se_{2n+1}(\eta,q_1)se_{2n+1}(\theta_I,q_1) +$$

$$+ \frac{Ms^{(1)'}_{2n+2}(\xi_0,q_1)}{Ms^{(3)'}_{2n+2}(\xi_0,q_1)} se_{2n+2}(\eta,q_1)se_{2n+2}(\theta_I,q_1)\Big\} \tag{3.19}$$

The function $A(\eta)$ is called the angular distribution factor of scattering amplitude.

3-5 Scattering Cross Section

When an object scatters a gravity water wave train, some of the energy carried by the incident wave is dispersed. The energy lost to the incident wave may be atsorbed by the object , or it may simply be deflected from its original course. The total amount of energy loss per second by an incident plane wave, divided by the incident wave intensity (energy per

second per unit area), is called the Total Cross section, Q , of the object. As far as the incident wave is concerned, it is as if an area Q of the incident wave is removed to give the same loss of energy. If the energy is absorbed by the object, the ratio is called the absorption cross section ; if the gravity wave is simply deflected, so it goes to infinity in different directions, it is called the scattering cross section. If both absorption and scattering occur, the sum is the total cross section. In any case, the incident wave is reduced in intensity because of the loss. In this work, we only consider a stationary rigid body which does not absorb energy, therefore we are only interested in the scattering cross section, and excluding the absorption cross section.

3-5-1 Differential Scattering Cross Section

The directivity characteristics for the energy of the scattered wave is determined by the function $|A(\eta)|^2$, which is customarily called the differential scattering cross section and denoted by $\sigma(\eta)$.

$$\sigma(\eta) = \frac{4}{\pi q_1^{\frac{1}{2}} \cosh \xi_0} \left| \sum_{n=0}^{\infty} \cdot \right.$$

$$\cdot \left\{ \frac{Mc_{2n}^{(1)\prime}(\xi_0, q_1)}{Mc_{2n}^{(3)\prime}(\xi_0, q_1)} ce_{2n}(\eta, q_1) ce_{2n}(\theta_2, q_1) + \right.$$

$$+ \frac{Mc_{2n+1}^{(1)\prime}(\xi_0, q_1)}{Mc_{2n+1}^{(3)\prime}(\xi_0, q_1)} ce_{2n+1}(\eta, q_1) ce_{2n+1}(\theta_2, q_1) +$$

$$+ \frac{Ms_{2n+1}^{(1)\prime}(\xi_0, q_1)}{Ms_{2n+1}^{(3)\prime}(\xi_0, q_1)} se_{2n+1}(\eta, q_1) se_{2n+1}(\theta_2, q_1) +$$

$$+ \frac{Ms^{(1)'}_{2m+2}(\xi_o,q_1)}{Ms^{(3)'}_{2m+2}(\xi_o,q_1)} se_{2m+2}(\eta,q_1)se_{2m+2}(\theta_1,q_1) \Big\} \Big|^2 \qquad (3.20)$$

and $\sigma(\eta)$ gives the energy scattered into one unit angular range per unit incident length of the wave front.

3-5-2 The Total Scattering Cross Section

The differential scattering cross section $\sigma(\eta)$ is used to indicate the angular intensity of scattered energy. Another scattering indicator is the total scattering cross section , denoted by Q , which is obtained by integrating $\sigma(\eta)$ over all solid angles.

$$Q = \int_0^{2\pi} \sigma(\eta) d\eta$$

$$= \frac{4}{q_1^{1/2}\cosh\xi_o} \sum_{n=0}^{\infty} \cdot$$

$$\cdot \Big\{ \Big| \frac{Mc^{(1)'}_{2n}(\xi_o,q_1)}{Mc^{(3)'}_{2n}(\xi_o,q_1)} ce_{2n}(\theta_1,q_1) \Big|^2 + \Big| \frac{Mc^{(1)'}_{2m+1}(\xi_o,q_1)}{Mc^{(3)'}_{2m+1}(\xi_o,q_1)} ce_{2m+1}(\theta_1,q_1) \Big|^2 +$$

$$+ \Big| \frac{Ms^{(1)'}_{2m+1}(\xi_o,q_1)}{Ms^{(3)'}_{2m+1}(\xi_o,q_1)} se_{2m+1}(\theta_1,q_1) \Big|^2 + \Big| \frac{Ms^{(1)'}_{2m+2}(\xi_o,q_1)}{Ms^{(3)'}_{2m+2}(\xi_o,q)} se_{2m+2}(\theta_1,q) \Big|^2 \Big\}$$

(3.21)

(see (B.31))

Q is evidently the total scattered energy per unit incident intensity. Physically, it is a hypothetical line segment (for plane wave) normal to the incident wave which intercepts an amount of incident energy equal to the scattered engergy.

4. THE SCATTERING OF GRAVITY WAVES BY A STRAIGHT SHORELINE WITH A SEMI-ELLIPTIC PENINSULA

The solutions for the elliptic cylinders can be used to construct the analogous solution for straight shoreline with a semi-elliptic peninsula such as shown in fig. 4.1(a). In order to satisfy the boundary condition on the shoreline, $\frac{\partial \Phi_h}{\partial x}\Big|_{x=0} = 0$, we can use the method of images. If $(\pi-\theta_1)$ is the direction of the incident wave of amplitude a_1, then the velocity potential for semi-elliptic cylinder, Φ_h, is

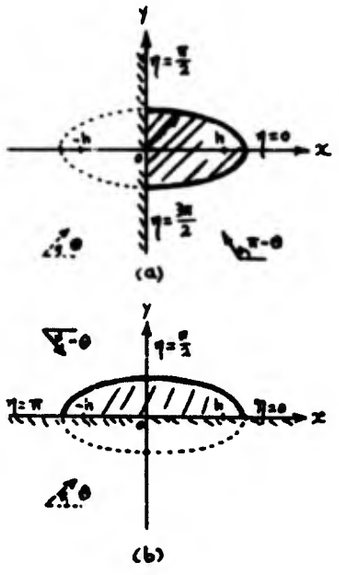

Fig. 4.1 (a) Semielliptic cylinder with major axis perpendicular to the straight shoreline, (b) Semielliptic cylinder with minor axis perpendicular to the straight shoreline.

$$\Phi_h = \Phi\Big|_{\theta_1=\theta_1} + \Phi\Big|_{\theta_1=\pi-\theta_1}$$

where Φ is given in equation(3.7), we obtain

$$\Phi_h = \frac{2gA_1}{\omega}\,\frac{\cosh k_1(z+d)}{\cosh k_1 d}\,e^{-i\omega t}\left[f(\xi,\eta)\Big|_{\theta_1=\theta_1} + f(\xi,\eta)\Big|_{\theta_1=\pi-\theta_1}\right]$$

$$= \frac{2gA_1}{\omega}\,\frac{\cosh k_1(z+d)}{\cosh k_1 d}\,e^{-i\omega t}\,f_h(\xi,\eta) \qquad (4.1)$$

where $f_h(\xi,\eta) = f(\xi,\eta)\Big|_{\theta_1=\theta_1} + f(\xi,\eta)\Big|_{\theta_1=\pi-\theta_2}$

$$= 2\sum_{n=0}^{\infty}(-1)^n \cdot$$

$$\cdot\Big\{ \Big[Mc_{2n}^{(1)}(\xi,q_1) - \frac{Mc_{2n}^{(1)'}(\xi_0,q_1)}{Mc_{2n}^{(3)'}(\xi_0,q_1)} Mc_{2n}^{(3)}(\xi,q_1)\Big] ce_{2n}(\eta,q_1)ce_{2n}(\theta_1,q_1) +$$

$$+ i\Big[Ms_{2n+1}^{(1)}(\xi,q_1) - \frac{Ms_{2n+1}^{(1)'}(\xi_0,q_1)}{Ms_{2n+1}^{(3)'}(\xi_0,q_1)} Ms_{2n+1}^{(3)}(\xi,q_1)\Big] se_{2n+1}(\eta,q_1)se_{2n+1}(\theta_1,q_1) \Big\} \qquad (4.1a)$$

Note that an important property : $ce_{2n+1}(\eta,q) = -ce_{2n+1}(\pi-\eta,q)$, $se_{2n+1}(\eta,q) = -se_{2n+1}(\pi-\eta,q)$ has been used, (B.17).

The corresponding pressure is,

$$P_h = -\rho\frac{\partial\Phi_h}{\partial t} = 2ga_I\rho i \frac{\cosh k_1(z+d)}{\cosh k_1 d} e^{-i\omega t} f_h(\xi,\eta) \qquad (4.2)$$

equation (4.2) is symmetric with respect to the y-axis, so does the pressure P_h .

The y-component force exerting on the semi-elliptic cylinder is

$$F_{hy} = -\int_{-d}^{0} dz \int_{\text{body surface}} P_h \cos(n,y)ds = -(h\cosh\xi_0)\int_{-d}^{0} dz \int_{-\frac{\pi}{2}}^{\frac{\pi}{2}} P_h \sin\eta d\eta \Big|_{\xi=\xi_0}$$

$$= -(2ga_I\rho i)(dh\cosh\xi_0)\Big(\frac{1}{d}\int_{-d}^{0}\frac{\cosh k_1(z+d)}{\cosh k_1 d} dz\Big)e^{-i\omega t}\int_{-\frac{\pi}{2}}^{\frac{\pi}{2}} f_h(\xi_0,\eta)\sin\eta d\eta$$

using equation (4.1a), Wronskian (B.23) and equations (B.16 a,b) , we have

$$\int_{-\frac{\pi}{2}}^{\frac{\pi}{2}} f_h(\xi_0,\eta)\sin\eta d\eta = 2\sum_{n=0}^{\infty}(-1)^{n+1}\frac{B_1^{(2n+1)}}{Ms_{2n+1}^{(3)'}(\xi_0,q_1)} se_{2n+1}(\theta_1,q_1) \qquad (4.3)$$

Hence,

$$F_{hy} = (2a_I \rho g)(2dh\cosh\xi_o)\left(\frac{\tanh k_1 d}{k_1 d}\right)e^{-i\omega t} \cdot \cdot \sum_{n=0}^{\infty}(-1)^n \frac{i\, B_1^{(2n+1)}}{Ms_{2n+1}^{(3)'}(\xi_o, q_1)}\, se_{2n+1}(\theta_I, q_1)$$

$$= (2a_I \rho g)(2dh\cosh\xi_o) C_{kd} \left| C_{Fy} \right| e^{i(\theta_{Fy} - \omega t)} \qquad (4.4)$$

where C_{Fy}, θ_{Fy} are the same as equations (3.12a,c), and C_{kd} is given by (3.10a).

Because of the symmetry of the waves and the geometry with respect to y-axis, it is no surprise that the y-component force for a semielliptic cylinder, equation (4.4), is the same as that for elliptic cylinder, equation (3.12).

The x-component force is

$$F_{hx} = -\int_{-d}^{0} dz \int_{\text{body surface}} P_h \cos(n,x)\, ds = -(h\sinh\xi_o)\int_{-d}^{0} dz \int_{-\frac{\pi}{2}}^{\frac{\pi}{2}} P_h \cos\eta\, d\eta \Big|_{\xi=\xi_o}$$

$$= -(2g a_I \rho i)(dh\sinh\xi_o)\left(\frac{1}{d}\int_{-d}^{0} \frac{\cosh k_1(z+d)}{\cosh k_1 d}\, dz\right)e^{-i\omega t} \cdot \cdot \int_{-\frac{\pi}{2}}^{\frac{\pi}{2}} f_h(\xi_o, \eta)\cos\eta\, d\eta$$

using (4.1a), Wronskian and (B.15a,b), we have

$$\int_{-\frac{\pi}{2}}^{\frac{\pi}{2}} f_h(\xi_o,\eta)\cos\eta\, d\eta = \frac{i2}{\pi}\sum_{n=0}^{\infty}(-1)^n \frac{\left[4A_o^{(2n)} + \sum_{j=1}^{\infty}(-1)^{j+1}\frac{A_{2j}^{(2n)}}{j^2-\frac{1}{4}}\right]}{Mc_{2n}^{(3)'}(\xi_o, q_1)}\, ce_{2n}(\theta_I, q_1) \qquad (4.5)$$

Therefore,

$$F_{hx} = (2a_I g\rho)(2dh\sinh\xi_o)\left(\frac{\tanh k_1 d}{k_1 d}\right)(e^{-i\omega t}) \cdot \cdot \left\{\frac{1}{\pi}\sum_{n=0}^{\infty}(-1)^n\left[4A_o^{(2n)} + \sum_{j=1}^{\infty}(-1)^{j+1}\frac{A_{2j}^{(2n)}}{j^2-\frac{1}{4}}\right]\frac{ce_{2n}(\theta_I, q_1)}{Mc_{2n}^{(3)'}(\xi_o, q_1)}\right.$$

$$= (2a_I g\rho)(2dh\sinh\xi_o) C_{K,d} \left| C_{hFx} \right| e^{i(\theta_{hFx} - \omega t)} \qquad (4.6)$$

where

$$C_{hFx} = \left|C_{hFx}\right| e^{i\theta_{hFx}}$$

$$= \frac{1}{\pi}\sum_{n=0}^{\infty}(-1)^n\left[4A_0^{(2n)} + \sum_{j=1}^{\infty}(-1)^{j+1}\frac{A_{2j}^{(2n)}}{j^2-(\frac{1}{2})^2}\right]\frac{ce_{2n}(\theta_z,q_1)}{Mc_{2n}^{(3)\prime}(\xi_0,q_1)} \tag{4.6a}$$

and

$$\left|C_{hFx}\right| = \left(\left[Re\{C_{hFx}\}\right]^2 + \left[Im\{C_{hFx}\}\right]^2\right)^{\frac{1}{2}} \tag{4.6b}$$

$$\theta_{hFx} = \tan^{-1}\left(\frac{Im\{C_{hFx}\}}{Re\{C_{hFx}\}}\right) \tag{4.6c}$$

The z-, x-, y-components moments acting on the semi-elliptic cylinder are calculated as follows:

$$M_{hz} = \int_{-d}^{0}dz\int_{-\frac{\pi}{2}}^{\frac{\pi}{2}}\left(-\frac{h^2}{2}P_h\sin 2\eta\right)d\eta\Big|_{\xi=\xi_0}$$

$$= -(2ga_I\rho 1)\left(\frac{dh^2}{2}\right)\left(\frac{1}{d}\int_{-d}^{0}\frac{\cosh k(z+d)}{\cosh kd}dz\right)\cdot$$

$$\cdot\int_{-\frac{\pi}{2}}^{\frac{\pi}{2}}f_h(\xi_0,\eta)\sin 2\eta\, d\eta$$

Using (4.1a), Wronskian, and (B.16a,b), we have

$$\int_{-\frac{\pi}{2}}^{\frac{\pi}{2}}f_h(\xi_0,\eta)\sin 2\eta\, d\eta = \frac{2}{\pi}\sum_{n=0}^{\infty}(-1)^{n+1}\frac{\sum_{j=0}^{\infty}\frac{(-1)^{j+1}B_{2j+1}^{(2n+1)}}{(j-\frac{1}{2})(j+\frac{3}{2})}}{Ms_{2n+1}^{(3)\prime}(\xi_0,q_1)}se_{2n+1}(\theta_z,q_1) \tag{4.7}$$

Hence

$$M_{hz} = (2ga_I\rho)\left(\frac{dh^2}{2}\right)\left(\frac{\tanh kd}{kd}\right)e^{-i\omega t}\left\{\frac{i2}{\pi}\sum_{n=0}^{\infty}(-1)^n\frac{\sum_{j=0}^{\infty}\frac{(-1)^{j+1}B_{2j+1}^{(2n+1)}}{(j-\frac{1}{2})(j+\frac{3}{2})}}{Ms_{2n+1}^{(3)\prime}(\xi_0,q_1)}se_{2n+1}(\theta_z,q_1)\right\}$$

$$= (2ga_I\rho)C_{kd}\left(\frac{dh^2}{2}\right)\left|C_{hMz}\right|e^{i(\theta_{hMz}-\omega t)} \tag{4.8}$$

where

$$C_{hMz} = \left|C_{hMz}\right| e^{i\theta_{hMz}}$$

$$= \frac{2}{\pi} \sum_{n=0}^{\infty} (-1)^n \left[\sum_{j=0}^{\infty} (-1)^{j+1} \frac{B_{2j+1}^{(2n+1)}}{(j-\frac{1}{2})(j+\frac{3}{2})} \right] \frac{1}{Ms_{2n+1}^{(3)'}(\xi_0, q_1)} se_{2n+1}(\theta_2, q_1) \tag{4.8a}$$

and

$$\left|C_{hMz}\right| = \left[(Re\{C_{hMz}\})^2 + (Im\{C_{hMz}\})^2 \right]^{\frac{1}{2}} \tag{4.8b}$$

$$\theta_{hMz} = \tan^{-1}\left(\frac{Im\{C_{hMz}\}}{Re\{C_{hMz}\}}\right) \tag{4.8c}$$

And following the same procedure, we obtain

$$M_{hx} = -\int_{-d}^{0} (z+d) \left[-\int_{\text{body surface}} P_h \cos(n,y) ds \right] dz = -F_{hy} dC_{kxy} \tag{4.9}$$

$$M_{hy} = \int_{-d}^{0} (z+d) \left[-\int_{\text{body surface}} P_h \cos(n,x) ds \right] dz = F_{hx} dC_{kxy} \tag{4.10}$$

where C_{kxy} is given by (3.13a), and F_{hy}, F_{hx} by (4.4), (4.6) respectively.

By subtracting the incident wave and its image, which would be the wave potential of a perfectly reflecting sea wall without the peninsula, the scattering potential for the semielliptic cylinder, Φ_{hs} , is from equation (4.1a)

$$\Phi_{hs} = \Phi_s \Big|_{\theta_i = \theta_I} + \Phi_s \Big|_{\theta_i = \pi - \theta_I}$$

$$= \frac{4ga_I}{\omega} \frac{\cosh k(z+d)}{\cosh kd} e^{-i\omega t} \sum_{n=0}^{\infty} (-1)^{n+1} \cdot$$

$$\cdot \left\{ \frac{Mc_{2n}^{(1)'}(\xi_0, q_1)}{Mc_{2n}^{(3)'}(\xi_0, q_1)} Mc_{2n}^{(3)}(\xi, q_1) ce_{2n}(\eta, q_1) ce_{2n}(\theta_I, q_1) + \right.$$

$$+ i \frac{Ms^{(1)\prime}_{2n+1}(\xi_0,q_1)}{Ms^{(3)\prime}_{2n+1}(\xi_0,q_1)} Ms^{(3)}_{2n+1}(\xi,q_1)se_{2n+1}(\eta,q_1)se_{2n+1}(\theta_I,q_1)\Big\} \tag{4.11}$$

The elevation of the scattered wave, ζ_{hs} , is

$$\zeta_{hs} = -\frac{1}{g}\frac{\partial \Phi_{hs}}{\partial t}\Big|_{z=0}$$

$$= 4a_I i e^{-i\omega t} \sum_{n=0}^{\infty}(-1)^{n+1} \cdot$$

$$\Big\{ \frac{Mc^{(1)\prime}_{2n}(\xi_0,q_1)}{Mc^{(3)\prime}_{2n}(\xi_0,q_1)} Mc^{(3)}_{2n}(\xi,q_1)ce_{2n}(\eta,q_1)ce_{2n}(\theta_I,q_1) +$$

$$+ i \frac{Ms^{(1)\prime}_{2n+1}(\xi_0,q_1)}{Ms^{(3)\prime}_{2n+1}(\xi_0,q_1)} Ms^{(3)}_{2n+1}(\xi,q_1)se_{2n+1}(\eta,q_1)se_{2n+1}(\theta_I,q_1) \Big\} \tag{4.12}$$

Using the asymptotic form for the modified Mathieu functions, the elevation of the scattered wave at far field (ξ large) is

$$\zeta_{hs} \sim a_I i \sqrt{\frac{h\cosh\xi_0}{h\cosh\xi}}\, A_h(\eta)\, e^{i(kh\cosh\xi-\omega t)} \tag{4.13}$$

where the scattering amplitude

$$A_h(\eta) = 4\sqrt{\frac{2}{\pi kh\cosh\xi_0}}\, e^{-i\frac{\pi}{4}} \sum_{n=0}^{\infty}(-1)^{n+1} \cdot$$

$$\cdot\Big\{ \frac{Mc^{(1)\prime}_{2n}(\xi_0,q_1)}{Mc^{(3)\prime}_{2n}(\xi_0,q_1)} ce_{2n}(\eta,q_1)ce_{2n}(\theta_I,q_1) +$$

$$+ \frac{Ms^{(1)\prime}_{2n+1}(\xi_0,q_1)}{Ms^{(3)\prime}_{2n+1}(\xi_0,q_1)} se_{2n+1}(\eta,q_1)se_{2n+1}(\theta_I,q_1) \Big\} \tag{4.13a}$$

The differential scattering cross section , $\sigma_h(\eta)$, is

$$\sigma_h(\eta) = \left| A_h(\eta) \right|^2$$

$$= \frac{16}{\pi q_1^{\frac{1}{2}} \cosh \xi_o} \left| \sum_{n=0}^{\infty} (-1)^{n+1} \cdot \right.$$

$$\cdot \left\{ \frac{Mc_{2n}^{(1)\prime}(\xi_o, q_1)}{Mc_{2n}^{(1)\prime}(\xi_o, q_1)} ce_{2n}(\eta, q_1) ce_{2n}(\theta_1, q_1) \right.$$

$$\left. \left. + \frac{Ms_{2n+1}^{(1)\prime}(\xi_o, q_1)}{Ms_{2n+1}^{(1)\prime}(\xi_o, q_1)} se_{2n+1}(\eta, q_1) se_{2n+1}(\theta_1, q_1) \right\} \right|^2 \qquad (4.14)$$

By using the same procedure as in §B-11 and using eqs. (B.16'a,b,c), we then have the total scattering cross section,

$$Q_h = \int_{-\frac{\pi}{2}}^{\frac{\pi}{2}} \sigma_h(\eta) d\eta = \frac{8}{q_1^{\frac{1}{2}} \cosh \xi_o} \sum_{n=0}^{\infty} \cdot$$

$$\left\{ \frac{Mc_{2n}^{(1)\prime}(\xi_o, q_1)}{Mc_{2n}^{(1)\prime}(\xi_o, q_1)} ce_{2n}(\theta_1, q_1) + \frac{Ms_{2n+1}^{(1)\prime}(\xi_o, q_1)}{Ms_{2n+1}^{(1)\prime}(\xi_o, q_1)} se_{2n+1}(\theta_1, q_1) \right\}$$

(4.15)

Using the same method, The case where the minor axis of the semi-elliptic cylinder is perpendicular to the shoreline, as shown in fig.4.1(b), can also be worked out[10] but omitted in this work.

5. RADIATED WAVE BY AN OSCILLATING ELLIPTIC CYLINDER

Gravity waves can be generated by the vibration of any solid body in contact with the fluid. The characteristics of the source determine the directional characteristics of the generated gravity wave field. Conversely, the directional properties of the wave field may be used to shed light on the nature of the source.

Although the radiation by a large body extending the whole depth is of relatively little practical interest in itself, it provides a means of calculating the wave forces on a stationary body by a scattered wave through Haskind's theorem. This indirect procedure can be of great value when the pressure distribution on the body due to incident waves is difficult to obtain.

5-1 The Radiated Wave

Consider a rigid elliptic cylinder which vibrates as a unit with the translational velocity $\vec{V}=(V_x e^{-i\omega t}, V_y e^{-i\omega t}, 0)$ and angular velocity $\vec{\Omega}=(\Omega_x e^{-i\omega t}, \Omega_y e^{-i\omega t}, \Omega_z e^{-i\omega t})$ about an axis passing through the point O' at the sea bottom

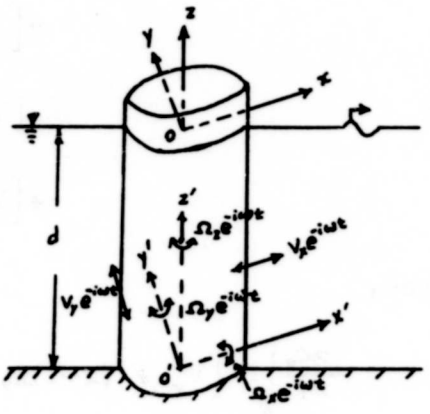

Fig. 5.1 Forces and Moments of an oscillating elliptic cylinder.

, as shown in fig. 6.1. The total fluid velocity of a point on the cylinder is $\vec{U}e^{-i\omega t}=(U_x e^{-i\omega t}, U_y e^{-i\omega t}, U_z e^{-i\omega t})=\vec{V}+\vec{\Omega}\times\vec{r}$, where $\vec{r}=(x,y,z+d)$, therefore,

$$\begin{aligned} U_x &= V_x + (z+d)\Omega_y - y\Omega_z \\ U_y &= V_y + x\Omega_z - (z+d)\Omega_x \\ U_z &= \quad y\Omega_x - x\Omega_y \end{aligned} \tag{5.1}$$

Applying the boundary condition on the normal velocity at the mean position of the solid, $\xi = \xi_o$, (equation (2.3)), the relation of coordinates systems: (equation (A.2)), and the outward unit normal (A.11), we have

$$\left.\frac{\partial\phi_R}{\partial n}\right|_{\xi=\xi_o} = \left.\frac{\partial\phi_R}{l_1\partial\xi}\right|_{\xi=\xi_o} = \vec{U}\cdot\vec{n}$$

$$= \left[V_x + (z+d)\Omega_y - y\Omega_z\right]\left(\frac{h\sinh\xi_o\cos\eta}{l_1}\right)$$

$$+\left[V_y + x\Omega_z - (z+d)\Omega_x\right]\left(\frac{h\cosh\xi_o\sin\eta}{l_1}\right)$$

$$= \left[V_x + (z+d)\Omega_y - h\sinh\xi_o\sin\eta\,\Omega_z\right]\left(\frac{h\sinh\xi_o\cos\eta}{l_1}\right)$$

$$+\left[V_y + h\cosh\xi_o\cos\eta\,\Omega_z - (z+d)\Omega_x\right]\left(\frac{h\cosh\xi_o\sin\eta}{l_1}\right)$$

Hence,

$$\left.\frac{\partial\phi_R}{\partial\xi}\right|_{\xi_o} = \left[V_x + (z+d)\Omega_y\right](h\sinh\xi_o\cos\eta) +$$

$$+\left[V_y - (z+d)\Omega_x\right](h\cosh\xi_o\sin\eta) + \frac{h}{2}\Omega_z\sin 2\eta \tag{5.2}$$

where ϕ_R is defined as the spatial part of velocity potential of the fluid, and equation (5.2) becomes the boundary condition on the body wall.

The solution of governing equation $\nabla^2\phi_R=0$, together with boundary conditions at the sea bottom, $\frac{\partial\phi_R}{\partial z}\Big|_{z=-d}=0$, and at the free surface, $\frac{\partial\phi_R}{\partial z}-\frac{\omega^2}{g}\phi_R=0\Big|_{z=0}$, and the radiation condition at far field, gives

$$\begin{aligned}\phi_R = \sum_{n=0}^{\infty}\sum_{m=1}^{\infty} \cosh k_m(z+d)\Big[& c_{2n}^{(m)} Mc_{2n}^{(1)}(\xi,q_m)ce_{2n}(\eta,q_m) + \\ & + c_{2n+1}^{(m)} Mc_{2n+1}^{(1)}(\xi,q_m)ce_{2n+1}(\eta,q_m) + \\ & + s_{2n+1}^{(m)} Ms_{2n+1}^{(1)}(\xi,q_m)se_{2n+1}(\eta,q_m) + \\ & + s_{2n+2}^{(m)} Ms_{2n+2}^{(1)}(\xi,q_m)se_{2n+2}(\eta,q_m)\Big] \qquad (5.3)\end{aligned}$$

where $c_n^{(m)}$, $s_n^{(m)}$ are constant coefficients to be determined by using the boundary condition on the solid wall, equation (5.2). We recall again $q_1>0$, and $q_m<0$ $(m\geq 2)$. Hence,

$$\begin{aligned}\frac{\partial\phi_R}{\partial\xi}\Big|_{\xi=\xi_0} = \sum_{n=0}^{\infty}\sum_{m=1}^{\infty} \cosh k_m(z+d)\Big[& c_{2n}^{(m)} Mc_{2n}^{(1)\prime}(\xi_0,q_m)ce_{2n}(\eta,q_m) + \\ & + c_{2n+1}^{(m)} Mc_{2n+1}^{(1)\prime}(\xi_0,q_m)ce_{2n+1}(\eta,q_m) + \\ & + s_{2n+1}^{(m)} Ms_{2n+1}^{(1)\prime}(\xi_0,q_m)se_{2n+1}(\eta,q_m) + \\ & + s_{2n+2}^{(m)} Ms_{2n+2}^{(1)\prime}(\xi_0,q_m)se_{2n+2}(\eta,q_m)\Big]\end{aligned}$$

$$\begin{aligned}= & \Big[V_x + (z+d)\Omega_y\Big]\ (\ h\sinh\xi_0\cos\eta\ ) + \\ & + \Big[V_y - (z+d)\Omega_x\Big](h\cosh\xi_0\sin\eta) + \frac{h}{2}\Omega_z\sin 2\eta\end{aligned}$$

(5.2')

In order to obtain the constants $c_n^{(m)}$, $s_n^{(m)}$, we multiply $\cosh k_m(z+d)$ and $ce_{2n}(\eta,q_m)$, ce_{2n+1}, se_{2n+1}, se_{2n+2} in turn on both sides of (5.2') and integrate from -d to 0 for z, and from 0 to 2π for η. Moreover, making use of orthogonal properties of $\cosh k_m(z+d)$ in the interval [-d,0], (2.5), and that of $ce_n(\eta,q_m)$, $se_n(\eta,q_m)$ in the interval $[0,2\pi]$, (B.12) with (B.27), (B.28). We recall that the coefficients of periodic Mathieu function $A^{(\ )}$, $B^{(\ )}$ are function of q only. Then we obtain

$$c_{2n}^{(m)} = 0$$

$$c_{2n+1}^{(m)} = \frac{h\sinh\xi_0 A_1^{(2n+1)}}{N_{k_m} Mc_{2n+1}^{(1)'}(\xi_0,q_m)} \int_{-d}^{0} \left[V_x + (z+d)\Omega_y\right] \cosh k_m(z+d)dz$$

$$s_{2n+1}^{(m)} = \frac{h\cosh\xi_0 B_1^{(2n+1)}}{N_{k_m} Ms_{2n+1}^{(1)'}(\xi_0,q_m)} \int_{-d}^{0} \left[V_y - (z+d)\Omega_x\right] \cosh k_m(z+d)dz$$

$$s_{2n+2}^{(m)} = \frac{\frac{1}{2}h^2 B_2^{(2n+2)}}{N_{k_m} Ms_{2n+2}^{(2)'}(\xi_0,q_m)} \int_{-d}^{0} \Omega_z \cosh k_m(z+d)dz$$

(5.4a,b,c,d)

where N_{k_m} is defined in equation (2.5).

In the far field $Mc_n^{(j)}(\xi,q_m)$, $Ms_n^{(j)}(\xi,q_m)$ $(m \geq 2)$ behave like modified Bessel function $K_m(k_m r) \sim 0$, (B.29). and give no contribution to the radiated wave potential. Physically, $q'_m s$ correspond to $k'_m s$ $(m \geq 2)$ which represent the evanescent modes having only local effects in the near field. Since $K_n(kr)$ is small enough, if kr, say, is equal to (or greater than) 10.

i.e. $\frac{r}{L}=\frac{kr}{2\pi}=\frac{10}{2\pi}\sim O(1)$, any distance longer than one wave length away from the body may be regarded as the far field. Hence, the velocity potential in the far field is

$$\phi_{R_\infty} \sim \cosh k_1(z+d)\sum_{n=0}^{\infty}\Big[c_{2n+1}^{(1)}Mc_{2n+1}^{(4)}(\xi,q_1)ce_{2n+1}(\eta,q_1) + s_{2n+1}^{(1)}Ms_{2n+1}^{(3)}(\xi,q_1)se_{2n+1}(\eta,q_1) + s_{2n+2}^{(1)}Ms_{2n+2}^{(3)}(\xi,q_1)se_{2n+2}(\eta,q_1)\Big] \qquad (5.5)$$

5-2 Haskind's Theorem and the Exciting forces on a stationary elliptic cylinder

In chapter 3 we have demonstrated that in order to determine the forces exerting on the cylinder, we have to know not only the hydrodynamic pressure in the incident wave system , but also that in the scattered wave system. A useful theorem by Haskind (1957) on the exciting forces and moments on a fixed body in an incident wave field, gives an expression which does not require a knowledge of the scattered wave effects, but depends instead on the velocity potential for the forced oscillation of the body in calm water. Moreover, the asymptotic characteristics of this velocity potential for large distance from the body is sufficient to determine the exciting forces for a given incident wave system.

Haskind's theorem [31] states that

$$X_j = i\omega\rho e^{-i\omega t} \iint_{S_\infty} \left(\phi_I \frac{\partial \phi_{Rj}}{\partial n} - \phi_{Rj} \frac{\partial \phi_I}{\partial n} \right) dS \qquad (5.6)$$

where ϕ_I is the velocity potential of the incident wave, ϕ_{Rj} the velocity potential of the radiated wave field due to the jth mode of oscillation, X_j the exciting force or moment relating to that mode of radiation. The precise correspondence is shown in Table 5.1, with n the unit normal vector into the fluid, and S the control surface at the far field.

Table 5.1 Correspondence between modes of forced motion and restoring forces

j	The jth mode of oscillation	forces (or moments) in the jth direction
1	surge (oscillation in x direction) ϕ_{R1}	x-component force X_1
2	sway (oscillation in y direction) ϕ_{R2}	y-component force X_2
3	heave (oscillation in z direction) ϕ_{R3}	z-component force X_3
4	roll (rotational oscillation about x-axis) ϕ_{R4}	moment about x-axis X_4
5	pitch (rotational oscillation about y-axis) ϕ_{R5}	moment about y-axis X_5
6	yaw (rotational oscillation about z-axis) ϕ_{R6}	moment about z-axis X_6

In elliptic cylinder coordinates and for the far field, $dS = l_1 d\eta dz$, $\frac{\partial}{\partial n} = -\frac{1}{l_1}\frac{\partial}{\partial \xi}$, (A.7). Hence equation (5.6)

can be written as

$$X_j = -i\omega\rho\, e^{-i\omega t}\int_{-d}^{0} dz \int_{0}^{2\pi}\left(\phi_I \frac{\partial \phi_{Rj}}{\partial \xi} - \phi_{Rj}\frac{\partial \phi_I}{\partial \xi}\right)\Big|_{\xi\to\infty} d\eta \qquad (5.7)$$

5-2-1 Surge and the x-component force

Consider the unit problem for the surge mode only ($V_x=1$, $V_y = \Omega_x = \Omega_y = \Omega_z = 0$). From (5.4)

$$c_{2n}^{(1)} = s_{2n+1}^{(1)} = s_{2n+2}^{(1)} = 0$$

$$c_{2n+1}^{(1)} = \frac{h\sinh\xi_0 A_1^{(2n+1)}}{N_{k_1} Mc_{2n+1}^{(3)}(\xi_0, q_1)}\int_{-d}^{0}\cosh k(z+d)dz = \frac{h\sinh\xi_0 A_1^{(2n+1)}\sinh kd}{N_{k_1} Mc_{2n+1}^{(3)}(\xi_0, q_1)\, k_1}$$

substitute into (5.5), we have the radiated velocity potential in the far field

$$\phi_{R1} \sim \cosh k_1(z+d)\sum_{n=0}^{\infty}\left[\frac{h\sinh\xi_0 A_1^{(2n+1)}\sinh kd}{N_{k_1} Mc_{2n+1}^{(3)}(\xi_0, q_1)\, k_1}\right] Mc_{2n+1}^{(3)}(\xi, q_1)\, ce_{2n+1}(\eta, q_1)$$

$$\sim \frac{\cosh k_1(z+d)}{N_{k_1}}(dh\sinh\xi_0)\left(\frac{\sinh kd}{kd}\right)\sum_{n=0}^{\infty} A_1^{(2n+1)}\frac{Mc_{2n+1}^{(3)}(\xi, q_1)}{Mc_{2n+1}^{(3)}(\xi_0, q_1)}\, ce_{2n+1}(\eta, q_1) \qquad (5.8)$$

Substituting equations (3.3), (5.8) into equation (5.7), we then have the x-component force exerting on the stationary cylinder.

$$X_1 = -i\omega\rho e^{-i\omega t}\left(\frac{2ga_x}{\omega}\right)\left(\frac{\tanh kd}{kd}\right)\left(\frac{dh\sinh\xi_0}{N_{k_1}}\right)\int_{-d}^{0}\cosh k(z+d)dz \cdot$$

$$\cdot \int_0^{2\pi}\Bigg(\Bigg\{\sum_{n=0}^{\infty}\Big[(-1)^n Mc_{2n}^{(1)}(\xi, q_1)ce_{2n}(\eta, q_1)ce_{2n}(\theta_1, q_1) +$$

$$+ (-1)^{n+1} Ms_{2n+2}^{(1)}(\xi, q_1)se_{2n+2}(\eta, q_1)se_{2n+2}(\theta_1, q_1) +$$

$$+ (-1)^n i\, Mc_{2n+1}^{(1)}(\xi, q_1)ce_{2n+1}(\eta, q_1)ce_{2n+1}(\theta_1, q_1) +$$

$$+ (-1)^n i\, Ms^{(1)}_{2n+1}(\xi, q_1) se_{2n+1}(\eta, q_1) se_{2n+1}(\theta_2, q_1)\Big]\Big\} \cdot$$

$$\cdot \left[\sum_{n=0}^{\infty} A_1^{(2n+1)} \frac{Mc^{(3)\prime}_{2n+1}(\xi_2, q_1)}{Mc^{(3)\prime}_{2n+1}(\xi_0, q_1)}\, ce_{2n+1}(\eta, q_1)\right] -$$

$$- \left\{\sum_{n=0}^{\infty}\Big[(-1)^n Mc^{(1)\prime}_{2n}(\xi, q_1) ce_{2n}(\eta, q_1) ce_{2n}(\theta_1, q_1) +\right.$$

$$+ (-1)^{n+1} Ms^{(1)\prime}_{2n+2}(\xi, q_1) se_{2n+2}(\eta, q_1) se_{2n+2}(\theta_2, q) +$$

$$+ (-1)^n i\, Mc^{(1)\prime}_{2n+1}(\xi, q_1) ce_{2n+1}(\eta, q_1) ce_{2n+1}(\theta_2, q_1) +$$

$$\left. + (-1)^n i\, Ms^{(1)\prime}_{2n+1}(\xi, q_1) se_{2n+1}(\eta, q_1) se_{2n+1}(\theta_2, q_1)\Big]\right\} \cdot$$

$$\cdot \left[\sum_{n=0}^{\infty} A_1^{(2n+1)} \frac{Mc^{(3)}_{2n+1}(\xi, q_1)}{Mc^{(3)}_{2n+1}(\xi_0, q_1)}\, ce_{2n+1}(\eta, q_1)\right]\Big)\, d\eta$$

$$= (-i)(2\rho g a_I)(dh \sinh\xi_0)\left(\frac{\tanh kd}{kd}\right) e^{-i\omega t} \int_0^{2\pi} \sum_{n=0}^{\infty} \cdot$$

$$\cdot \left\{(-1)^n \frac{iA_1^{(2n+1)}\left[Mc^{(1)}_{2n+1}(\xi, q_1) Mc^{(3)\prime}_{2n+1}(\xi, q_1) - Mc^{(1)\prime}_{2n+1}(\xi, q_1) Mc^{(3)}_{2n+1}(\xi, q_1)\right]}{Mc^{(3)\prime}_{2n+1}(\xi_0, q_1)} \cdot \right.$$

$$\cdot ce_{2n+1}(\theta_1, q_1) ce^2_{2n+1}(\theta_1, q_1) + \Big[\text{other terms with}$$

$$ce_{2n}(\eta, q_1) cc_i(\eta, q_1) \text{ and } ce_{2n+1}(\eta, q_1) se_i(\eta, q_1)\ i \neq 2n+1\Big]\Big\}\, d\eta$$

$$= (2\rho g a_I)(2dh \sinh\xi_0)\left(\frac{\tanh kd}{kd}\right) e^{-i\omega t} \cdot$$

$$\cdot \sum_{n=0}^{\infty} (-1)^n \frac{iA_1^{(2n+1)}}{Mc^{(3)\prime}_{2n+1}(\xi_0, q_1)}\, ce_{2n+1}(\theta_1, q_1)$$

thus,

$$X_1 = (2\rho g a_I)(2dh \sinh\xi_0)\left(\frac{\tanh kd}{k_1 d}\right) e^{-i\omega t} \sum_{n=0}^{\infty} (-1)^n \frac{iA_1^{(2n+1)}}{Mc^{(3)\prime}_{2n+1}(\xi_0, q_1)} ce_{2n+1}(\theta_1, q_1) \tag{5.9}$$

5-2-2 Sway and the y-component force

Following the same procedure, the radiated velocity potential due to unit sway only (V_y=1, others=0) gives

$$\phi_{R2} \sim \frac{\cosh k_1(z+d)}{N_{k_1}} (dh\cosh\xi_o)\left(\frac{\sinh kd}{kd}\right) \cdot \sum_{n=0}^{\infty} \frac{B_1^{(2n+1)} Ms_{2n+1}^{(4)}(\xi, q)}{Ms_{2n+1}^{(3)\prime}(\xi_o, q)} se_{2n+1}(\eta, q) \qquad (5.10)$$

and the y-component force is,

$$X_2 = (2g\rho a_I)(2dh\cosh\xi_o)\left(\frac{\tanh kd}{kd}\right)e^{-i\omega t} \cdot \sum_{n=0}^{\infty} (-1)^n \frac{iB_1^{(2n+1)}}{Ms_{2n+1}^{(3)\prime}(\xi_o, q_1)} se_{2n+1}(\eta_1, q_1) \qquad (5.11)$$

5-2-3 Roll and the Moment about x'-axis

For the roll mode with unit amplitude (Ω_x=1, others=0) the radiated velocity potential leads to

$$\phi_{R4} \sim -\frac{\cosh k_1(z+d)}{N_{k_1}} (dh\cosh\xi_o)\left(\frac{\sinh kd}{k_1 d}\right)d\left(1-\frac{\coth kd}{k_1 d} + \frac{\operatorname{csch} kd}{k_1 d}\right) \cdot \sum_{n=0}^{\infty} B_1^{(2n+1)} \frac{Ms_{2n+1}^{(3)}(\xi, q_1)}{Ms_{2n+1}^{(3)\prime}(\xi_o, q)} se_{2n+1}(\eta, q_1) \qquad (5.12)$$

and the moment about x'-axis at bottom is,

$$X_4 = -(2g\rho a_I)(2dh\cosh\xi_o)\left(\frac{\tanh k_1 d}{k_1 d}\right)d\left(1-\frac{\coth k_1 d}{k_1 d} + \frac{\operatorname{csch} k_1 d}{k_1 d}\right) \cdot e^{-i\omega t} \sum_{n=0}^{\infty}(-1)^n \frac{iB_1^{(2n+1)}}{Ms_{2n+1}^{(3)\prime}(\xi_o, q_1)} se_{2n+1}(\eta_1, q_1) \qquad (5.13)$$

5-2-4 Pitch and the moment about y'-axis

For unit pitch mode (Ω_y=1, others=0), the radiated velocity potential is

$$\Phi_{R5} \sim \frac{\cosh k_1(z+d)}{N_{k_1}} (dh\sinh\xi_0)\left(\frac{\sinh k_1 d}{k_1 d}\right) d\left(1-\frac{\coth k_1 d}{k_1 d}+\frac{\operatorname{csch} k_1 d}{k_1 d}\right) \cdot \sum_{n=0}^{\infty} A_1^{(2n+1)} \frac{Mc_{2n+1}^{(3)}(\xi, q_1)}{Mc_{2n+1}^{(3)\prime}(\xi_0, q_1)} ce_{2n+1}(\eta, q_1) \qquad (5.14)$$

and the moment about y'-axis at bottom is,

$$X_5 = (2g\rho a_I)(2dh\sinh\xi_0)\left(\frac{\tanh k_1 d}{k_1 d}\right) d\left(1-\frac{\coth k_1 d}{k_1 d}+\frac{\operatorname{csch} k_1 d}{k_1 d}\right) \cdot e^{-i\omega t} \sum_{n=0}^{\infty}(-1)^n \frac{iA_1^{(2n+1)}}{Mc_{2n+1}^{(3)\prime}(\xi_0, q_1)} ce_{2n+1}(\theta_1, q_1) \qquad (5.15)$$

5-2-5 Yaw and the moment about z'-axis

For the yaw mode with unit amplitude (Ω_Z=1, others=0), the radiated velocity potential is

$$\Phi_{R6} \sim \frac{\cosh k_1(z+d)}{N_{k_1}} \left(\frac{1}{2}dh^2\right)\left(\frac{\sinh k_1 d}{k_1 d}\right) \sum_{n=0}^{\infty} B_2^{(2n+2)} \frac{Ms_{2n+2}^{(3)}(\xi, q_1)}{Ms_{2n+2}^{(3)\prime}(\xi_0, q_1)} se_{2n+2}(\eta, q_1) \qquad (5.16)$$

and the moment about z'-axis at bottom is,

$$X_6 = (2\rho g a_I)(dh^2)\left(\frac{\tanh k_1 d}{k_1 d}\right) e^{-i\omega t} \sum_{n=0}^{\infty}(-1)^{n+1} \frac{B_2^{(2n+2)}}{Ms_{2n+2}^{(3)\prime}(\xi_0, q_1)} se_{2n+2}(\theta_1, q_1) \qquad (5.17)$$

We note that equations (5.9), (5.11), (5.13), (5.15) and (5.17) are the same as equations (3.9), (3.10), (3.11), (3.12) and (3.13) respectively.

In this work we are not interested in the heaving mode (j=3).

5-3 Radiation Damping

The restoring force on an oscillating body is defined as the force required to drive a body in harmonic oscillation about its mean position. It is usually taken as the negative of the hydrodynamic reaction on the body in forced motion and must be added to the hydrostatic buoyancy force in the equation of motion of a floation body. The hydrodynamic force can be written as

$$X_j = -A_j \frac{d^2 s_i}{dt^2} - B_j \frac{ds_i}{dt} \tag{5.18}$$

where j corresponds to the jth mode, s is body displacement, and both A_j and B_j are real.

The term A_j is called the added mass coefficient and it amounts to an additional inertia for having to accelerate the fluid near the body. B_j is defined as the damping coefficient and the term $B_j \frac{ds_i}{dt}$ represents the force component in phase with the velocity of the body and accounts for energy irretrievably transfered to the fluid as outgoing waves.

The knowledge of the far-field radiated wave potential, where only the propagating mode is significant, may be used to establish the damping coefficient through a consideration of energy balance. However, the added mass coefficient is associated with the near-field radiated wave potential and may be computed only by including all evanescent and propagating

wave modes; a much larger amount of numerical work is needed and is not attempted in this work.

If the body velocity is given by

$$\frac{ds_j}{dt} = U_j e^{-i\omega t} \tag{5.19}$$

then the averaged rate of energy transfered from the body to the fluid is

$$\frac{d\bar{E}}{dt} = \frac{1}{T}\int_0^T X_j \cdot \frac{ds_j}{dt}\, dt \tag{5.20}$$

where $T=\frac{2\pi}{\omega}$.

Substituting equations (5.18), (5.19) into (5.20), we can obtain the damping coefficient in terms of input energy:

$$B_j = -\frac{2}{|U_j|^2}\frac{d\bar{E}}{dt} \tag{5.21}$$

In a quasi-steady motion of an inviscid fluid, the mean energy imparted to the fluid is exactly equal to the energy radiated away by wave motion. The time average rate of energy flux across a large control surface S_∞ enclosing the body is given by

$$\frac{d\bar{E}_j}{dt} = \frac{1}{T}\int_0^T \left[\rho \int_{S_\infty} \mathrm{Re}\left\{\frac{\partial \Phi_{Rj}}{\partial t}\right\} \mathrm{Re}\left\{\frac{\partial \Phi_{Rj}}{\partial n}\right\} ds\right] dt \tag{5.22}$$

where the normal gradient is oriented into the fluid domain. The damping coefficients are calculated for each individual mode as demonstrated below.

5-3-1 Radiation Damping due to surge

For the far field, equation (5.8) can be written as

$$\Phi_{R1} \sim \frac{\cosh k_1(z+d)}{N_{k_1}} (dh\sinh\xi_0) \left(\frac{\sinh k_1 d}{k_1 d}\right) e^{-i\omega t} \sqrt{\frac{2}{\pi k_1 r}} \cdot$$

$$\cdot \sum_{n=0}^{\infty} A_1^{(2n+1)} \frac{i}{Mc_{2n+1}^{(3)'}(\xi_0, q_1)} e^{i\left(k_1 r - \frac{(2n+1)\pi}{2} - \frac{\pi}{4}\right)} ce_{2n+1}(\eta, q_1) \tag{5.23}$$

where $r = h\cosh\xi$.

The real parts of $\frac{\partial \Phi_{R1}}{\partial t}$ and $\frac{\partial \Phi_{R1}}{\partial n}$ are

$$Re\left\{\frac{\partial \Phi_{R1}}{\partial t}\right\} = \frac{\cosh k_1(z+d)}{N_{k_1}} (dh\sinh\xi_0) \left(\frac{\sinh k_1 d}{k_1 d}\right) \sqrt{\frac{2}{\pi k_1 r}}\, \omega \cdot$$

$$\cdot \sum_{n=0}^{\infty} \frac{A_1^{(2n+1)}}{Mc_{2n+1}^{(1)'}(\xi_0, q_1) + Mc_{2n+1}^{(3)'}(\xi_0, q_1)} \cdot$$

$$\cdot \left[Mc_{2n+1}^{(1)'}(\xi_0, q_1) \sin\left(k_1 r - \frac{2n+1}{2}\pi - \frac{\pi}{4} - \omega t\right) - \right.$$

$$\left. - Mc_{2n+1}^{(2)'}(\xi_0, q_1) \cos\left(k_1 r - \frac{2n+1}{2}\pi - \frac{\pi}{4} - \omega t\right) \right] \cdot$$

$$\cdot ce_{2n+1}(\eta, q_1) \tag{5.24}$$

$$Re\left\{\frac{\partial \Phi_{R1}}{\partial n}\right\} = Re\left\{\frac{\partial \Phi_{R1}}{\partial r}\right\}$$

$$= \frac{\cosh k_1(z+d)}{N_{k_1}} (dh\sinh\xi_0) \left(\frac{\sinh k_1 d}{k_1 d}\right) \sqrt{\frac{2k_1}{\pi r}} \cdot$$

$$\cdot \sum_{n=0}^{\infty} \frac{A_1^{(2n+1)}}{Mc_{2n+1}^{(1)'}(\xi_0, q_1) + Mc_{2n+1}^{(2)'}(\xi_0, q_1)} \cdot$$

$$\cdot \left[- Mc_{2n+1}^{(1)'}(\xi_0, q_1) \sin\left(k_1 r - \frac{2n+1}{2}\pi - \frac{\pi}{4} - \omega t\right) \right.$$

$$+ Mc^{(3)'}_{2m+1}(\xi_o,q_1)\cos(k_1 r-\frac{2n+1}{2}\pi-\frac{\pi}{4}-\omega t)\Big]\cdot$$

$$\cdot ce_{2m+1}(\eta,q_1) \qquad (5.25)$$

Substituting equation (5.24), (5.25) into (5.22) and integrate along a great ellipse in the far field from $\eta=0$ to 2π, $z=-d$ to 0, equation (5.21) (with $U_j=1$) reduces to

$$B_1 = 2\rho\omega\left(\frac{\sinh k_1 d}{k_1 d}\right)^2 (dh\sinh\xi_o)^2\left(\frac{1}{N_{k_1}}\right)C_{B1} \qquad (5.26)$$

where

$$C_{B1} = \sum_{n=0}^{\infty} \frac{\left[A_1^{(2n+1)}\right]^2}{Mc^{(1)'}_{2m+1}(\xi_o,q_1)+Mc^{(3)'}_{2m+1}(\xi_o,q_1)} \qquad (5.26a)$$

5-3-2 Radiation Damping due to other modes

Following the same procedures, and from equations (5.10), (5.12), (5.14), (5.16), we can obtain the four other radiation damping coefficients.

(1) Radiation Damping due to Sway

$$B_2 = 2\rho\omega\left(\frac{\sinh k_1 d}{k_1 d}\right)^2 (dh\cosh\xi_o)^2\left(\frac{1}{N_{k_1}}\right)C_{B2} \qquad (5.27)$$

where

$$C_{B2} = \sum_{n=0}^{\infty} \frac{\left[B_1^{(2n+1)}\right]^2}{Ms^{(1)'}_{2m+1}(\xi_o,q_1)+Ms^{(3)'}_{2m+1}(\xi_o,q_1)} \qquad (5.27a)$$

(2) Radiation Damping due to Roll

$$B_4 = 2\rho\omega\left(\frac{\sinh k_1 d}{k_1 d}\right)^2 (dh\cosh\xi_o)^2\left(\frac{1}{N_{k_1}}\right)(dC_{k_1 xy})^2 C_{B2} \qquad (5.28)$$

where $C_{k_1 xy}$ is defined in equation (3.11a)

(3) Radiation Damping due to Pitch

$$B_5 = 2\rho\omega\left(\frac{\sinh kd}{kd}\right)^2 (dh\cosh\xi_0)^2 \left(\frac{1}{N_{k_1}}\right)(dC_{k_1xy})^2 C_{B1} \qquad (5.29)$$

(4) Radiation Damping due to Yaw

$$B_6 = 2\rho\omega\left(\frac{\sinh kd}{kd}\right)^2 \left(\frac{dh^2}{2}\right)\left(\frac{1}{N_{k_1}}\right) C_{B6} \qquad (5.30)$$

where

$$C_{B6} = \sum_{n=0}^{\infty} \frac{[B_2^{(2n+1)}]^2}{Ms_{2n+1}^{(1)}(\xi_0, q_1) + Ms_{2n+1}^{(2)}(\xi_0, q_1)} \qquad (5.30a)$$

6. COMPUTATIONAL ASPECTS AND NUMERICAL RESULTS

To an engineer or a physicist a formal solution is seldom sufficient, but is merely a stepping stone to quantative results.

Although a considerable amount of analytical knowledge concerning the solutions of differential equations of the Mathieu type is available for almost over a hundred years, the existing numerical results of these solutions seem still incomplete and insufficient for applications. Furthermore, the various notations and definitions of the Mathieu functions due to different normalizations used by different authors increase the inconvenience of using these numerical results. Recently, Clemm (1969)[11] published a rather complete computer program for all coefficients, characteristic values and various solutions and their first derivatives of both the Mathieu functions and the modified Mathieu functions. For a justification of the method using in his computer program, the reader is referred to Blanch's paper[4].

We employ Clemm's program to calculate the values concerning the Mathieu functions.

6-1 Mathieu functions

We use Ince's normalization for the Mathieu functions and Blanch's definition for the modified Mathieu functions which were adopted in previous chapters of this work.

The periodic Mathieu functions; $ce_m(\eta,q)$, $se_m(\eta,q)$, have been calculated by Ince only for the ranges $q = 1, (1), 10$; $m = 0, (1), 5$ for $ce_m(\eta,q)$ and m up to 6 for $se_m(\eta,q)$. The modified Mathieu functions and its first derivatives; $Mc_m^{(i)}(\xi,q)$, $Ms_m^{(i)}(\xi,q)$ and $Mc_m^{(i)\prime}(\xi,q)$, $Ms_m^{(i)\prime}(\xi,q)$, (i=1,2), have been calculated by Blanch for $q = 0.00, (0.05), 1$; $m = 0, (1), 15$; $\xi = 0.00, (0.01), 1$. For our purposes, these tabulated results are still incomplete in the fineness of intervals and insufficient in range, and new calculations are necessary.

We computed the characteristic values $a_1(q)$, the coefficients $A_m^{(n)}(q)$, $B_m^{(n)}(q)$, $ce_m(\eta,q)$, $se_m(\eta,q)$, $Mc_m^{(i)\prime}(\xi,q)$ and $Ms_m^{(i)\prime}(\xi,q)$ (i=1,2), with arguements as follows:

(1°) Since large body-sizes (comparing with the wavelength) are of interest and since for $q = 10$, $\frac{h}{L} \sim 0(1)$, we chose $q = 0.5, (0.5), 10$. We also computed some values for $q=0.1, 0.2, 0.226717$, in order to compare with Burke's results etc. It is possible to perform calculations for higher q. But for higher q, we tend to encounter overflow or underflow in computer execution in calculating $A_m^{(n)}(q)$, $B_m^{(n)}(q)$, $Mc_m^{(i)\prime}(\xi,q)$ and $Ms_m^{(i)\prime}(\xi,q)$.

(2°) $m = 0, (1), 20$: Since there are two sets of solutions ; $ce_{2n}(\eta,q)$, $ce_{2n+1}(\eta,q)$ ... etc. this is equivalent to first ten orders of either odd-ordered or even-ordered Mathieu functions. In calculating quantities such as forces,

scattering cross-sections and radiation damping coefficients, $m \leq 20$ are sufficiently accurate for the series to converge except for large ξ ($\xi \sim 3$) with large q. We also have some values with m = 21 , (1) , 40 in order to study the convergence of the series for $\xi = 3$.

(3) $\eta = 0.0^\circ$, (7.5°) , 90°; values greater than 90 with same interval can be obtained by using Reduction formulae (B.17).

(4) $\xi = 0.0$, 0.2 , 0.6 , 1 , 3 : For $\xi = 0.0$, the ratio of minor axis radius to major axis radius is $\frac{b}{a} = 0$. The ellipse reduces to a plate with length 2h ; For $\xi = 3$, $\frac{b}{a} = 0.99505$, the ellipse almost reduces to a circle. Even for $\xi = 1$, $\frac{b}{a} = 0.76159$, the ellipse is not far from a circle. We also computed some values for $\xi = 0.01$, 0.55 for comparison with other published results. Because of the slow convergence of the series for $\xi = 3$, most calculations of the series are carried out for $\xi = 0.0 \sim 1$.

The Mathieu functions with parameters in the range of Ince's and Blanch's tables have been checked and are correct.

Total execution computer time for these functions with the range of the various parameters metioned above is approximately 45 min. It takes longer time to compute the modified Mathieu functions than the Mathieu functions. The properties of Mathieu functions are first computed and stored for the stated range of parameters, use is then made of these

values to compute the physical quantities.

Once we have the numerical results of Mathieu functions, the calculation of the physical quantities (forces, scattering cross sections, and the radiation damping coefficients) becomes straightforward. In order to avoid overflow or underflow in computer execution, the values of Mathieu solutions less than 10^{-5} is considered to be zero. All series tend to converge very slowly for large ξ and q . Methods of linear and parabolic extrapolations used by Garrett [13] are used to calculate the series. The method states that we can use S_N , the sum of first N-terms in a series, and $\frac{1}{N}$ as the Cartesian coordinates, then extrapolate S_N to $\frac{1}{N}=0$, as shown is Fig.6.1. When the two methods give indistinguishable results, the series convergence is good.

In our cases, the maximum N is N=10.

In most cases in this work N=10 is sufficiently accurate for the series to converge except for large ξ ($\xi=3$) and large q.

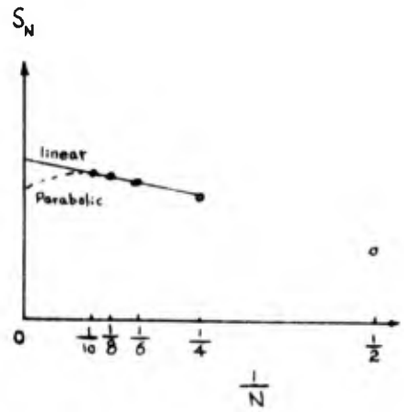

Fig. 6.1 Extrapolation

6-2 Forces and Moments

The quantities of $|C_{Fx}|$, Θ_{Fx}, $|C_{Fy}|$, Θ_{Fy}, $|C_{Mz}|$, Θ_{Mz}; i.e. equations (3.10c), (3.10d), (3.12b), (3.12c), (3.16b), (3.16c), are calculated and shown in Figs (6.3) - (6.16).

These series converge very fast even for $\xi_0=3$ and $q=10$. By using 3-terms through 10-terms of these series the results are the same.

We note that if we use asymptotic forms with $\xi_0 \to \infty$, $h \to 0$, and $h\cosh\xi_0 \sim h\sinh\xi_0 \sim r_0$ for Mathieu functions, (in this limit case, the ellipse reduces to a circle), the forces, scattering cross sections and radiation damping coefficients for the elliptical cylinder should reduce to those for the circular cylinder. (Appendix C)

Since the ellipse is almost a circle for $\xi_0=3$, the results of the force systems of $\xi_0=3$ with $\theta_1=0$ are compared with the results which are directly obtained from the circular cylinder (C.5a). The comparisons are shown in Tables 6.1 . 6.2 , and the results are in very good agreement with only slight discrepancy in phase angles.

For a semi-elliptic cylinder protruding from a straight coast, the results given by equations (4.6b), (4.6c), (4.8b), (4.8c) ; $|C_{hFx}|$, Θ_{hFx}, $|C_{hMz}|$, Θ_{hMz}, are shown in figures (7.1)—(7.2).

Table 6.1 Comparison of force coefficients on a circular cylinder and an elliptical cylinder with equal projected area ; $r_o = h\sinh\xi_o$, $\theta_I = 0°$. (this table is calculated from eqs. (3.10c,d), (C.5a))

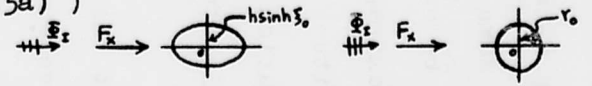

q	0.5	1	1.5	2	2.5	3	3.5	4	4.5	5	5.5	6	6.5	7	7.5	8	8.5	9	9.5	10
$\lvert C_x \rvert$	0.333	0.280	0.253	0.235	0.223	0.213	0.205	0.198	0.192	0.187	0.183	0.179	0.175	0.172	0.169	0.166	0.164	0.162	0.159	0.157
$\lvert C_{Fx} \rvert$	0.332	0.279	0.252	0.235	0.222	0.212	0.204	0.198	0.192	0.187	0.182	0.178	0.175	0.172	0.169	0.166	0.164	0.161	0.159	0.157
$\theta_x - \pi$	-2.448	-2.015	-0.227	2.265	-1.076	2.186	-0.593	3.104	0.674	-1.624	2.473	0.385	-1.618	2.737	0.877	-0.922	-2.665	1.925	0.278	-1.326
$\theta_{Fx} - \pi$	-2.519	-2.115	-0.349	2.124	-1.234	2.013	-0.779	2.904	0.663	-1.847	2.234	0.141	-1.872	2.474	0.604	-1.203	-2.956	1.626	-0.029	-1.641

(phase angle is counted from $-\pi$ to π)

Table 6.2 Comparison of force coefficients on a circular cylinder and an elliptical cylinder with equal projected area ; $r_o = h\cosh\xi_o$, $\theta_I = 90°$. (this table is calculated from eqs. (3.12b,c), (C.5a))

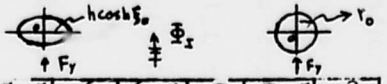

q	0.5	1	1.5	2	2.5	3	3.5	4	4.5	5	5.5	6	6.5	7	7.5	8	8.5	9	9.5	10
$\lvert C_x \rvert$	0.332	0.279	0.252	0.235	0.222	0.212	0.204	0.198	0.192	0.187	0.182	0.178	0.175	0.172	0.169	0.166	0.164	0.161	0.159	0.157
$\lvert C_{Fy} \rvert$	0.333	0.280	0.253	0.235	0.223	0.213	0.205	0.198	0.192	0.187	0.183	0.179	0.175	0.172	0.169	0.166	0.164	0.162	0.159	0.157
$\theta_x - \pi$	-2.518	-2.115	-0.349	2.124	-1.234	2.013	-0.779	2.904	0.663	-1.846	2.240	0.141	-1.872	2.474	0.604	-1.203	-2.956	1.626	0.029	-1.641
$\theta_{Fy} - \pi$	-2.448	-2.015	-0.227	2.265	-1.076	2.186	-0.593	3.104	0.672	-1.624	2.474	0.385	-1.618	2.737	0.877	-0.922	-2.665	1.925	0.278	-1.326

(phase angle is counted from $-\pi$ to π)

6-3 Differential Scattering Cross Section

The results of differential scattering cross section, $\sigma(\eta)$; equation (3.20), are shown in figure 6.17 . Equation (3.20) converges very well for $\xi_0 \leq 1$. (no calculations were made for $\xi_0 > 1$, for which convergence is expected to deteriorate). The numerical results show that the 6-terms, 8-terms, and 10-terms of the series are almost the same. Even for $\xi_0 = 1$, $q_1 = 10$, the difference between the results by using linear extrapolation and those by using parabolic extrapolation is within 5%. The results of small q is consitent with Burke's[10] . Burke used the low-frequency approximation ($ka \to 0$, $\Rightarrow$ q small) for the Mathieu functions in his study of electromagnetic waves.

It is interesting to note from the results that the change in directionality of the scattered waves as the wavelength is changed. For long wavelength compared with the dimension of the body ($q_1 < 0.1$) little is scattered. As the wavelength decreases (q_1 increases), the distribution in angle becomes more and more complicated ; scattering peaks appear and move forward. For very short wavelengths a very sharp peak is concentrated in the forward direction. In some unsymmetrical cases there is also a sharp peak as a reflected wave. It is usual to call the half of the scattered wave spreading backward as the reflected wave, and the forward half as the shadow-forming wave.

6-4 Total Scattering Cross-section

The results of total scattering cross-section, Q, equation (3.21), is shown in Fig 6.18. The numerical behavior of (3.21) is almost the same as (3.20). We also have the case of $\xi_0=3$, but the convergence of (3.21) for $q_1>3$ is so poor that using 10-terms in the series is still not enough to get an accurate result by extrapolation. It is interesting to note that the total scattering cross section, Q, for $q_1=3$ is almost 4, which is the asymptotic limit of Q for a full circular cylinder.

We checked the results for small q_1 ($0<q_1<1$) with Barakat's[2,7], and there are some discrepancies. In Barakat's results the labeling in certain figures appears to be wrong.

6-5 Differential Scattering Cross Section and Total Scattering Cross Section of Semi-Elliptic Cylinder

The results of differential and total scattering cross sections, (4.14), (4.15) ; $\sigma_h(\eta)$, Q_h, of a semi-elliptic cylinder with straight shoreline for $\theta_1=45°$ are shown in figures (7.3), (7.4).

6-6 Radiation Damping

The results of damping coefficients, (5.26a), (5.27a), (5.30a) ; C_{B1}, C_{B2}, C_{B6}, are shown in figure 6.19. These series converge as well as the coefficients of the forces, equations (3.10c)—(3.16c).

6-7 Summary of numerical results

(1) Symbols :

k_1 : Wave number of the incident wave = 2π/wavelength

d : Still water depth

θ_I : Angle of incidence with respect to a principal axis of the ellipse

a : Half length of major axis of ellipse

b : Half length of minor axis of ellipse

ξ_o : Parameter characterizing the ellipticity of the cross section. $b/a = \tanh \xi_o$

ξ_o	0	0.2	0.55	0.6	1	3	∞
b/a	0 Flat Plate	0.197	0.500	0.537	0.762	0.995	1 Circle

h : Focal distance of ellipse, $\sqrt{a^2 - b^2}$

$q_1 = (k_1 h/2)^2$

(2) List of Figures :

Elliptic cylinder

Figure	Caption	Equation	Parameters
6.2	$C_{k_1 d}$: Depth factor for F_x , F_y & M_z	3.10a	$k_1 d$
	$C_{k_1 xy}$: Depth factor for M_x & M_y	3.13a	

Elliptic cylinder (cont'd)

Figure	Caption	Equation	Parameters
6.3-6.6	x-component force coefficient $\|C_{Fx}\|$: magnitude θ_{Fx} : phase	 3.10c 3.10d	θ_I=0°, (15°), 90°
6.7-	y-component force coefficient $\|C_{Fy}\|$: magnitude θ_{Fy} : phase	 3.12b 3.12c	q_1=0, (0.5), 10 ξ_0=0,
6.12-	Moment about z-axis $\|C_{Mz}\|$:magnitude θ_{Mz} :phase	 3.16b 3.16c	0.2, 0.6, 1, 3
6.17a-6.17f	Differential cross section $\sigma(\eta)$	 3.20	θ_I=0°, 45°, 90° η q_1=0.1, 0.2, 0.5, 1, 4, 10 ξ_0=0, 0.2, 0.6, 1

Elliptic cylinder (cont'd)

Figure	Caption	Equation	Parameters
6.17g	Differential cross section and comparison with Burke[10] (underlined)	3.20	θ_I=0°, <u>45°</u>, 90° η q_1=<u>0.227</u> ξ_o=0, 0.2, <u>0.55</u>, 0.6, 1
6.18a-6.18e	Total scattering cross section	3.21	θ_I=0°, (15°), 90° q_1 ξ_o=0, 0.2 0.6, 1, 3
6.19a	Radiation damping coefficient, oscillation in x-direction C_{B1}	5.26a	q_1 ξ_o=0, 0.2 0.6, 1, 3
6.19b	Radiation damping coefficient, oscillation in y-direction C_{B2}	5.27a	

Elliptic cylinder (cont'd)

Figure	Caption	Equation	Parameters
6.19c	Radiation damping coefficient, yawing about z-axis C_{B6}	5.30a	q_1 ξ_o =0, 0.2, 0.6, 1, 3

Semi-elliptic cylinder on a straight coast

Figure	Caption	Equation	Parameters
	x-component force coefficient		$\theta_I = 45°$
7.1	C_{hFx} : magnitude	4.6b	q_1
7.1a	$_{hFx}$: phase	4.6c	ξ_o = 0, 0.2, 0.6
	Moment coefficient about z-axis		
7.2	$\lvert C_{hMz} \rvert$: magnitude	4.8b	
7.2a	θ_{hMz} : phase	4.8c	
7.3	Differential scattering cross section $\sigma_h(\eta)$	4.14	$\theta_I = 45°$ η q_1 = 0.1, 0.5, 2 ξ_o = 0, 0.2, 0.6

Semi-elliptic cylinder on a straight coast (cont'd)

Figure	Caption	Equation	Parameters
7.4	Total scattering cross section Q_h	4.15	$\theta_I = 45^\circ$ $q_1 = 0,$ (0.5), 10 $\xi_0 = 0,$ 0.2, 0.6

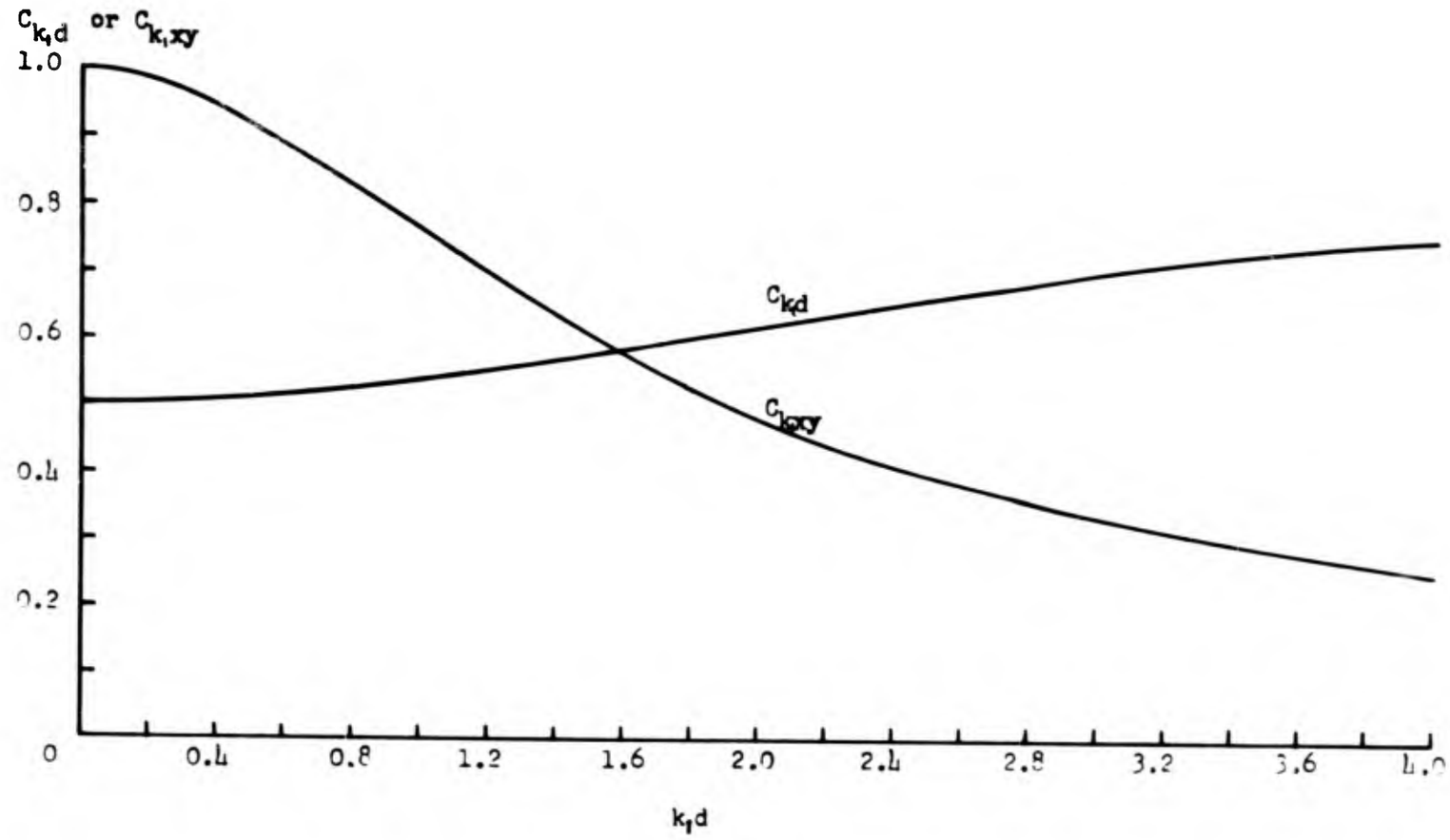

Figure 6.2 Depth factors C_{k_1d} and C_{k_1xy}

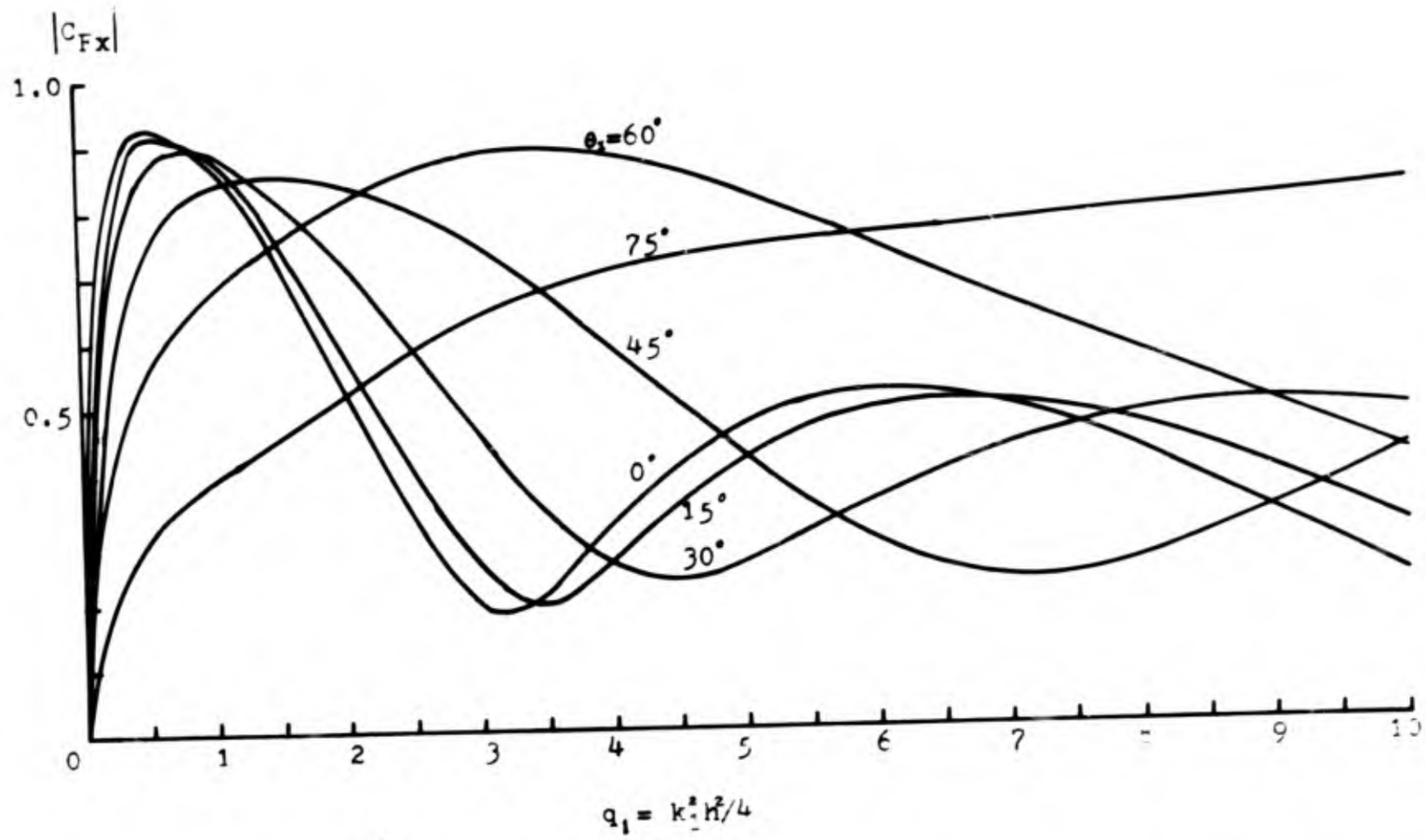

Figure 6.3 The magnitude of x-component force coefficient for γ_0=0.1 (b/a=0.197) and for various incident wave angles θ_1.

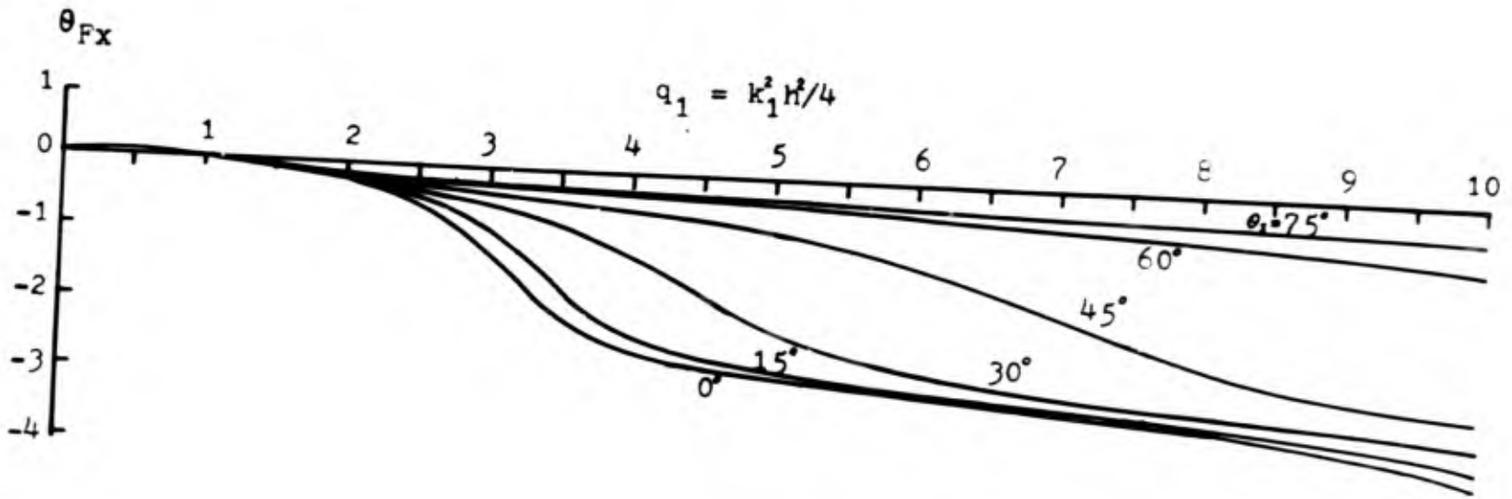

Figure 6.3a The phase of x-component force coefficient for ξ_0=0.2 and for various incident wave angles θ_1.

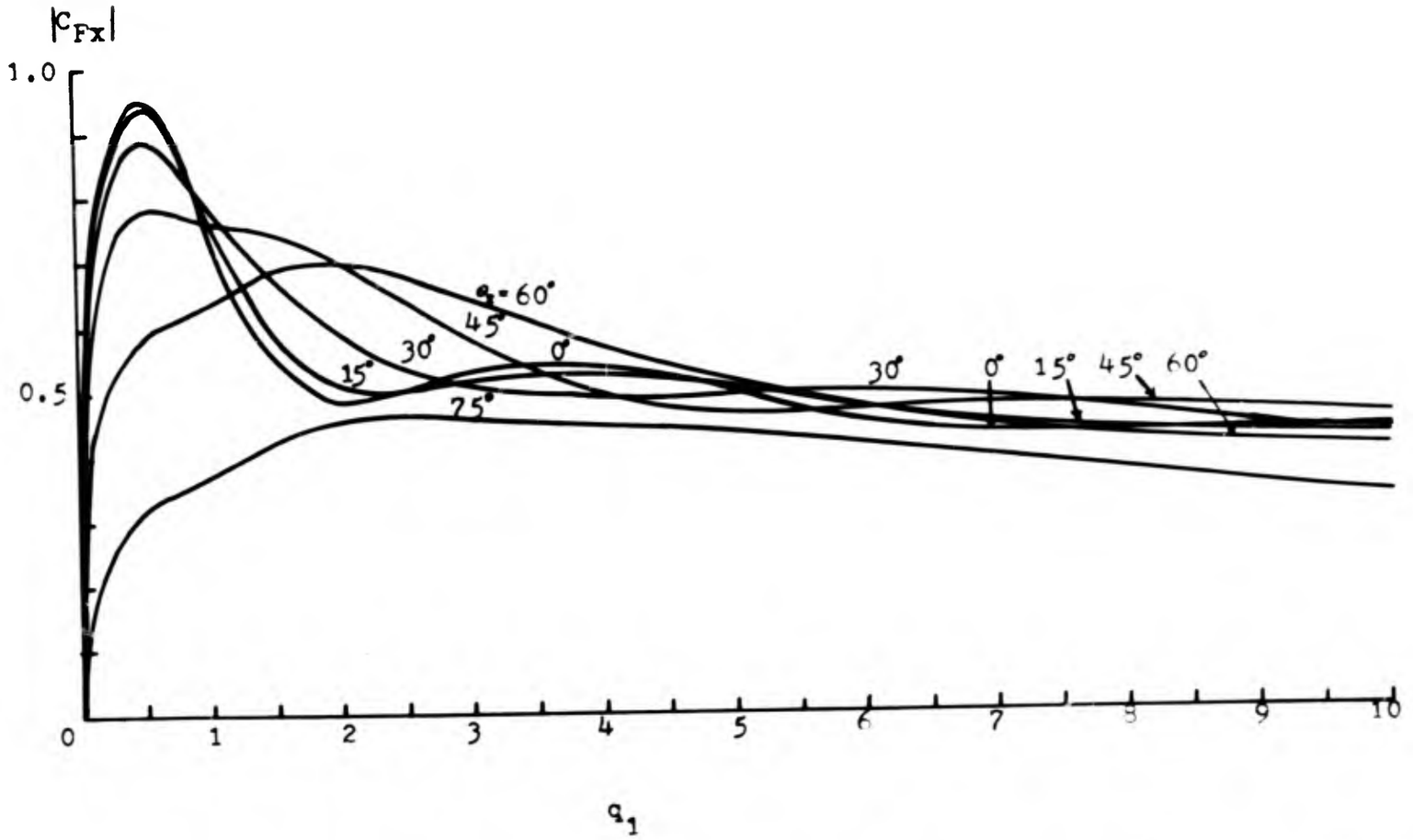

Figure 6.4 The magnitude of x-component force coefficient for γ_s=0.6 (b/a=0.537) and for various incident wave angles θ_1.

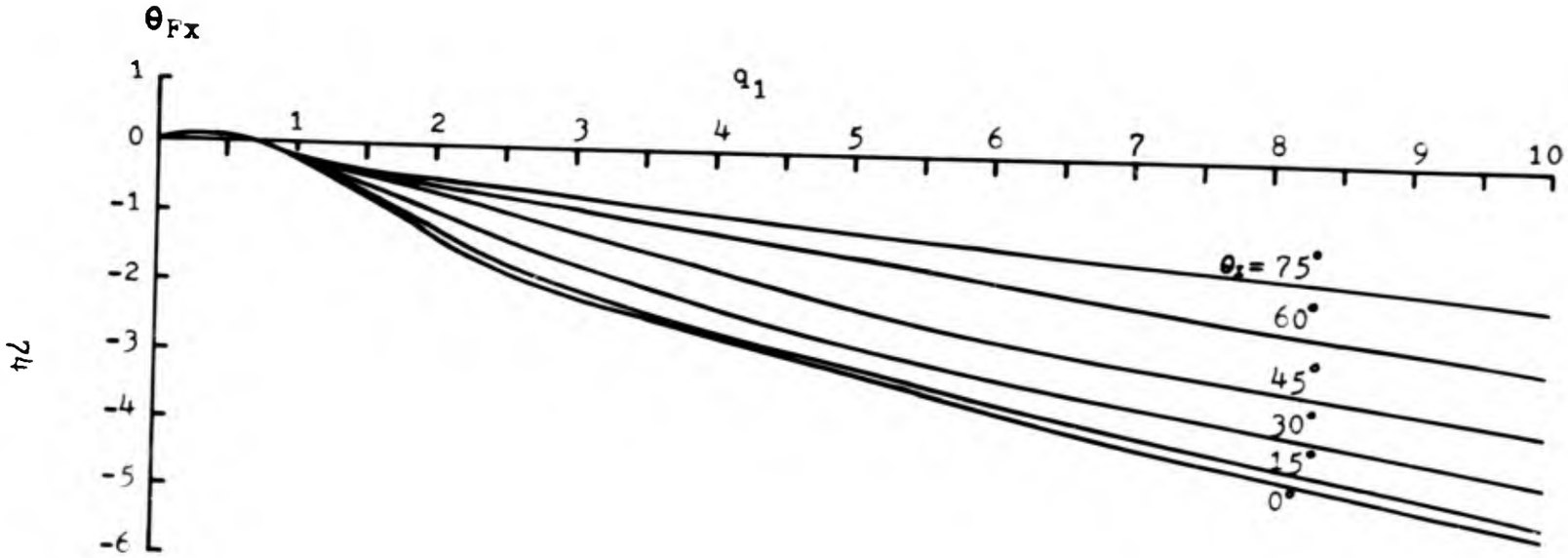

Figure 6.4a The phase of x-component force coefficient for ξ_0=0.6 and for various incident wave angles θ_I.

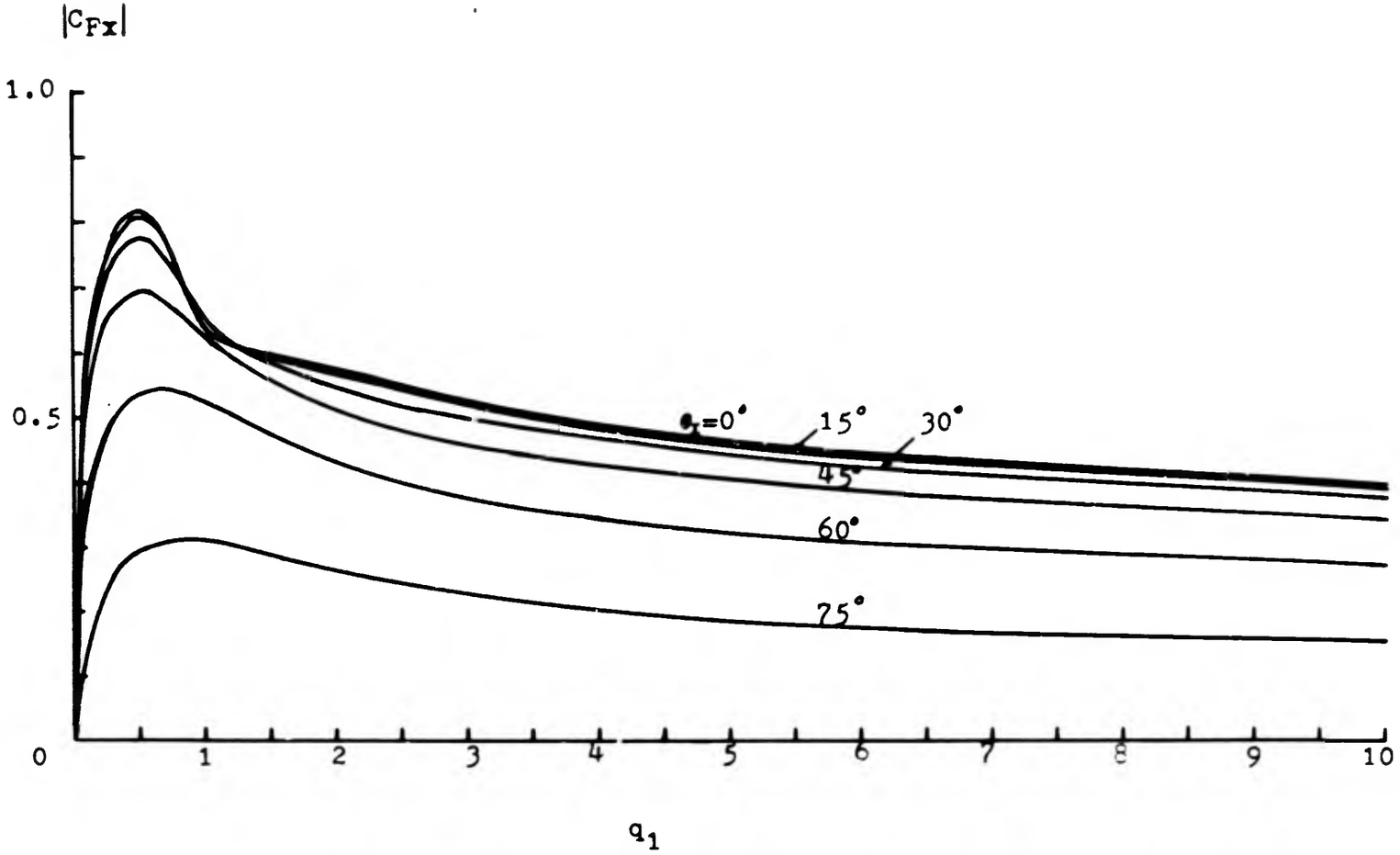

Figure 6.5 The magnitude of x-component force coefficient for ξ_∞=1.0 (b/a=0.762) and for various incident wave angles θ_i.

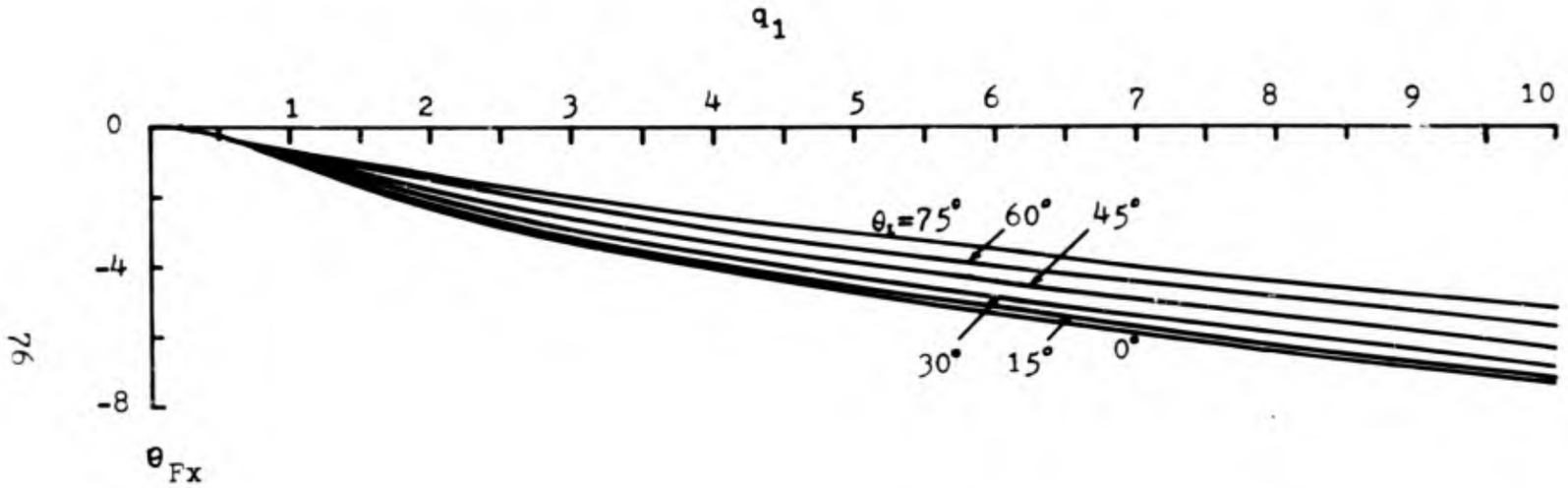

Figure 6.5a The phase of x-component force coefficient for ξ_0=1.0 and for various incident wave angles θ_r.

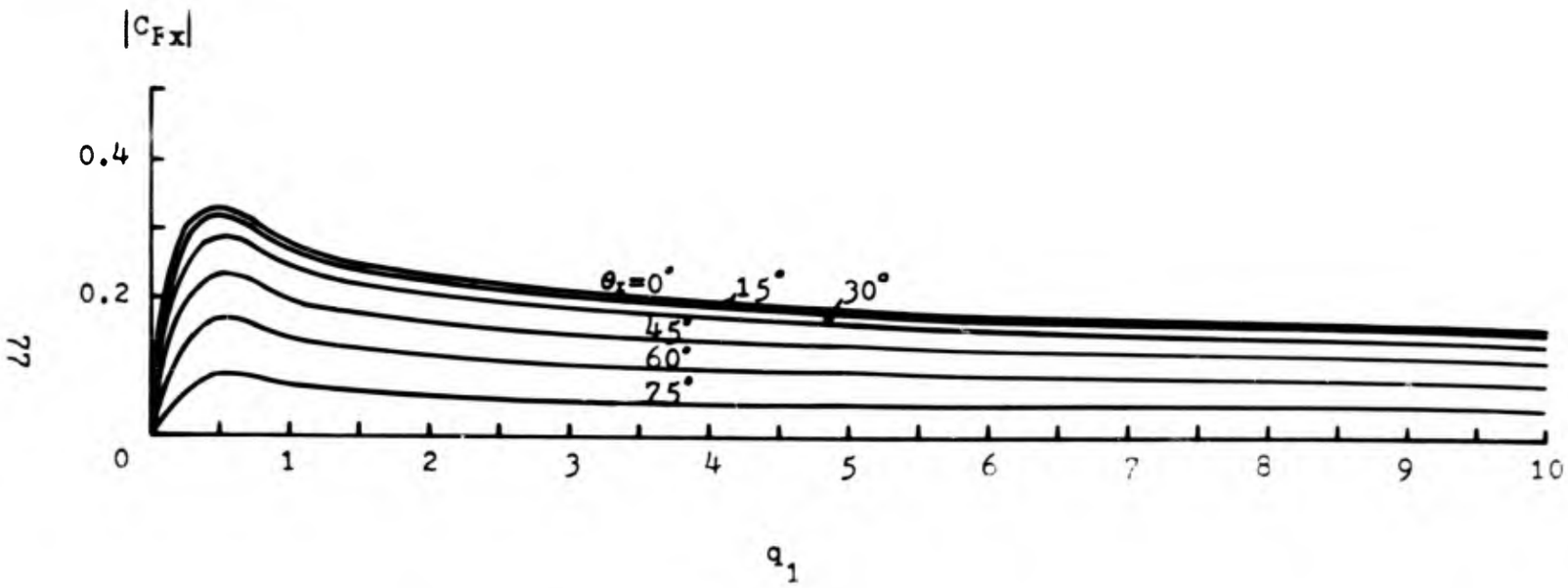

Figure 6.6 The magnitude of x-component force coefficient for ξ_0=3.0 (b/a=0.995) and for various incident wave angles θ_i.

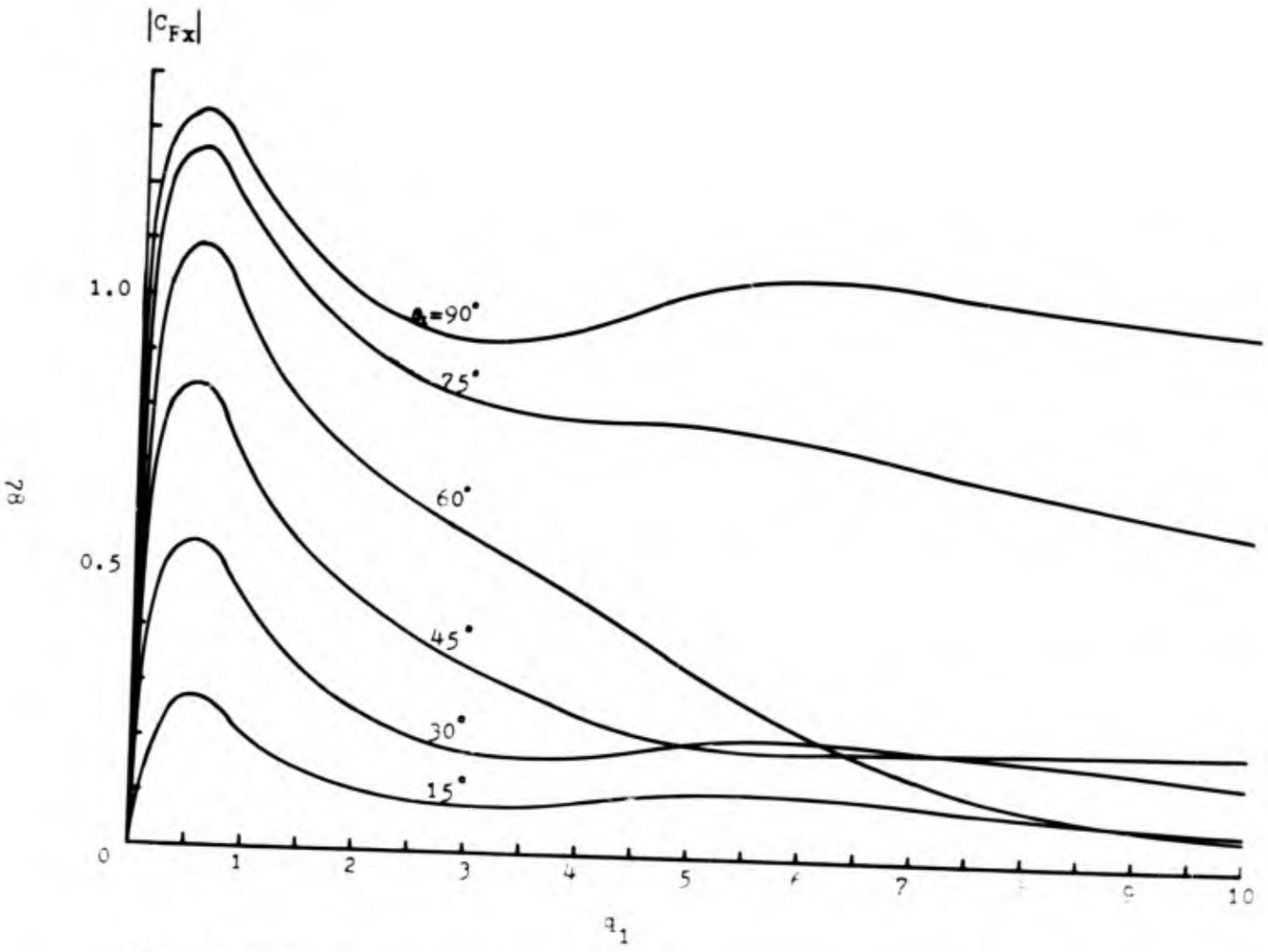

Figure 4.7 The magnitude of y-component force coefficient for ξ_0=0.0 (b/a=0) and for various incident wave angles θ_1.

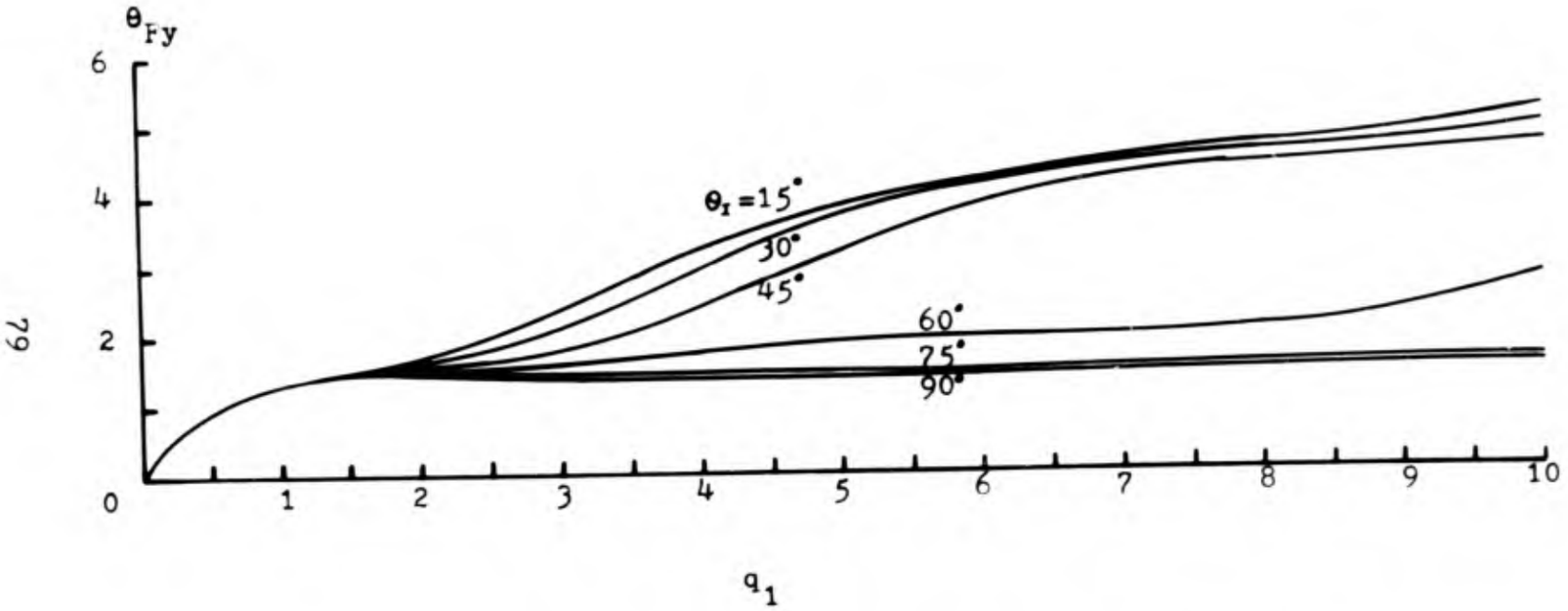

Figure 6.7a The phase of y-component force coefficient for ξ_0=0.0 and for various incident wave angles θ_I.

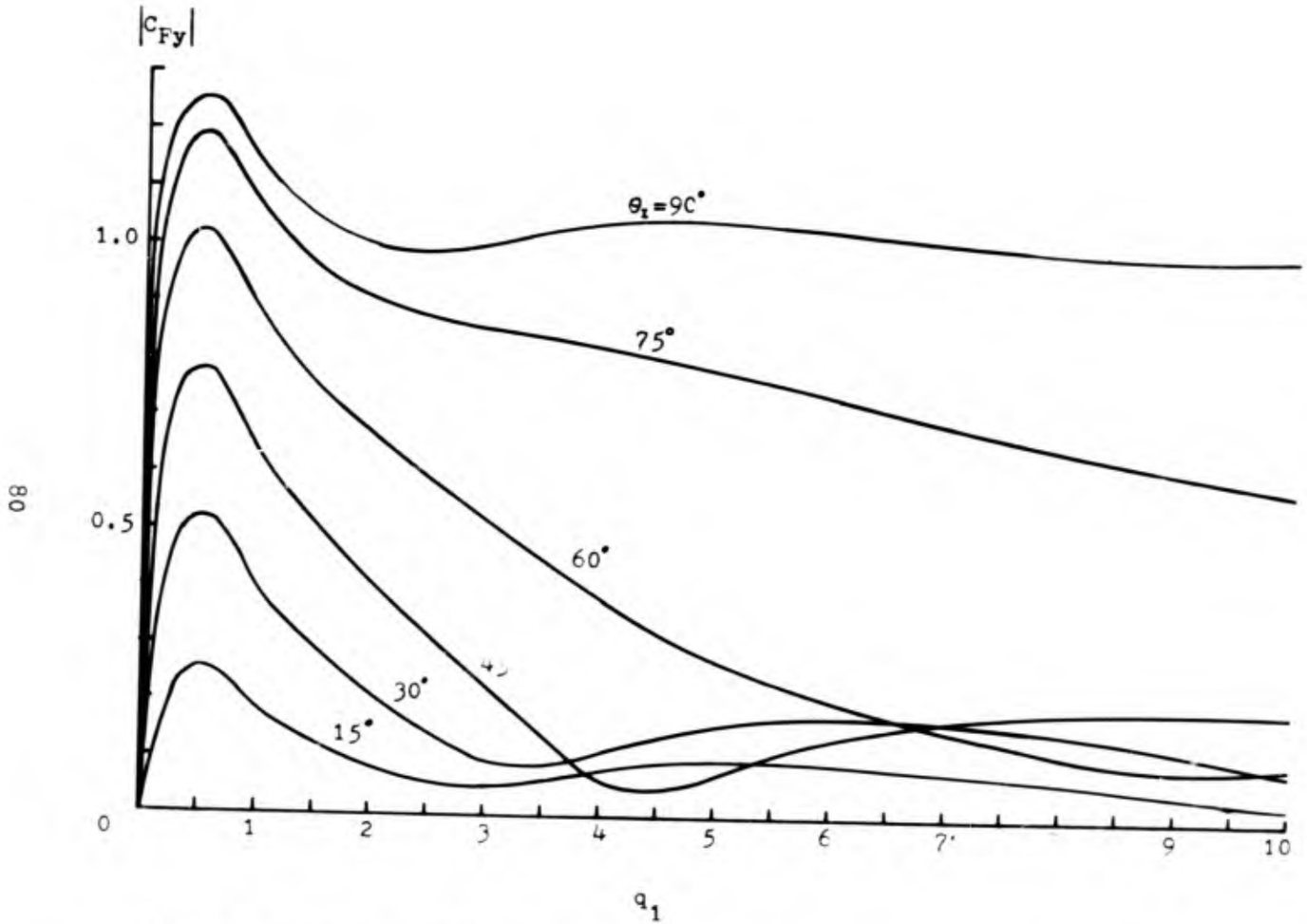

Figure 6.8 The magnitude of y-component force coefficient for γ_e=0.2 (b/a=0.197) and for various incident wave angles θ_i.

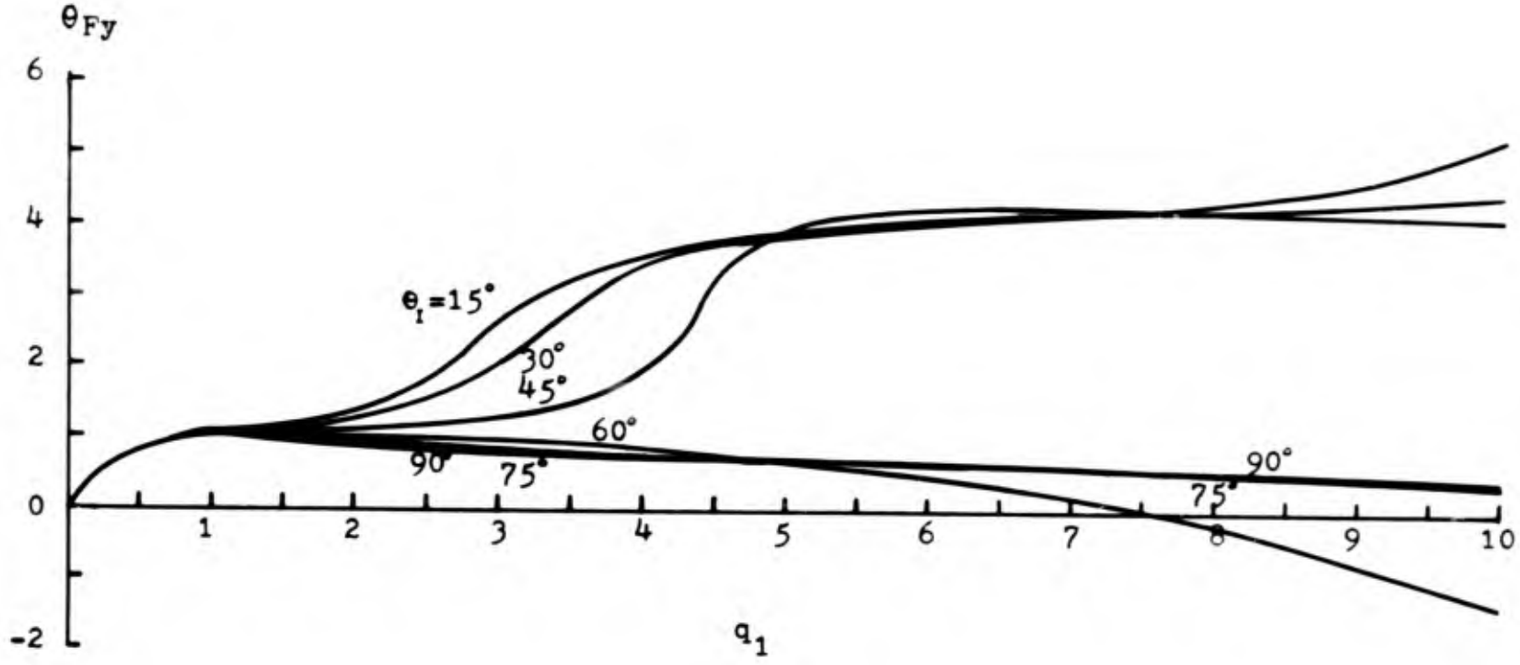

Figure 6.8a The phase of y-component force coefficient for ξ_0=0.2 and for various incident wave angles θ_I.

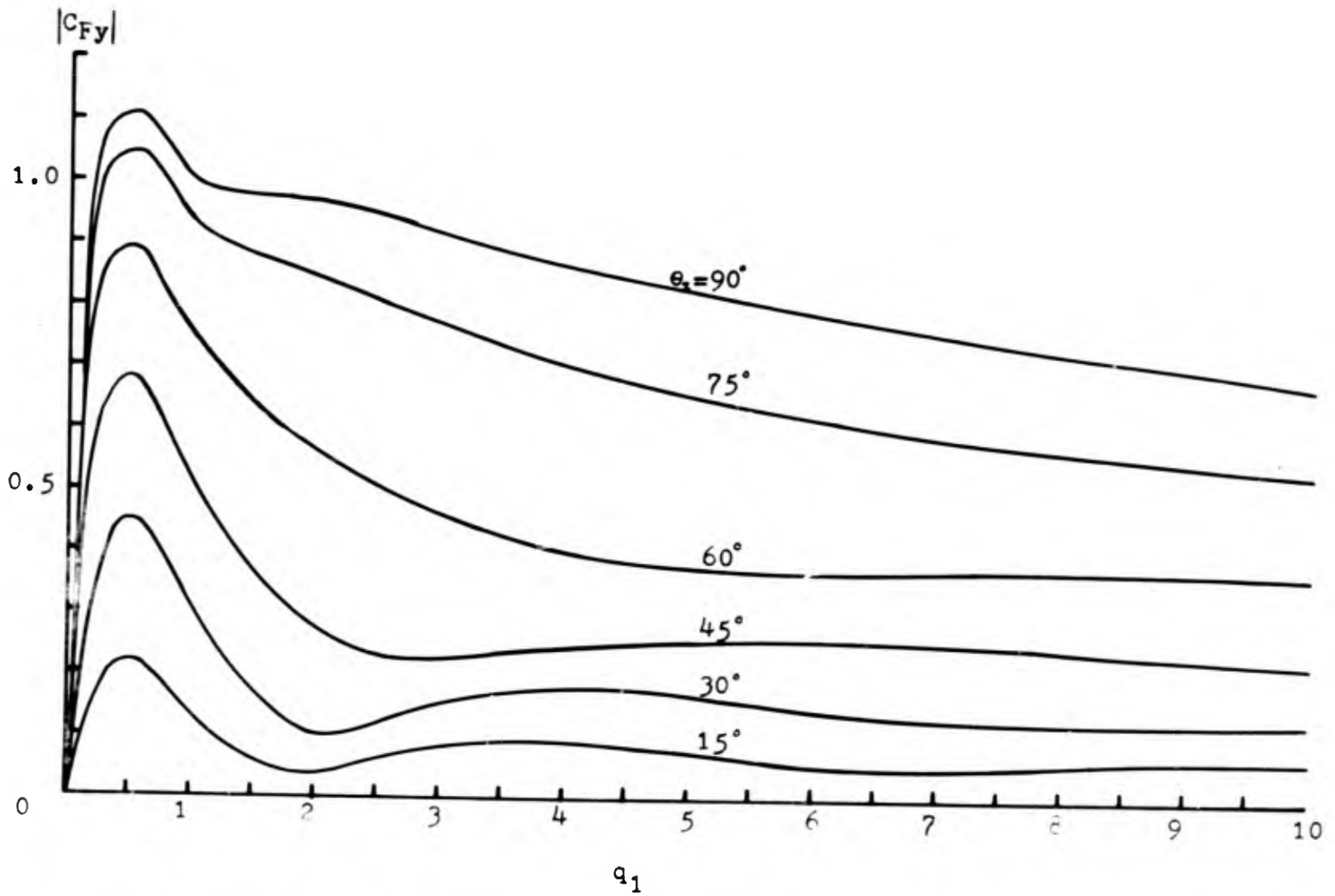

Figure 6.9 The magnitude of y-component force coefficient for ξ_o=0.6 (b/a=0.537) and for various incident wave angles θ_i.

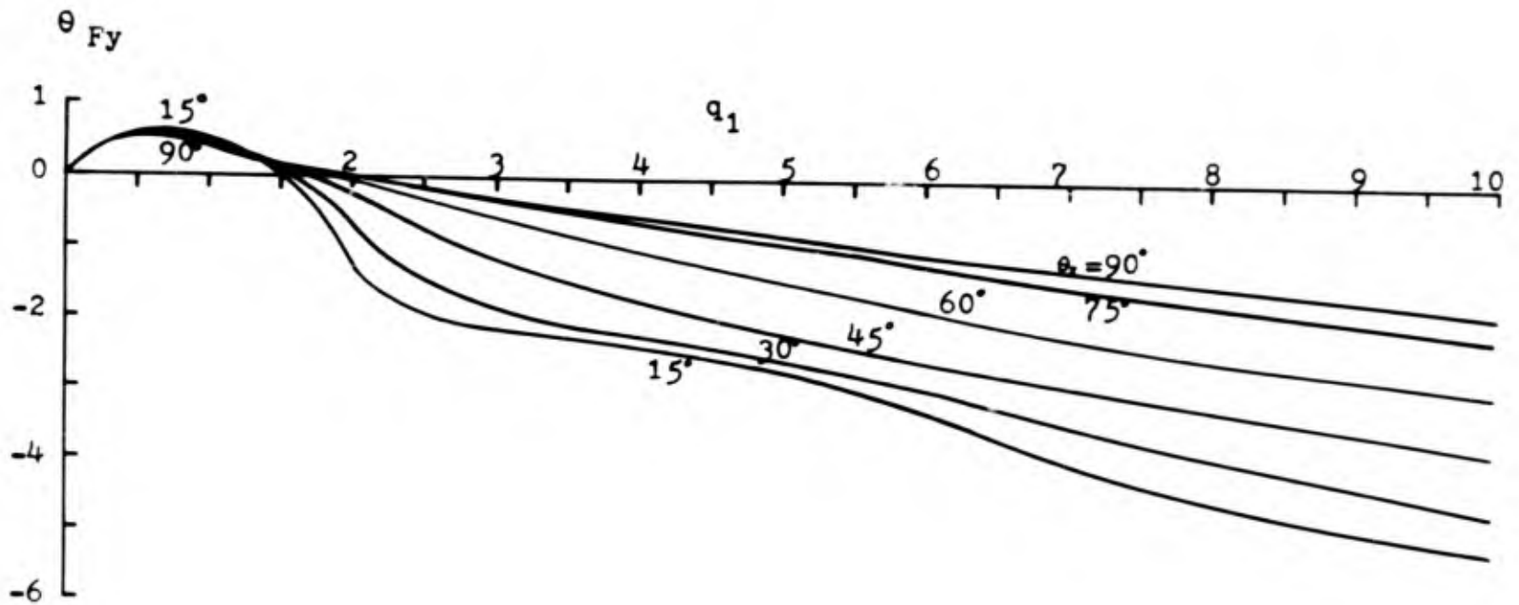

Figure 6.9a The phase of y-component force coefficient for ξ_0=0.6 and for various incident wave angles θ_I.

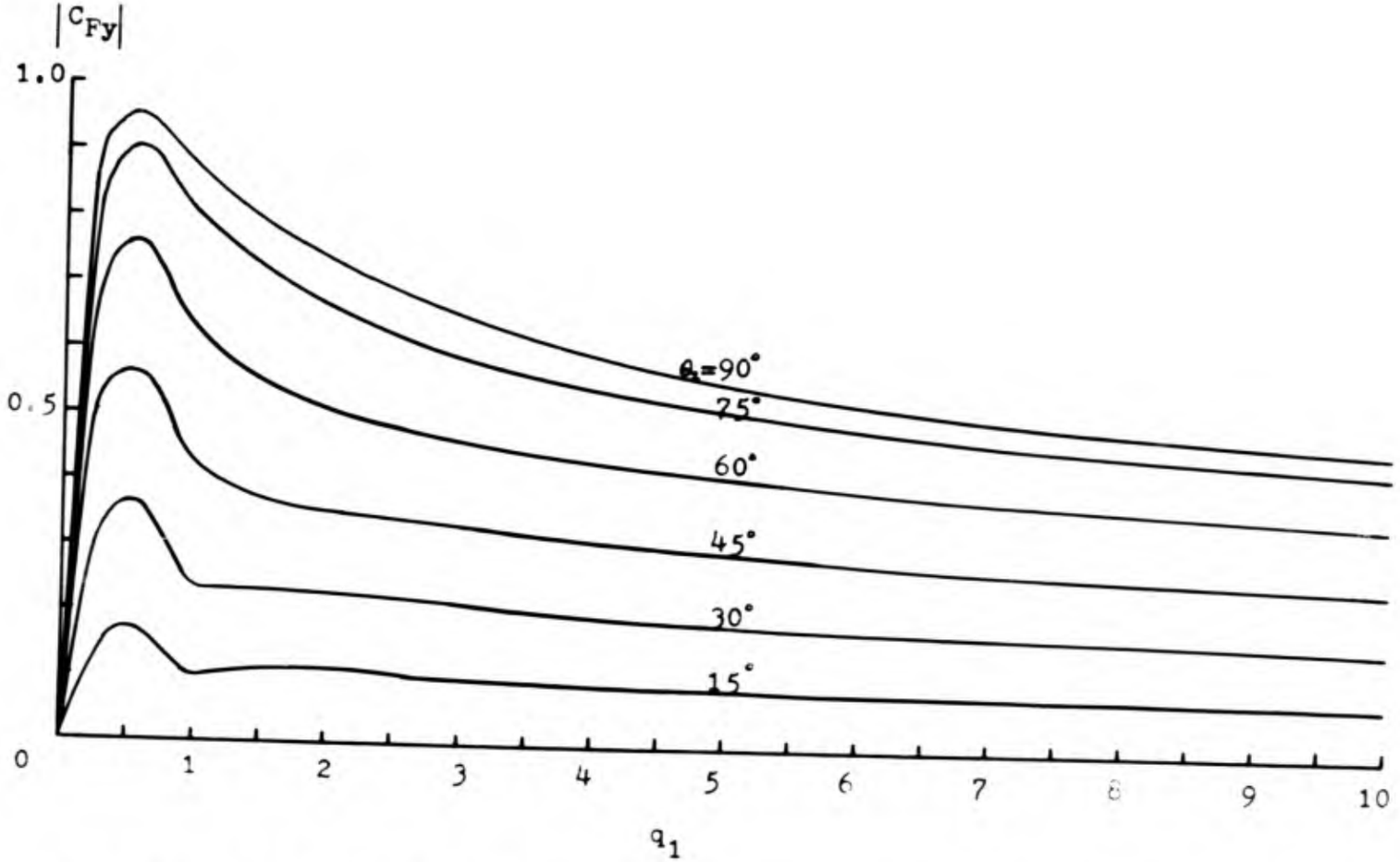

Figure 6.10 The magnitude of y-component force coefficient for f_c=1.0 (b/a=0.762) and for various incident wave angles θ_i.

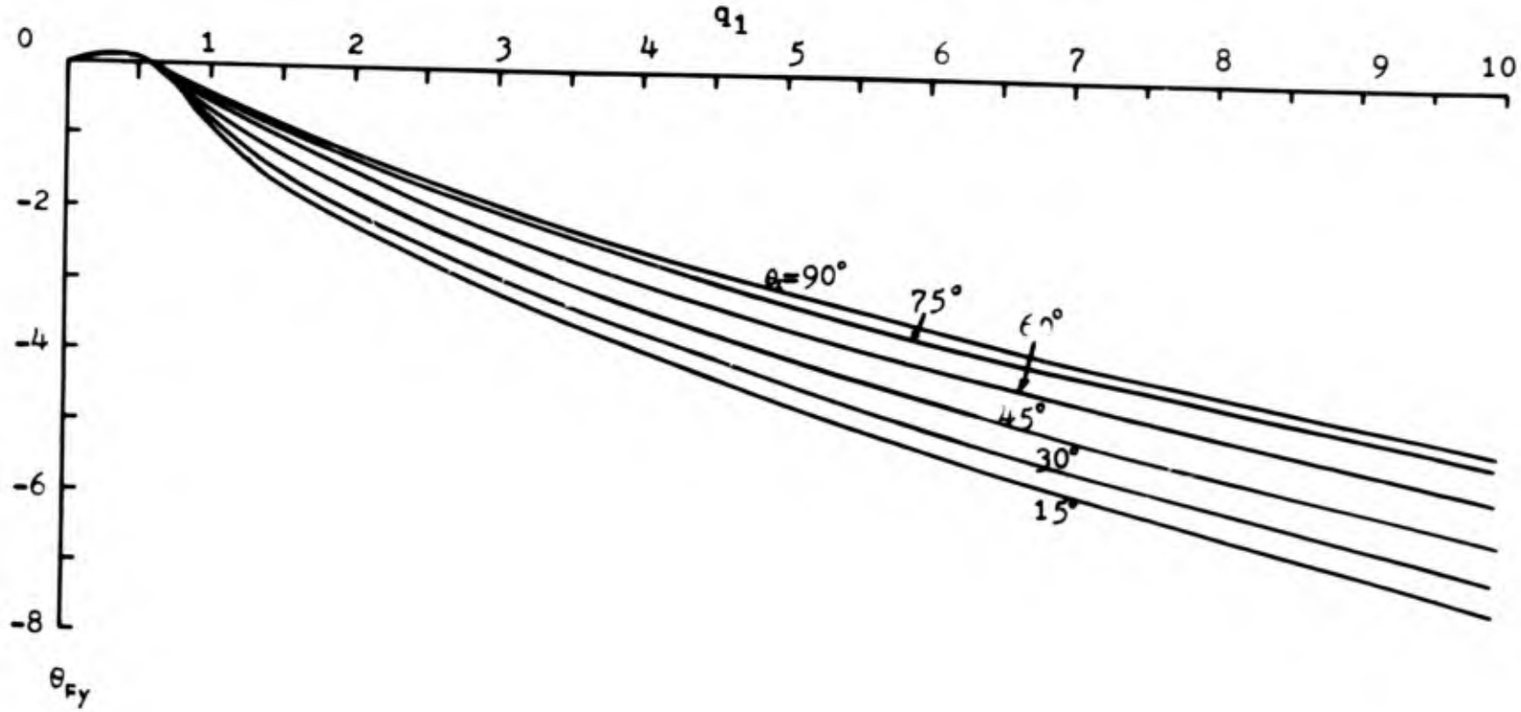

Figure 6.10a The phase of y-component force coefficient for r_0=1.0 and for various incident wave angles θ_i.

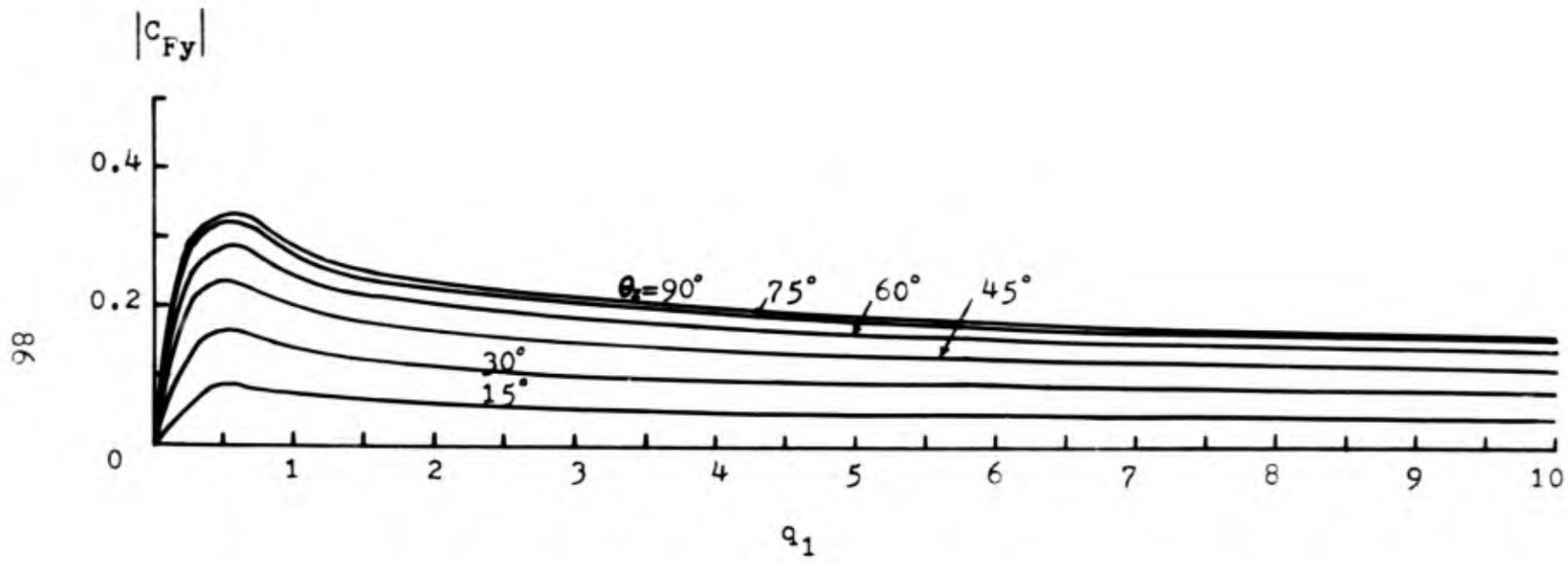

Figure 6.11 The magnitude of y-component force coefficient for ξ_0=3.0 (b/a=0.995) and for various incident wave angles θ_1.

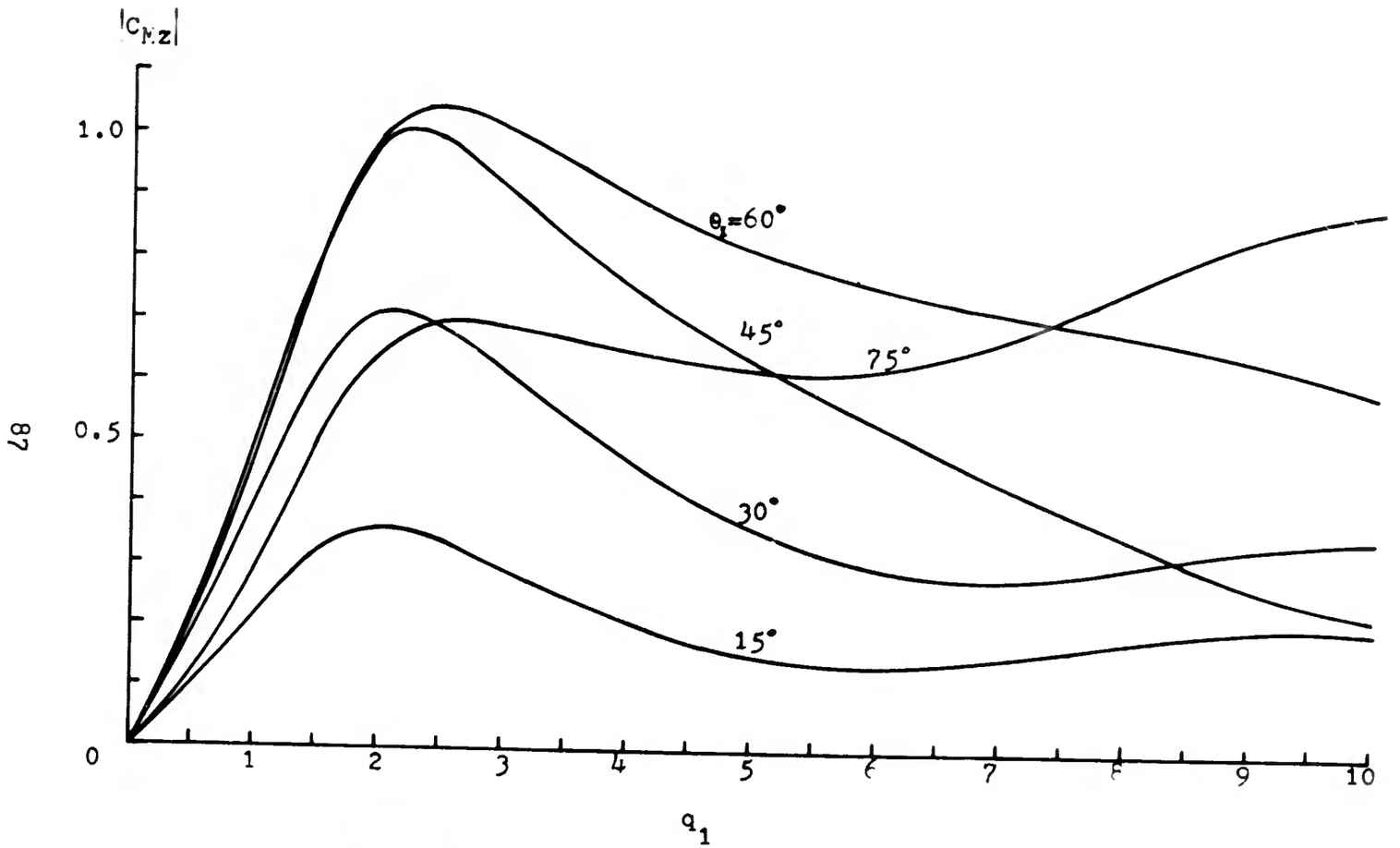

Figure 6.12 The magnitude of coefficient of moment about z-axis for ξ_0=0.0 (b/a=0.0) and for various incident wave angles θ_i.

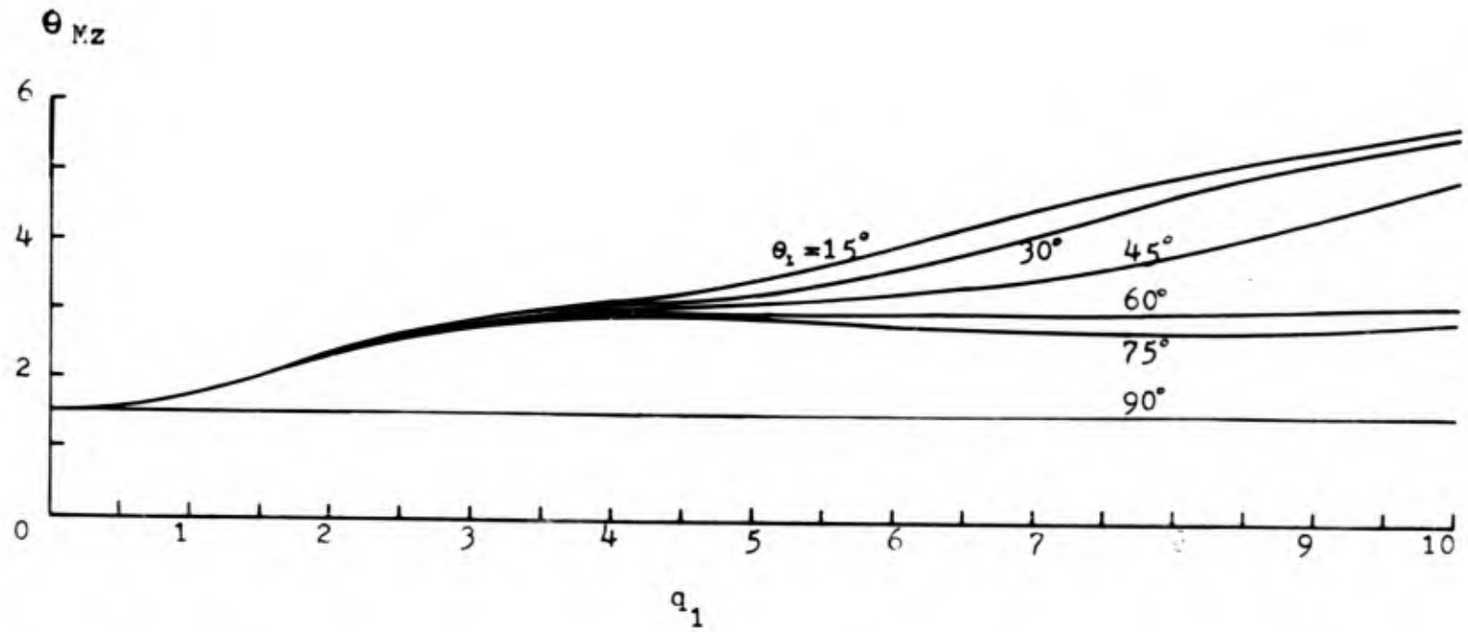

Figure 6.12a The phase of coefficient of moment about z-axis for ξ_o=0.0 and for various incident wave angles θ_1.

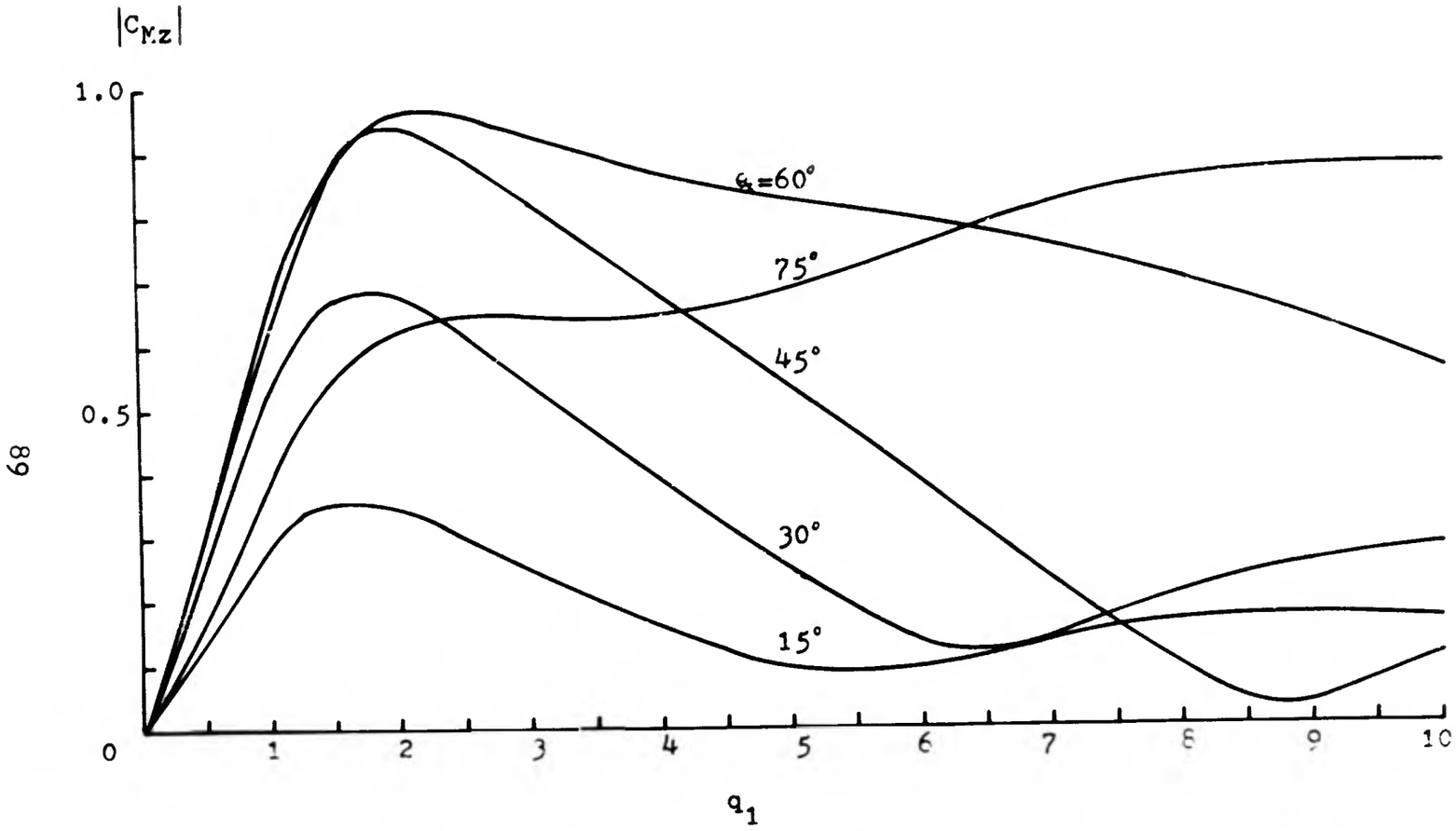

Figure 6.13 The magnitude of coefficient of moment about z-axis for ξ_0=0.2 (b/a=0.197) and for various incident wave angles θ_1.

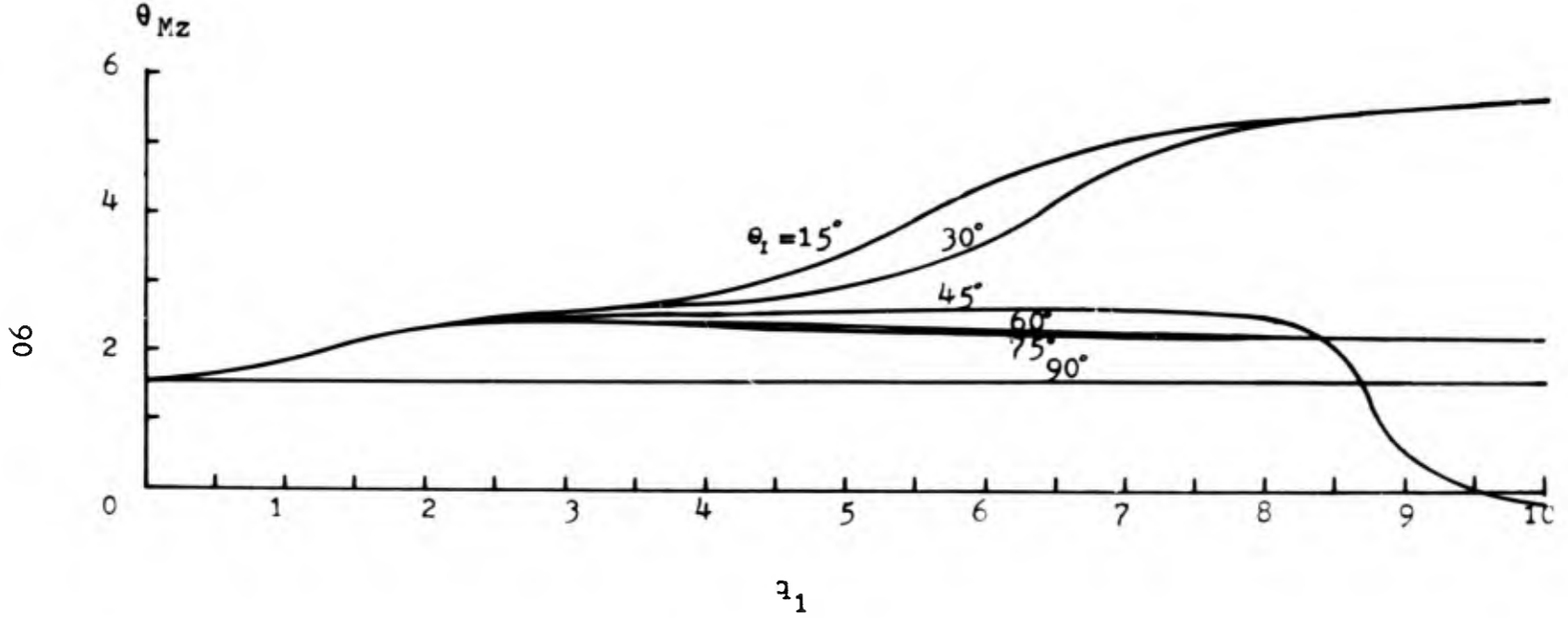

Figure 6.13a The phase of coefficient of moment about z-axis for ξ_0=0.2 and for various incident wave angles θ_I.

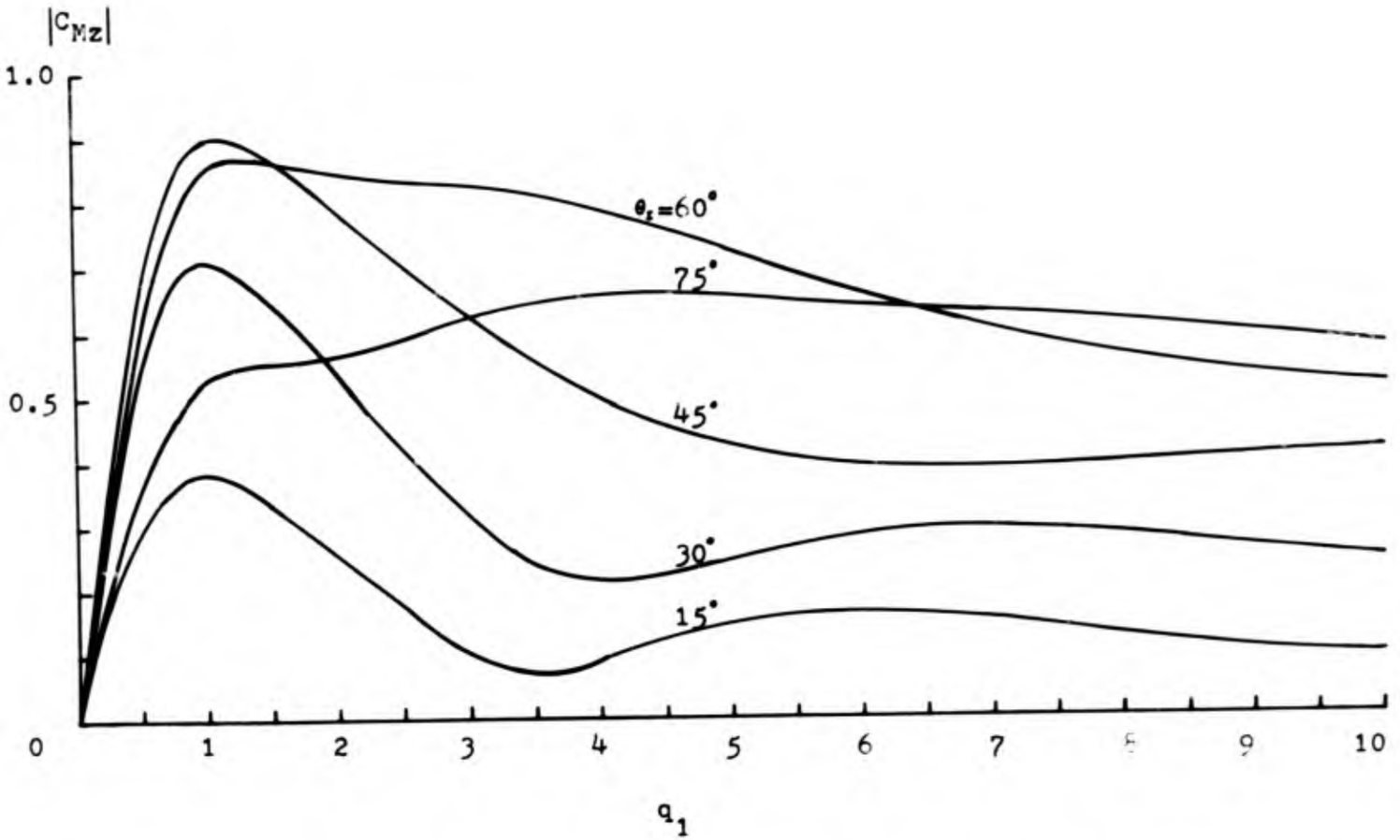

Figure 6.14 The magnitude of coefficient of moment about z-axis for ξ_0=0.6 (b/a=0.537) and for various incident wave angles θ_i.

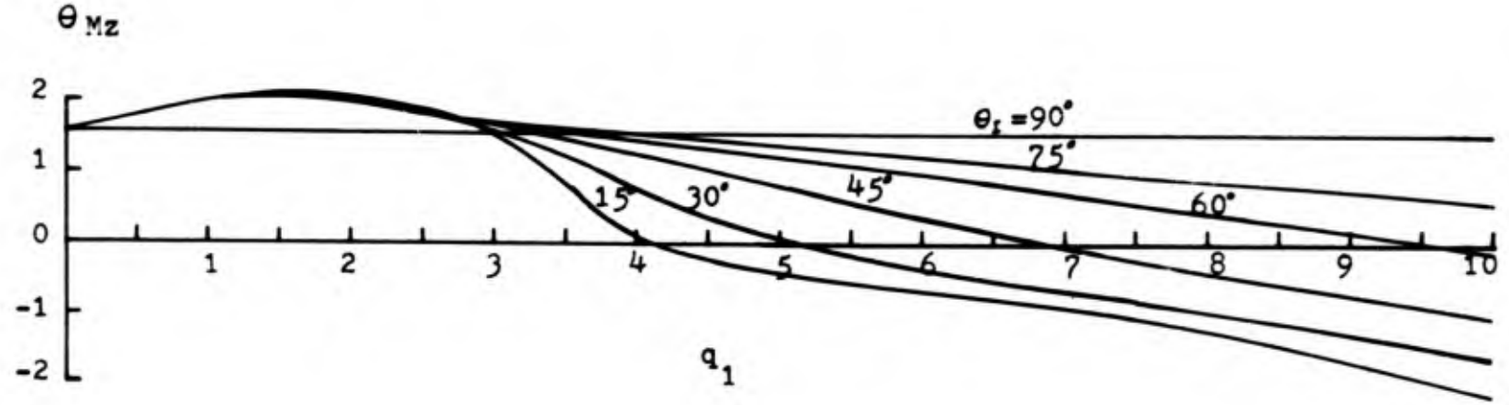

Figure 6.14a The phase of coefficient of moment about z-axis for ξ_0=0.6 and for various incident wave angles θ_i.

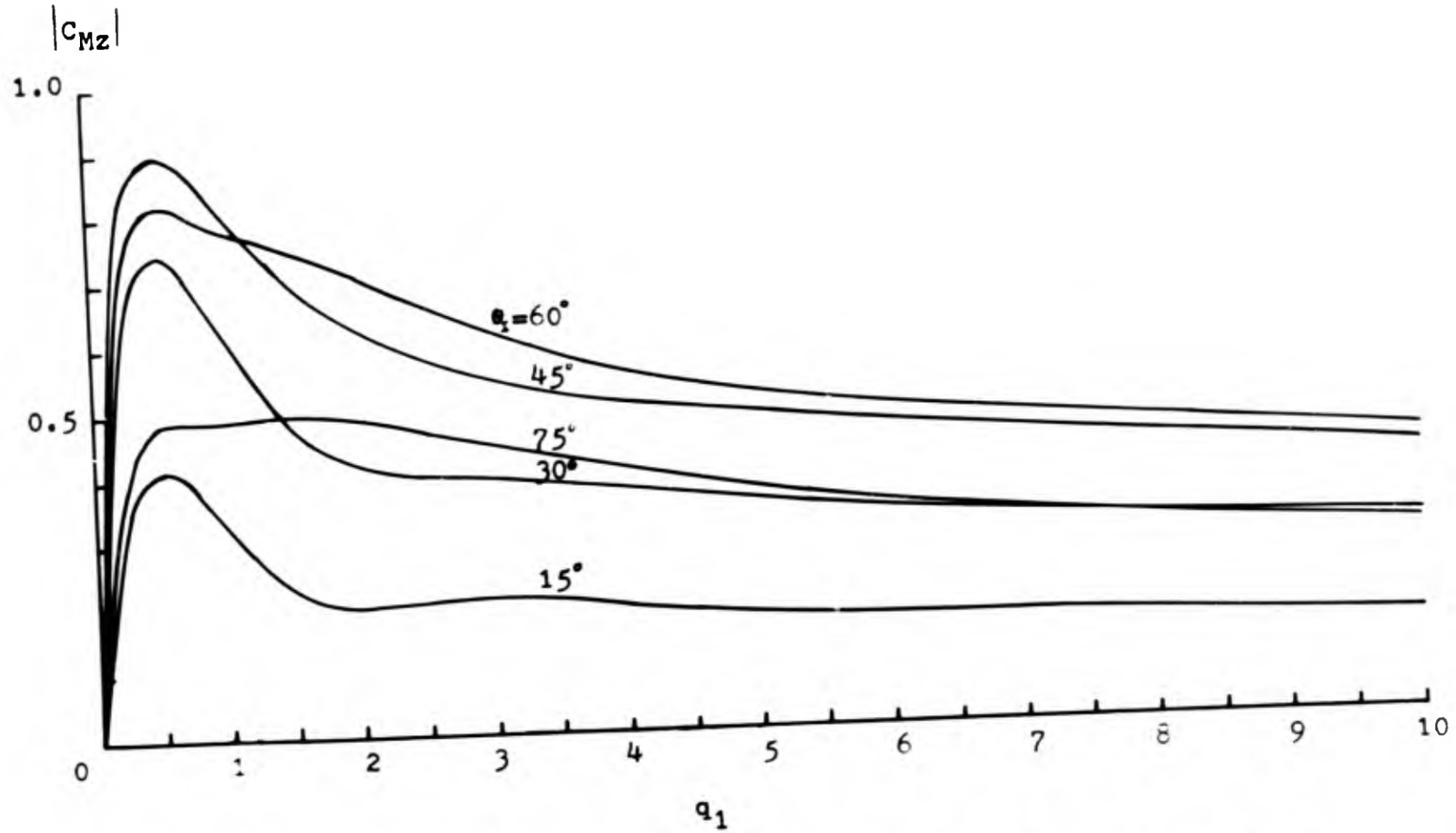

Figure 6.15 The magnitude of coefficient of moment about z-axis for ξ_0=1.0 (b/a=0.762) and for various incident wave angles θ_1.

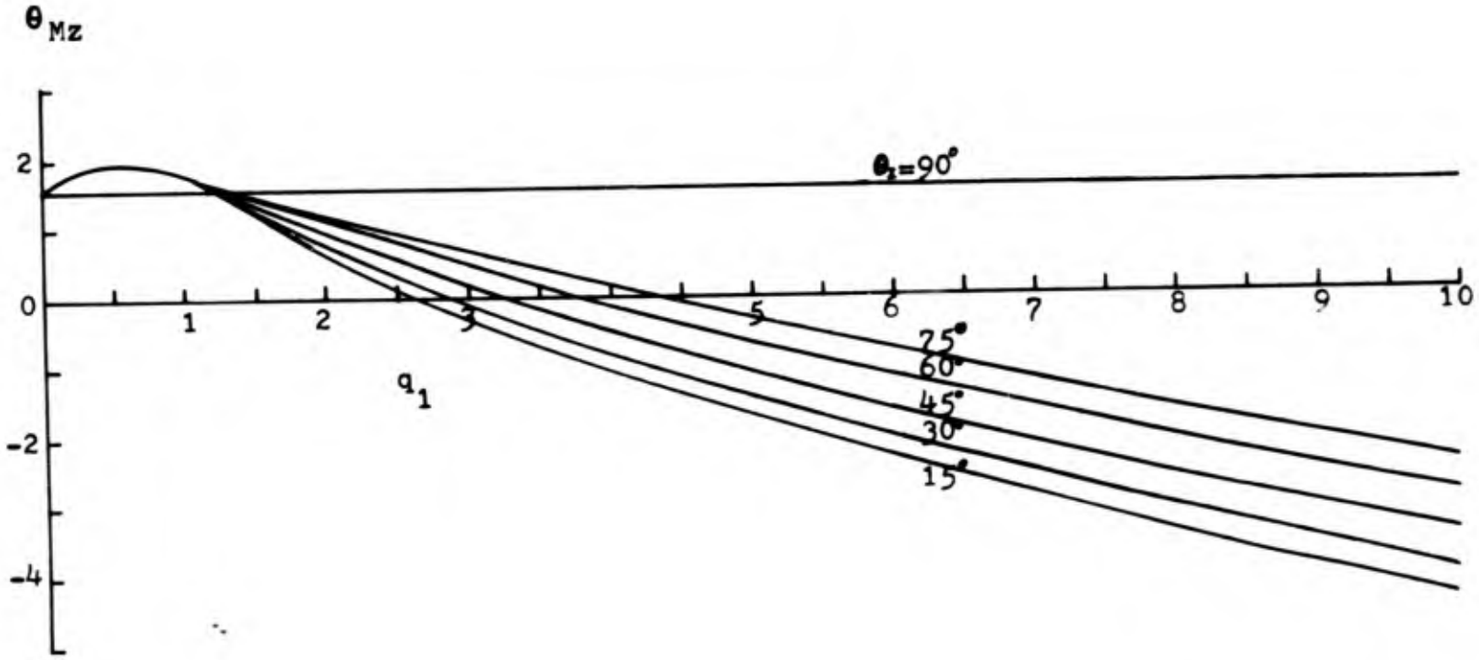

Figure 6.15a The phase of coefficient of moment about z-axis for ξ_o=1.0 and for various incident wave angles θ_r.

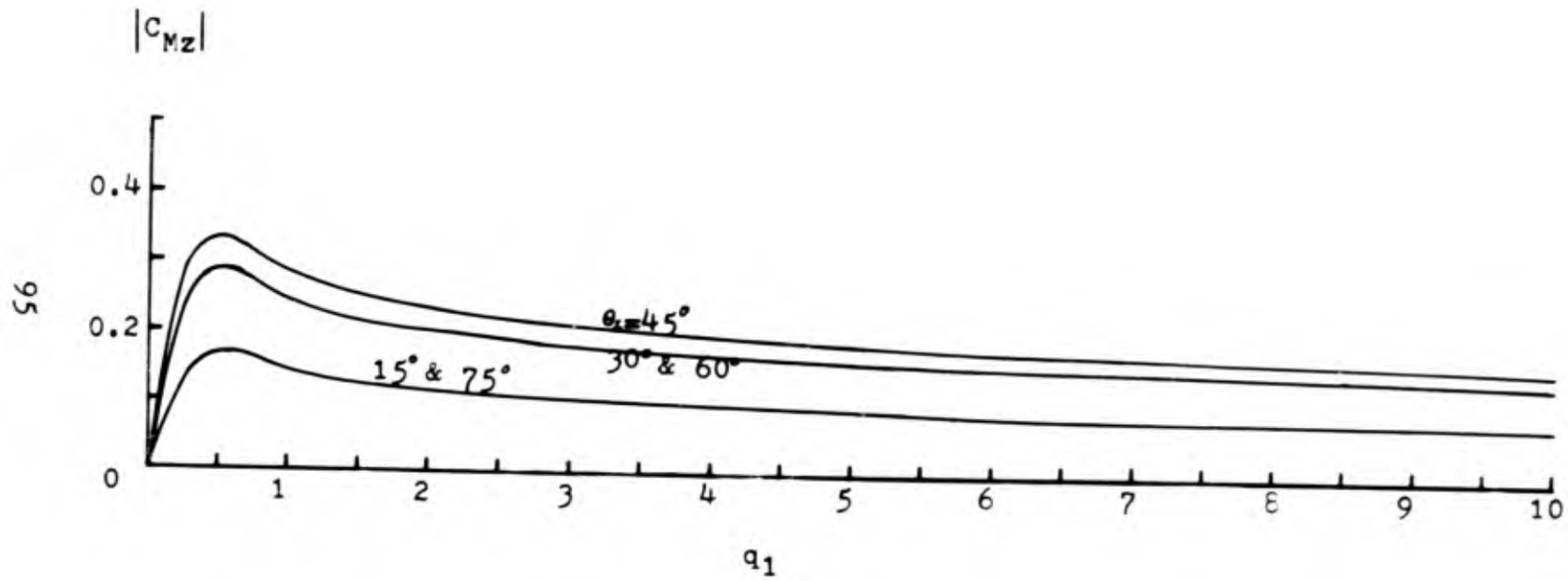

Figure 6.16 The magnitude of coefficient of moment about z-axis for γ_o=3.0 (b/a=0.995) and for various incident wave angles θ_I.

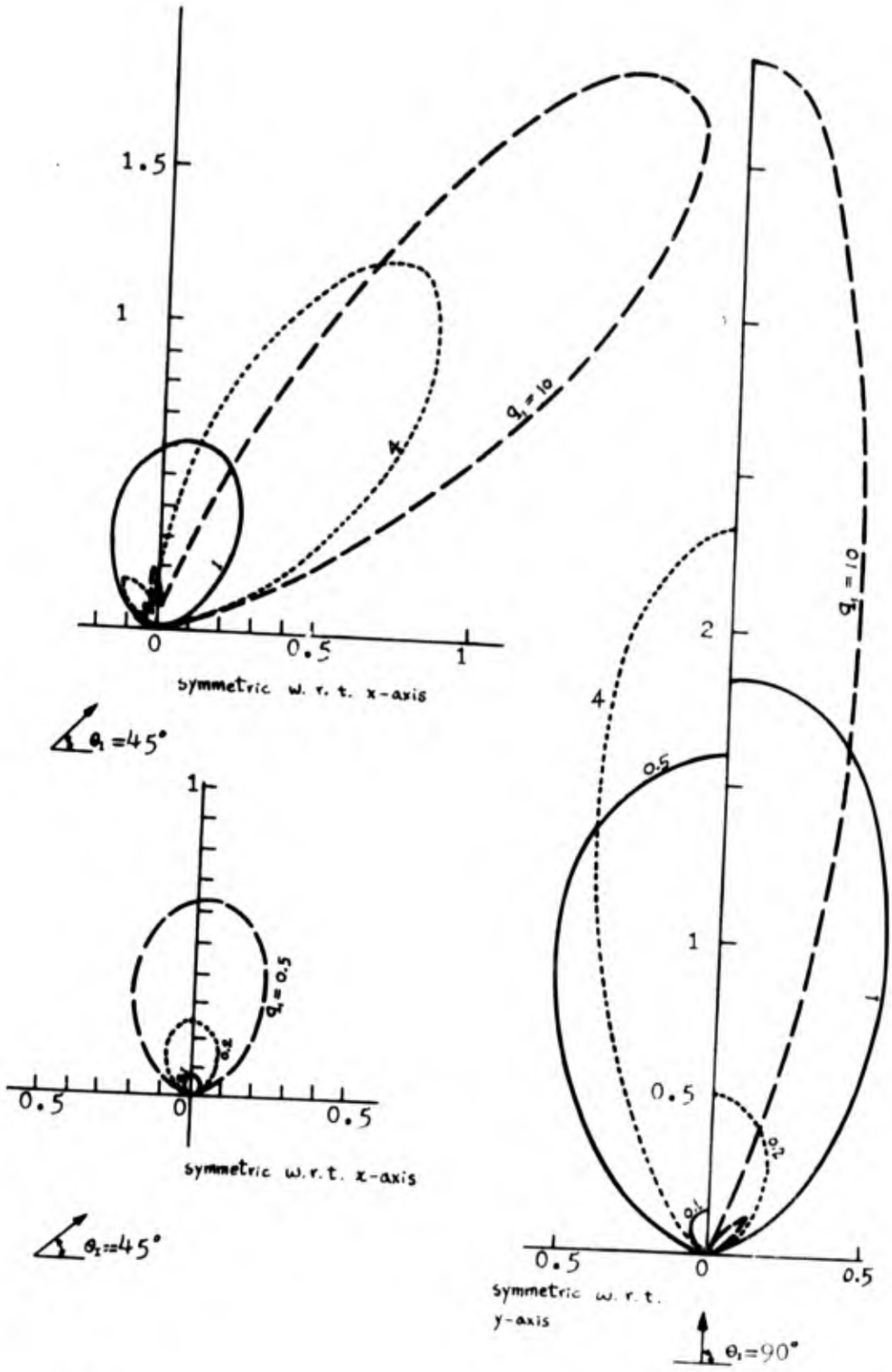

Figure 6.17a Differential cross section of a thin plate barrier, $\xi_0=0$.

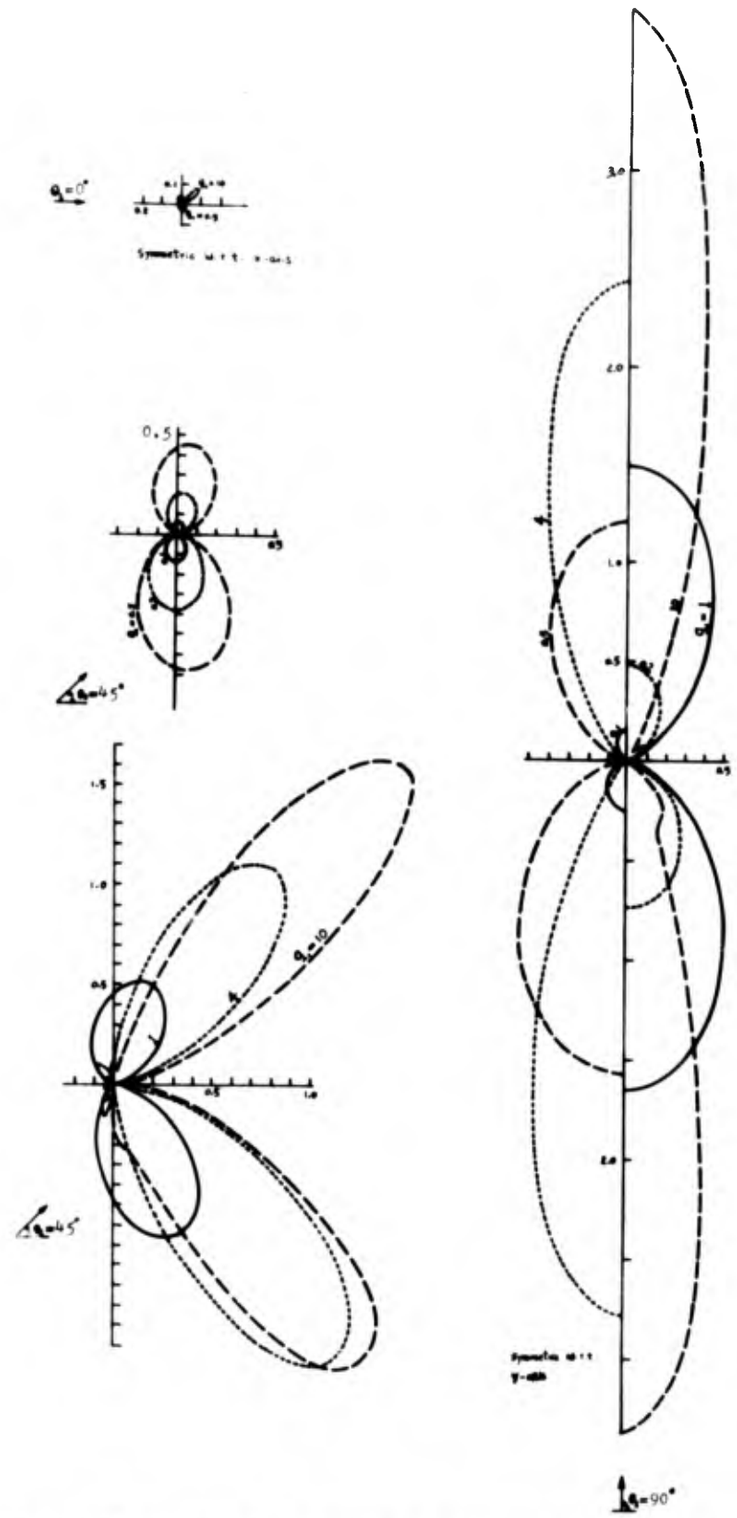

Figure 7.17b Differential cross section of an elliptic cylinder of $\xi=0.2$.

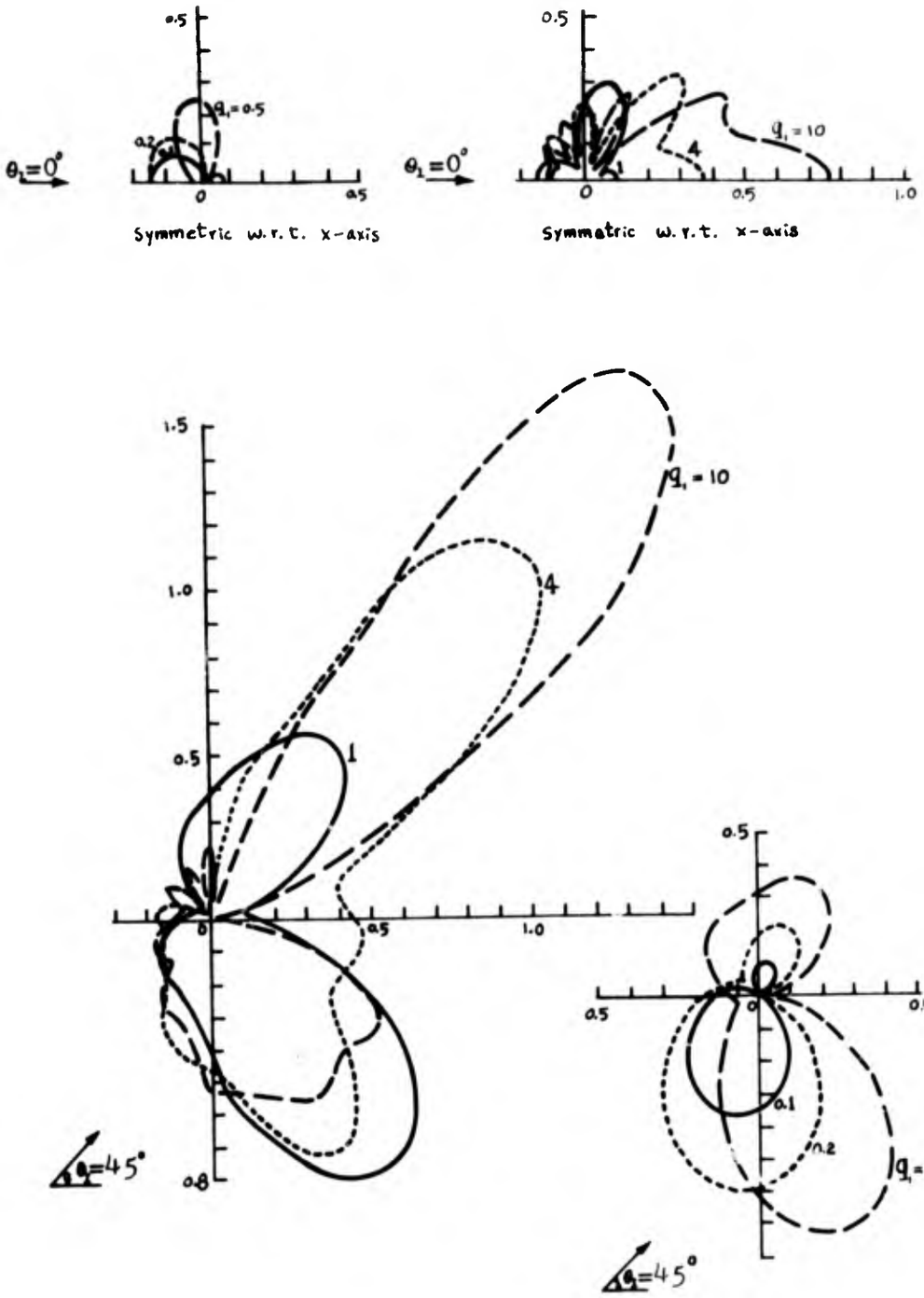

Figure 6.17c Differential cross section of an elliptic cylinder of $\frac{b}{a}$=0.6.

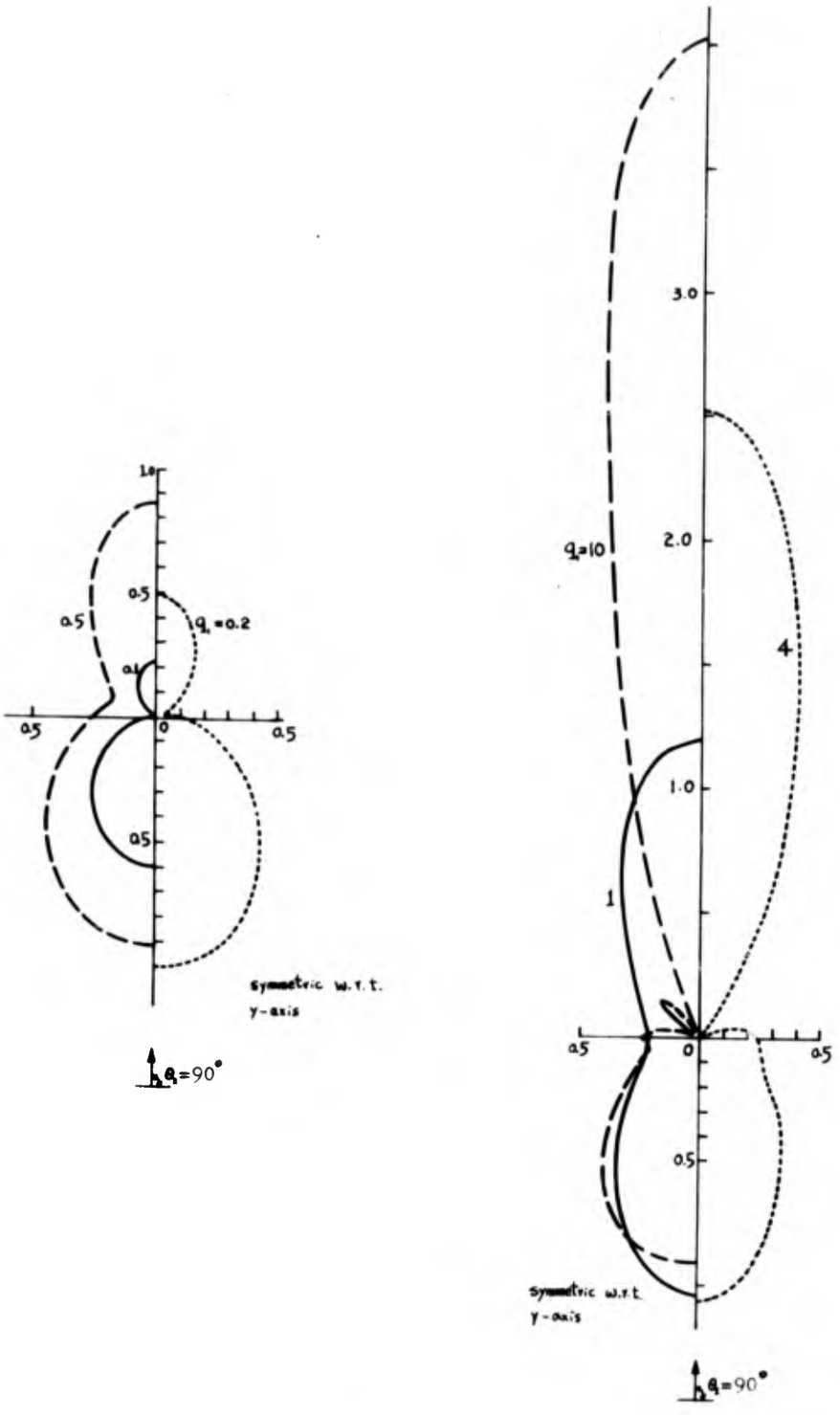

Figure 6.17d Differential cross section of an elliptic cylinder of $\xi_0=0.6$.

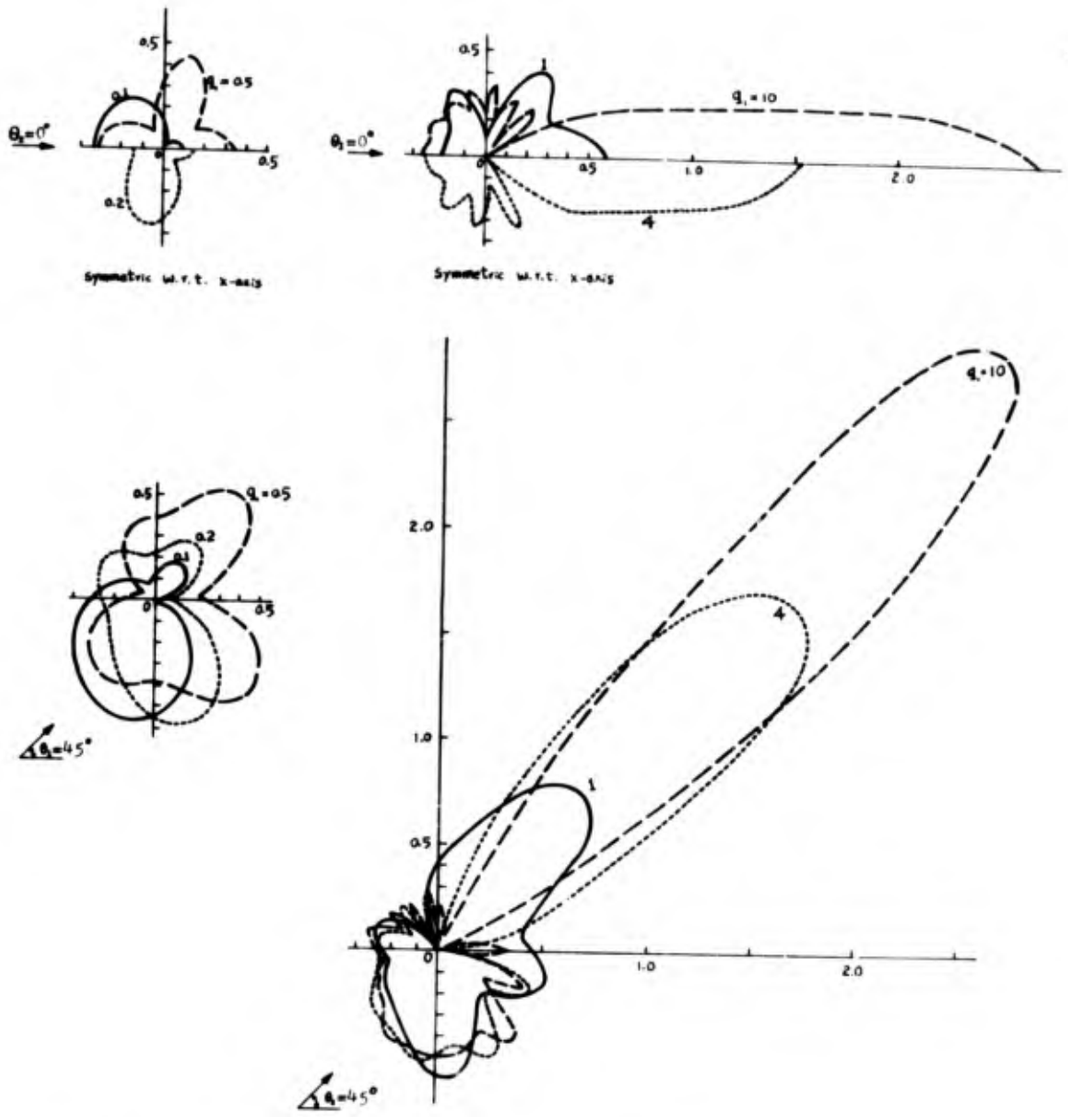

Figure 7.17e Differential cross section of an elliptic cylinder of $\xi_0=1.0$.

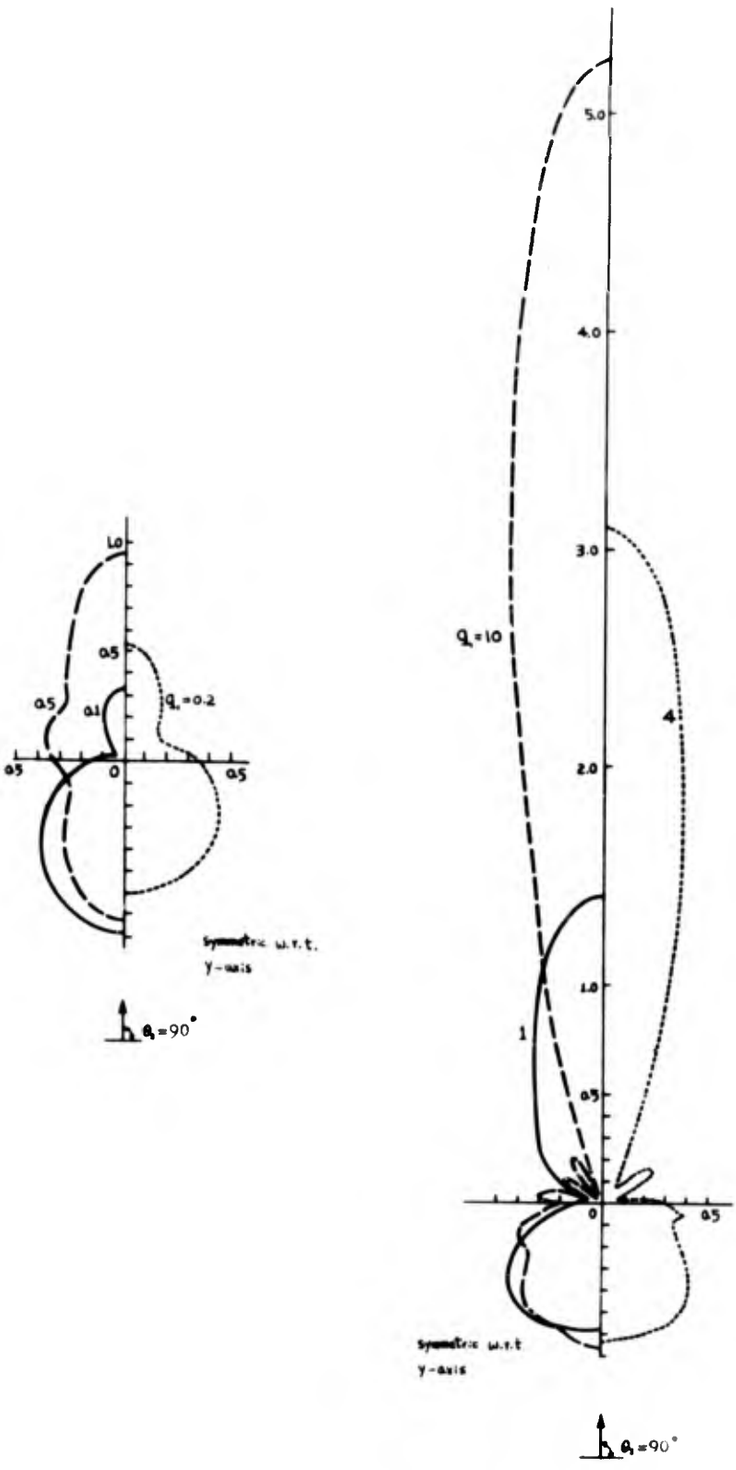

Figure 6.12f Differential cross section of an elliptic cylinder of χ=1.0.

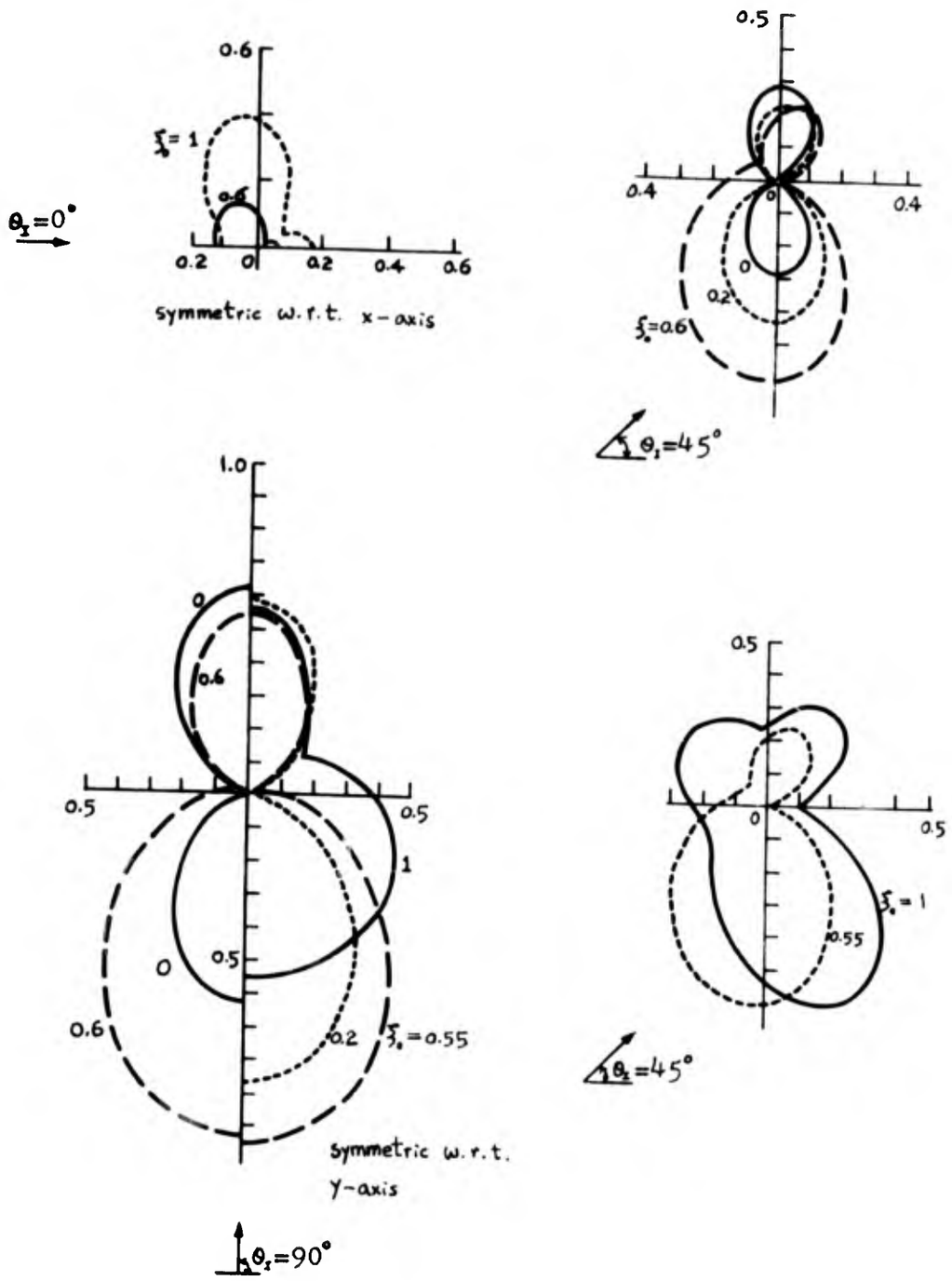

Figure 6.17g Differential cross section of an elliptic cylinder with q_1=0.2267.

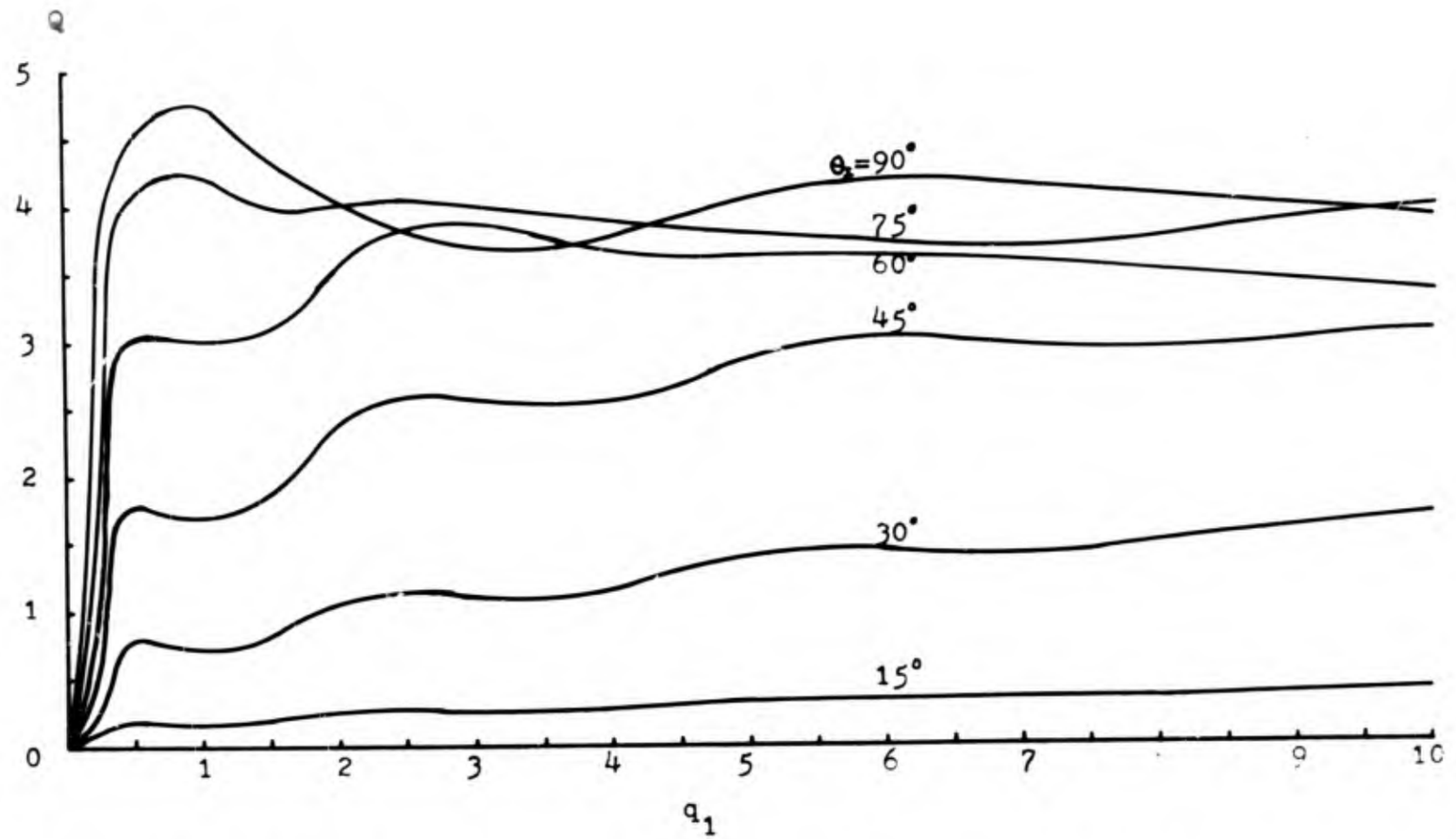

Figure 6.18a Total cross section of an thin plate barrier, χ_0=0.0.

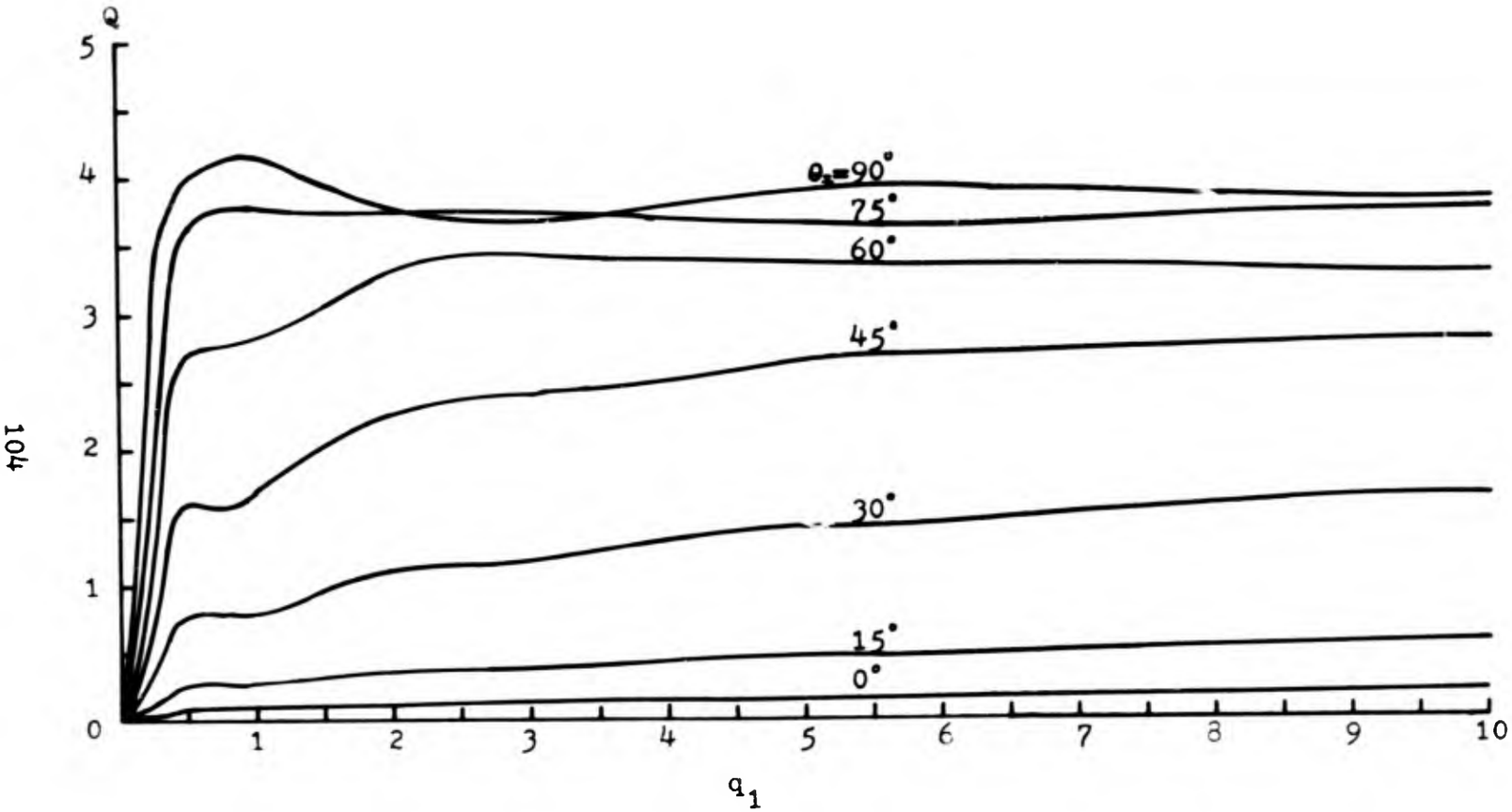

Figure 6.18b Total cross section of an elliptic cylinder of $\xi_0=0.2$.

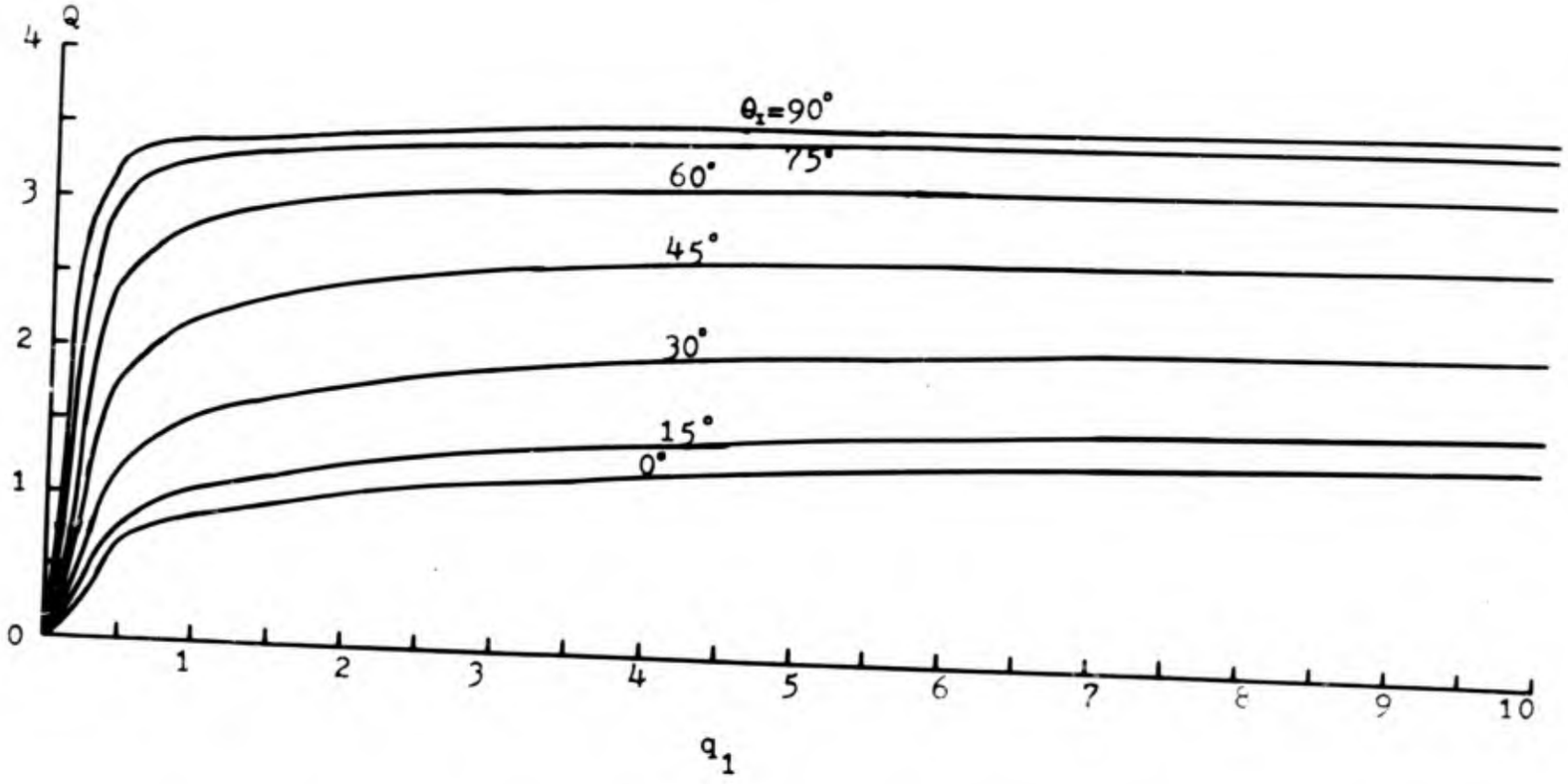

Figure 6.18c Total cross section of an elliptic cylinder of ξ_0=0.6.

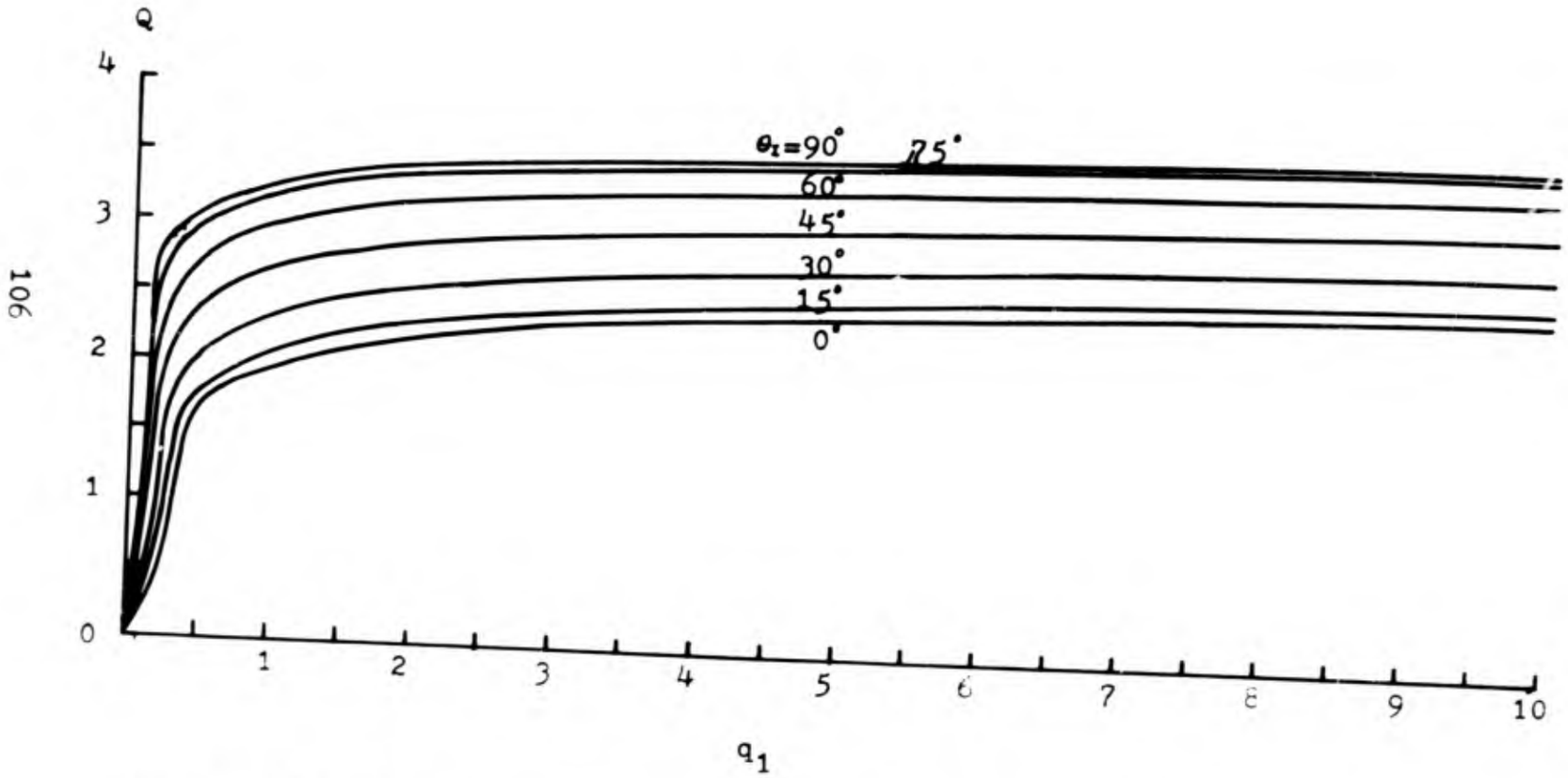

Figure 6.18d Total cross section of an elliptic cylinder of ξ_0=1.0.

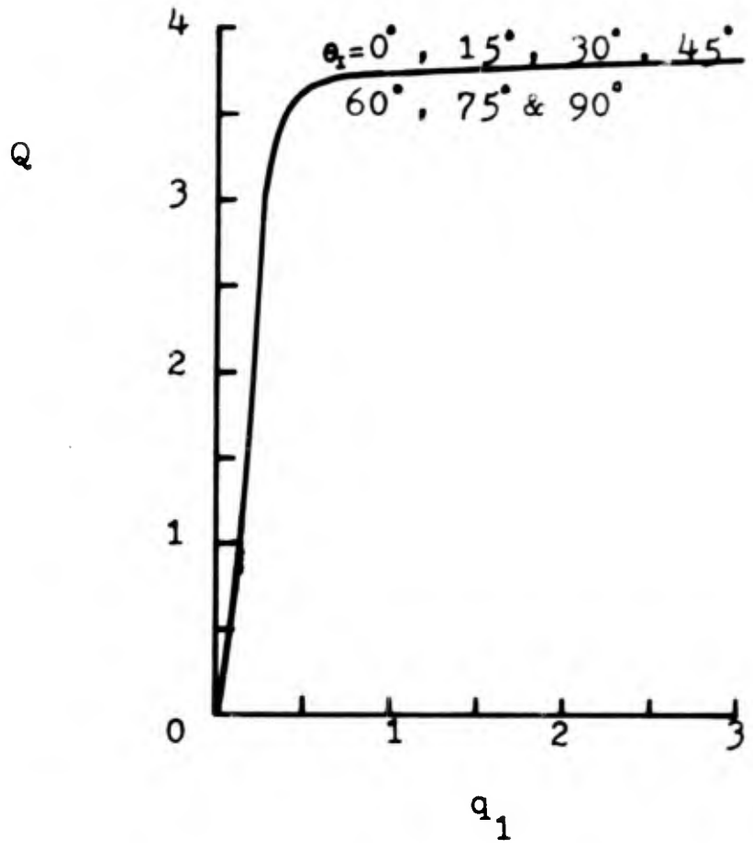

Figure 6.18e Total cross section of an elliptic cylinder of ξ_0=3.0.

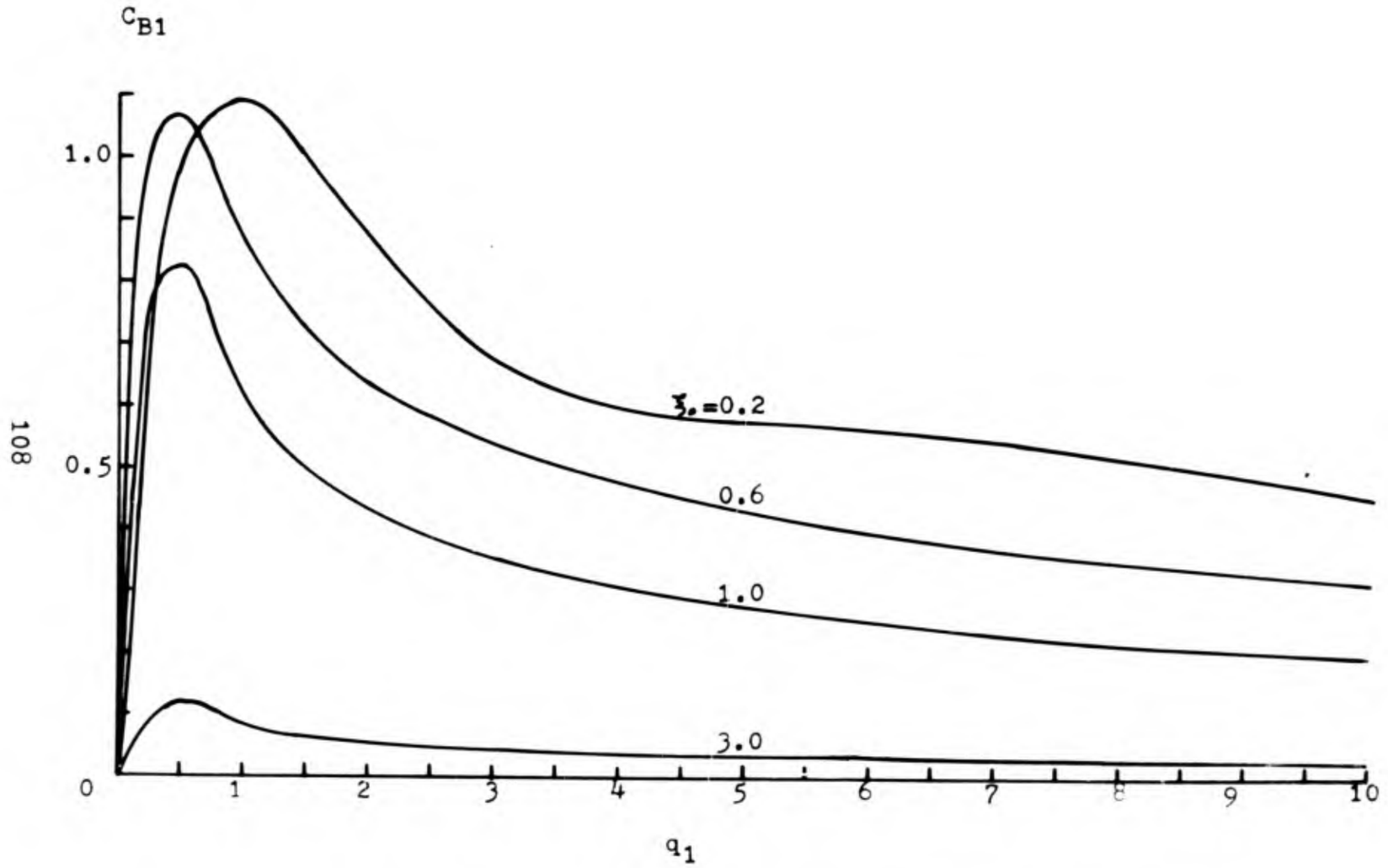

Figure 6.19a Radiation damping coefficient, oscillation in x direction.

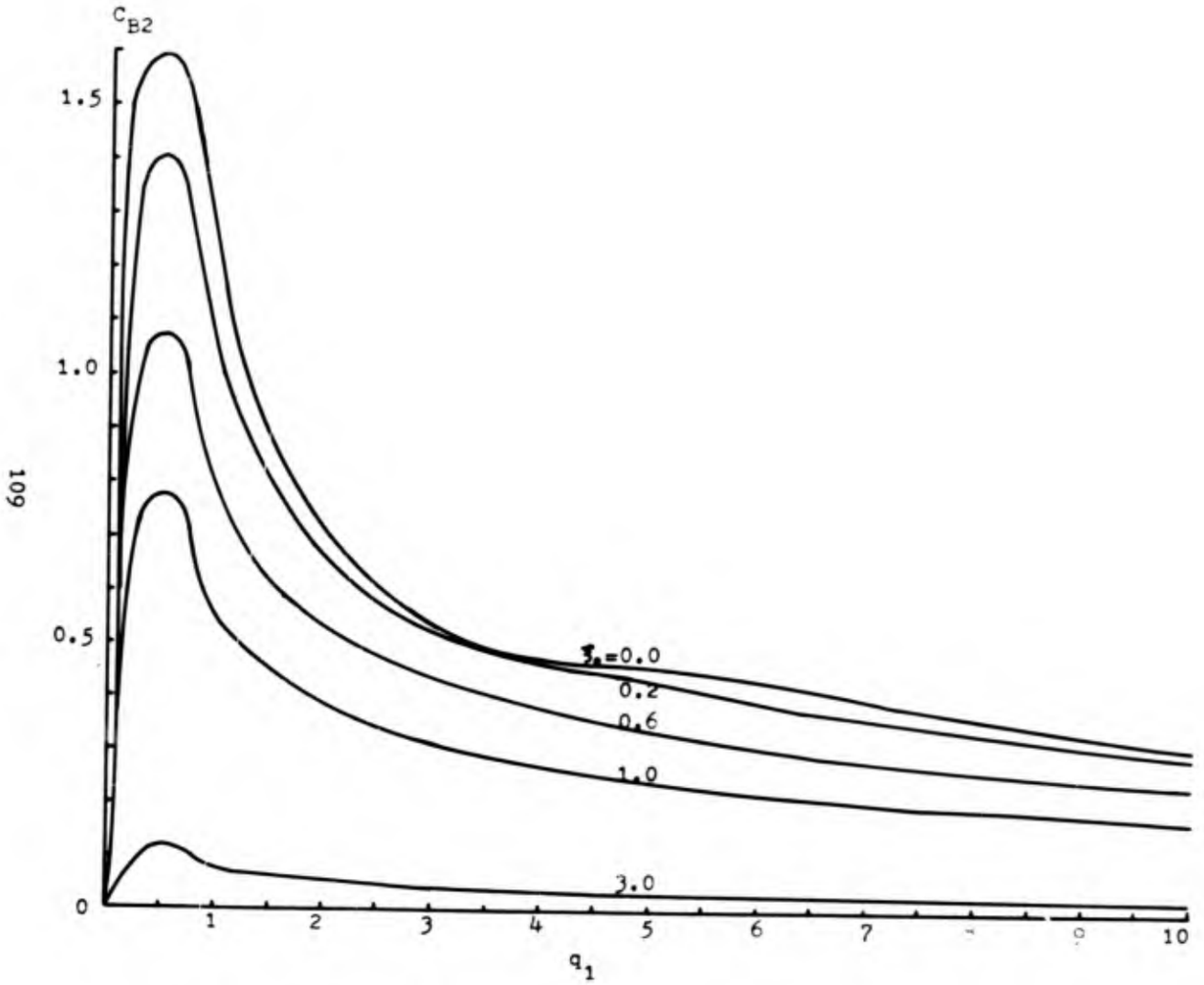

Figure 6.19b Radiation damping coefficient, oscillation in y direction.

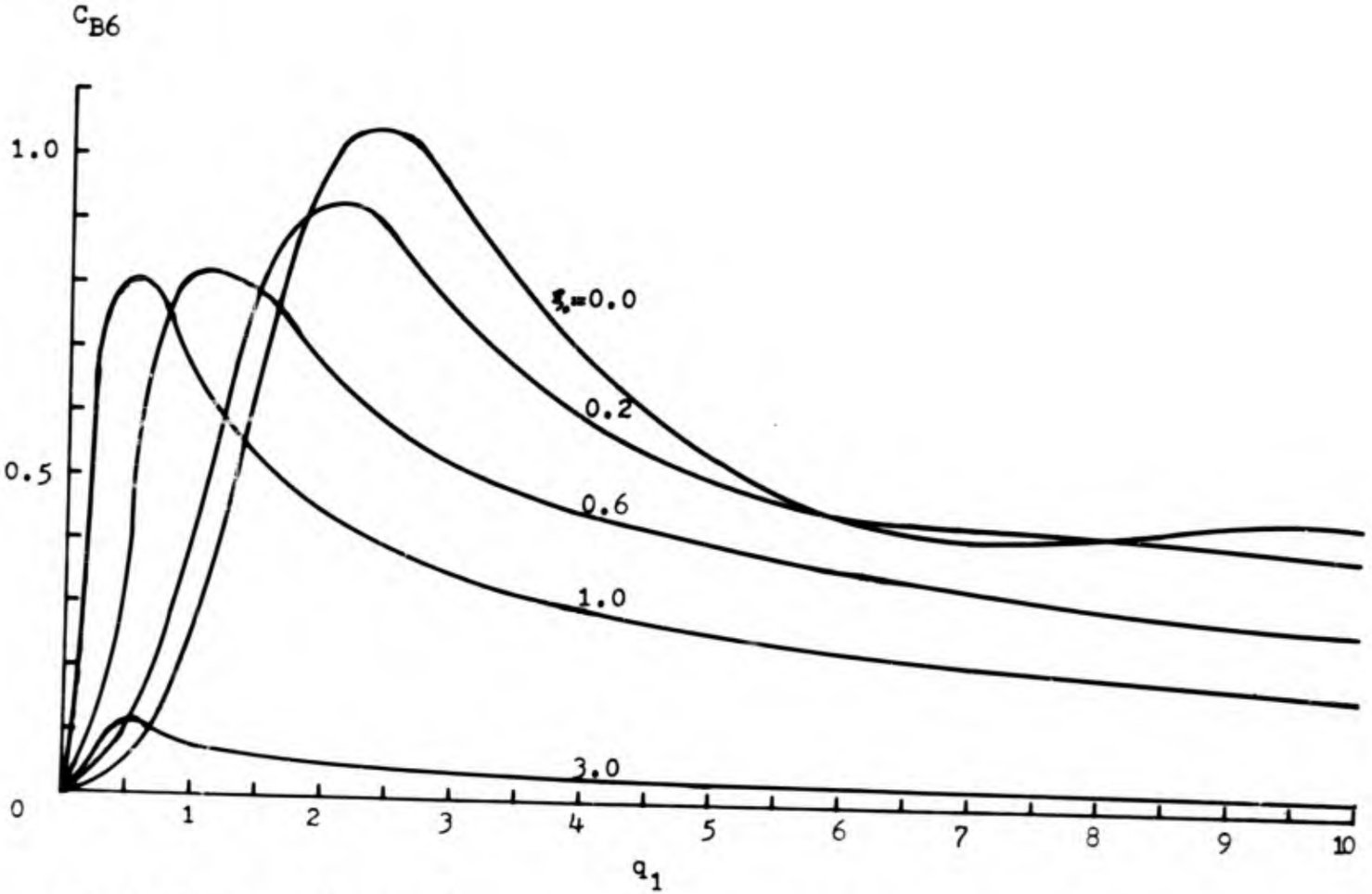

Figure 6.19c Radiation damping coefficient, yawing about z-axis.

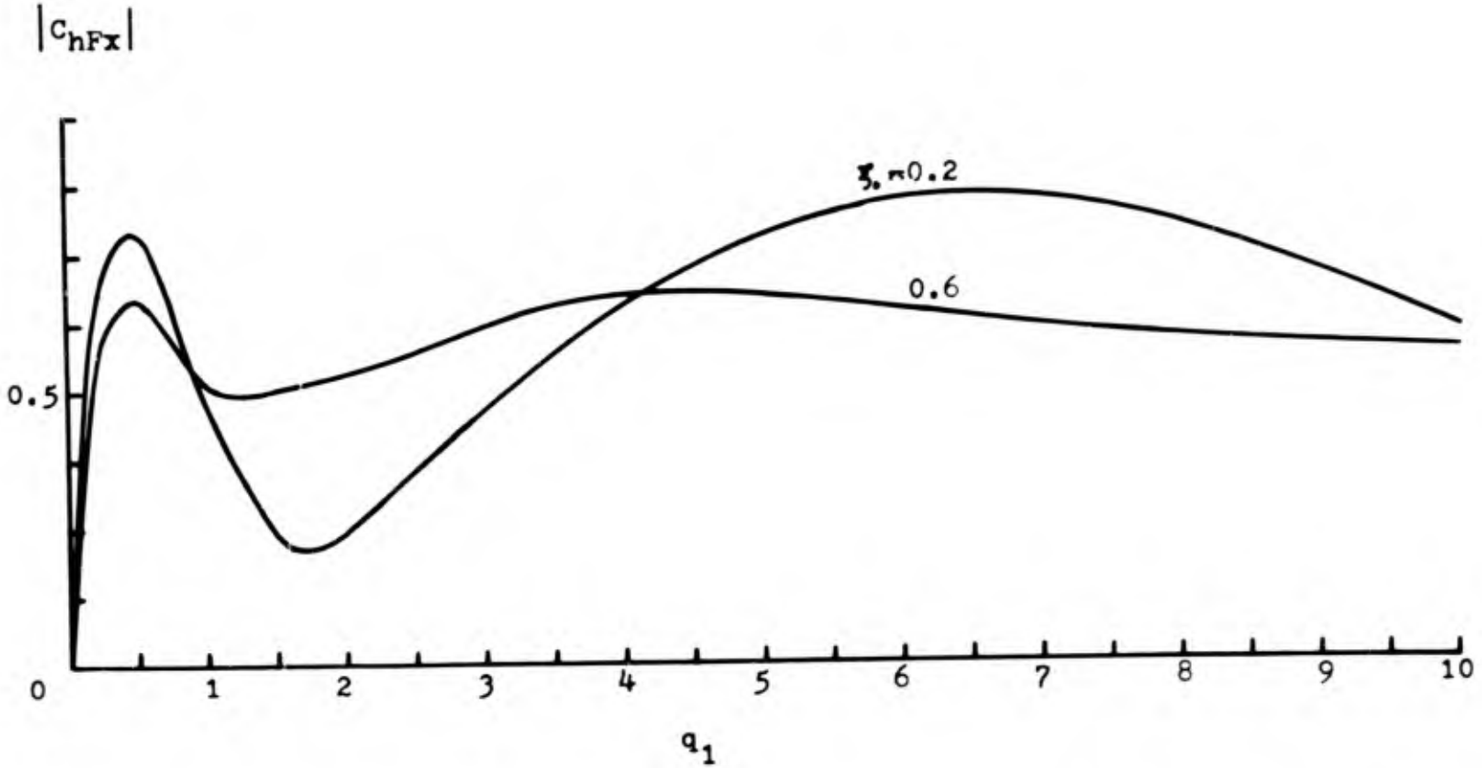

Figure 7.1 The magnitude of x-component force coefficient for a semi-elliptic cylinder with straight shoreline and θ_1=45°.

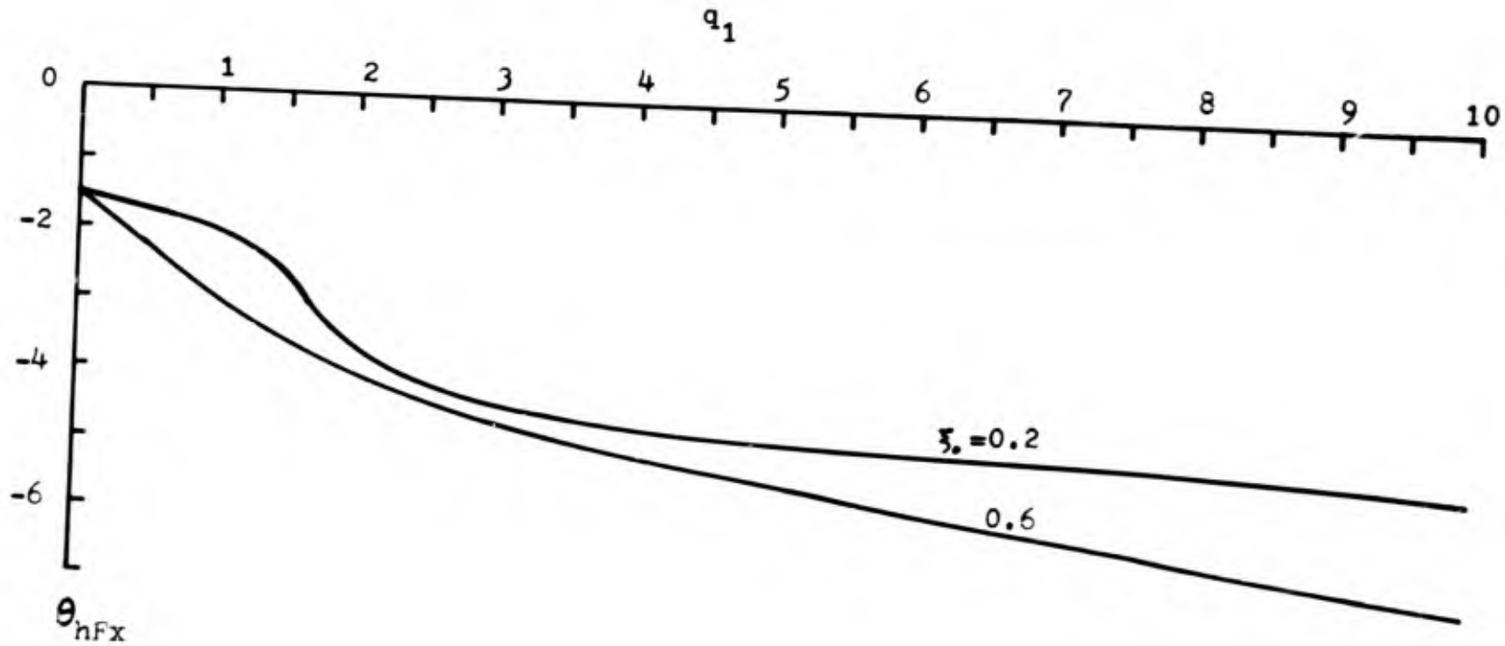

Figure 7.1a The phase of x-component force coefficient for a semi-elliptic cylinder with straight shoreline and $\theta_1=45°$.

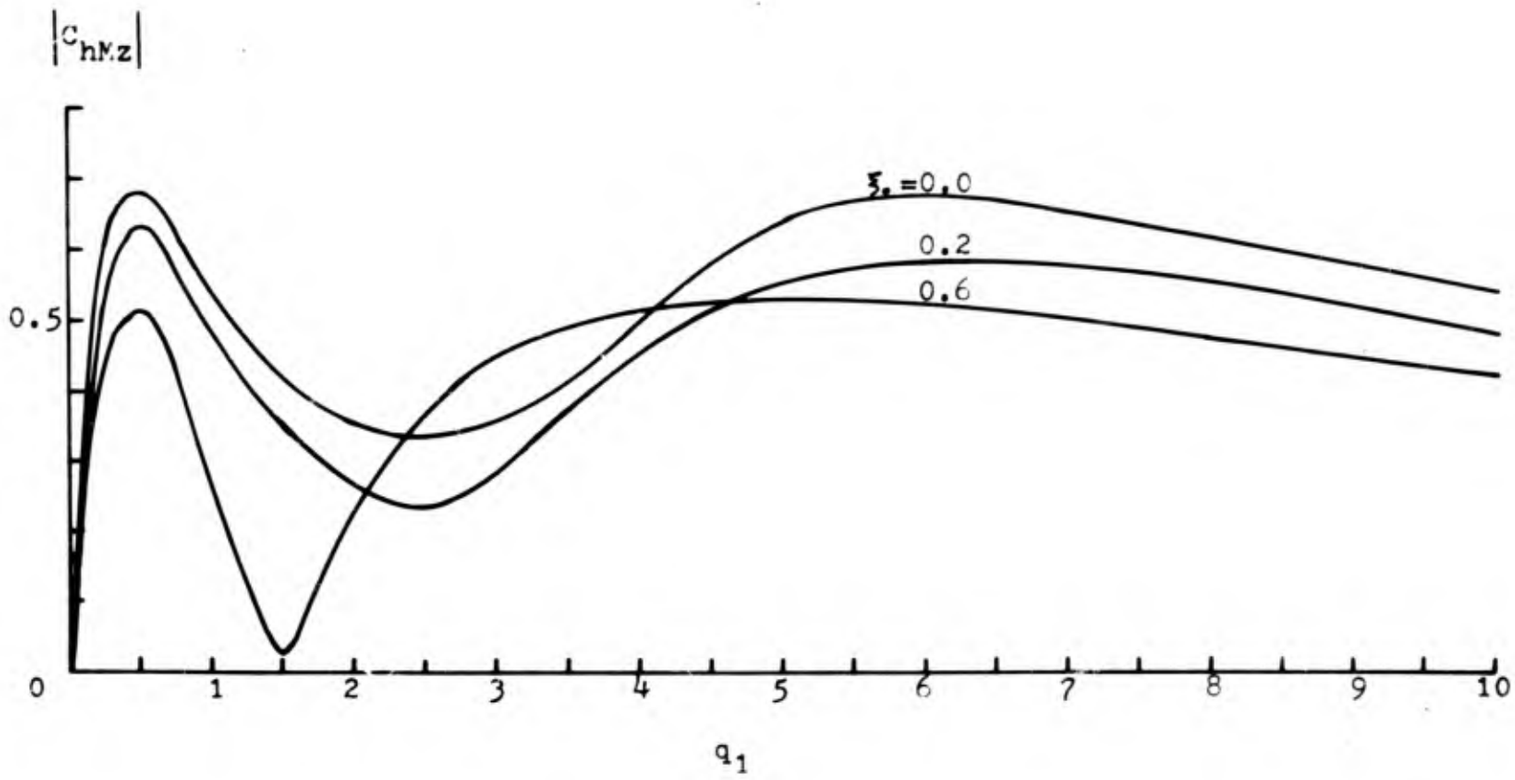

Figure 7.2 The magnitude of coefficient of moment about z-axis for a semi-elliptic cylinder with straight shoreline and $\theta_i=45°$.

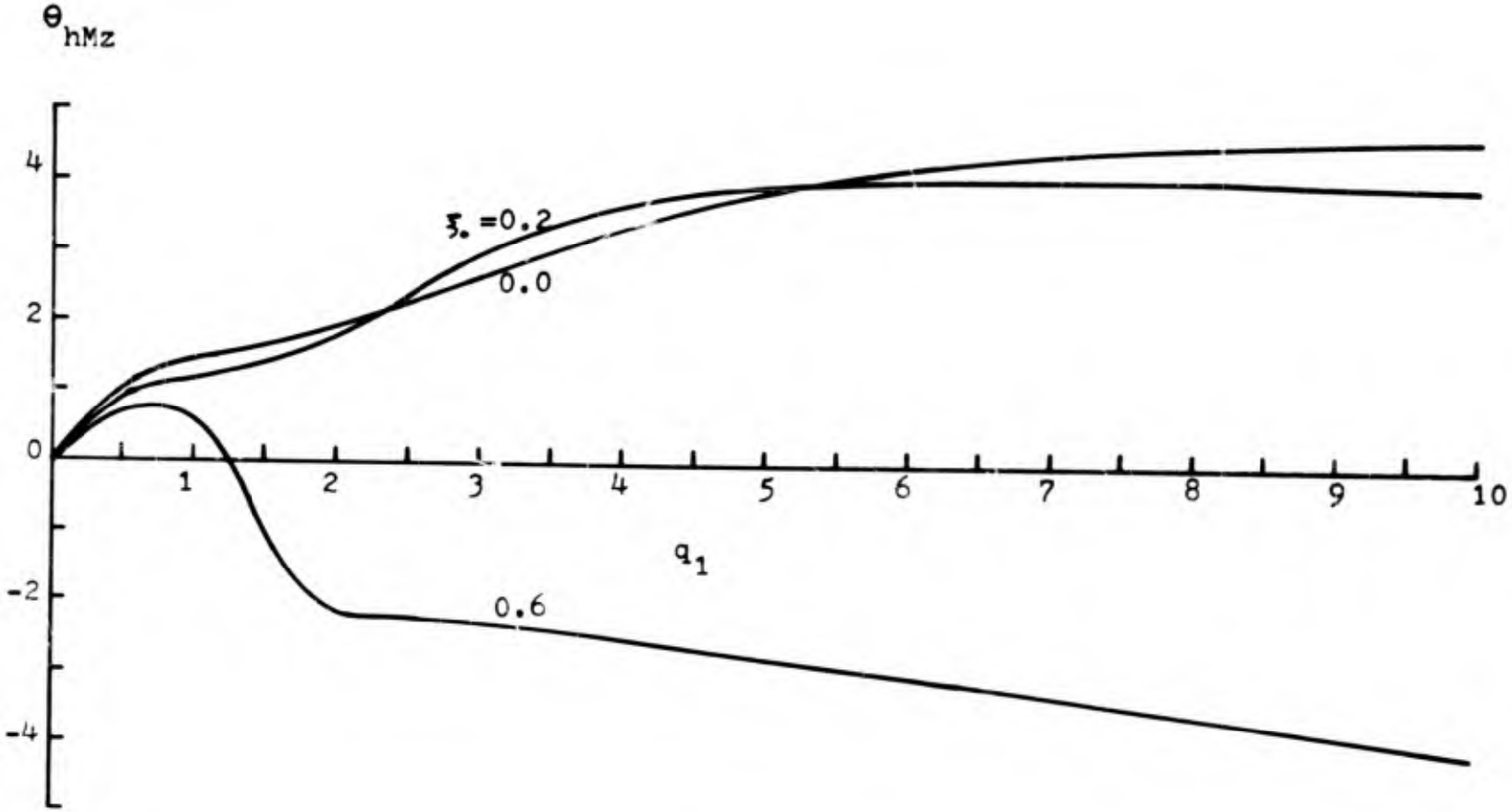

Figure 7.2a The phase of coefficient of moment about z-axis for a semi-elliptic cylinder with straight shoreline and θ_I=45°.

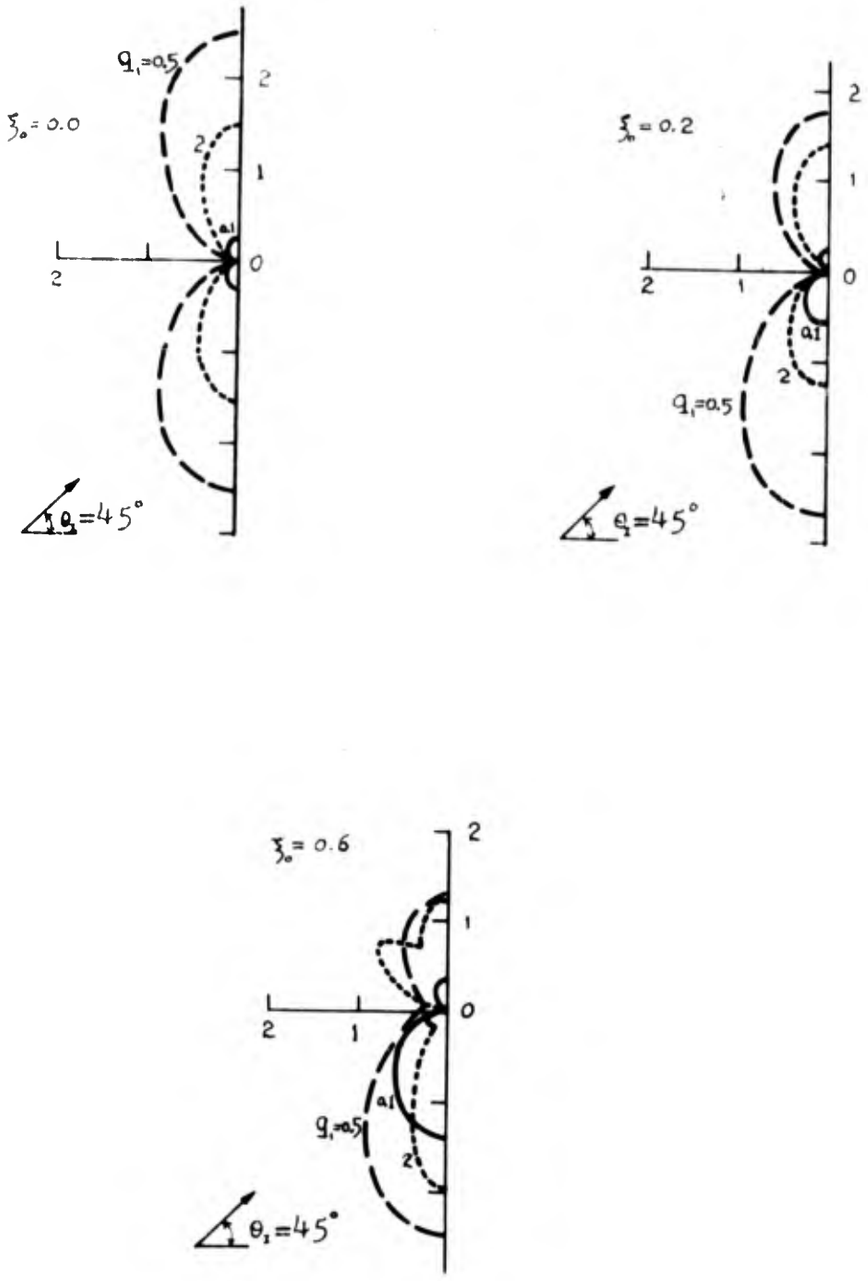

Figure 7.3 Differential cross section of a semi-elliptic cylinder with straight shoreline and $\theta_1 = 45°$.

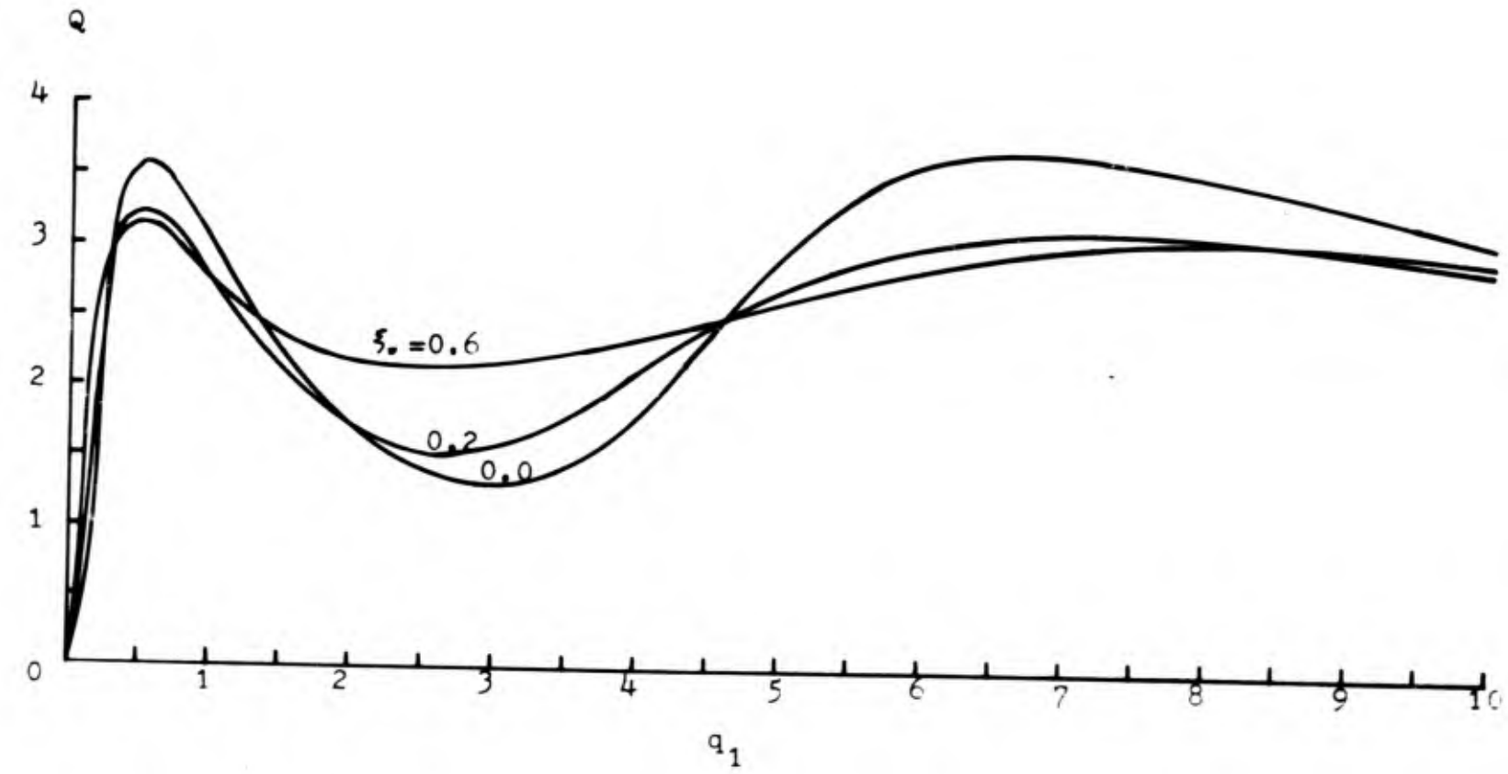

Figure 7.4 Total cross section of semi-elliptic cylinder with straight shoreline and θ_I=45°.

REFERENCES

1. Abramowitz, M. and Stegun, I.A. "Handbook of Mathematical Functions with Formulas, Graphs, and Mathematical Tables" Chapter 20. U.S. Department of Commerce, National Bureau of Standards, Applied Mathematics Series 55. June, 1964

2. Barakat, R. "Diffraction of plane waves by an elliptic cylinder" The J. of the Acoustical Society of America, vol.35, no.12, December, 1963

3. Black, J.L. and Mei, C.C. "Scattering and radiation of water waves" MIT, Water Resources and Hydrodynamics Laboratory report no.121, April, 1970

4. Blanch, G. "Numerical aspects of Mathieu eigenvalues" Circolo Matematico Di Palermo Rendiconti, Serie, 14-15, 1965-66

5. Blanch, G. and Clemm, D.S. "Tables relating to the radial Mathieu functions" vol.1, vol.2, Aerospace Research Laboratories, Office of Aerospace Research, United States Air Force. 1965

6. Blanch, G. and Clemm, D.S. "Mathieu's equation for complex parameters, Tables of Characteristic values" Aerospace research Laboratories, Office of Aerospace Research, United States Air Force. .1969

7. Bowman, J.J., Senior, T.B.A. and Uslenghi, P.L.E. " Electromagnetic and Acoustic scattering by simple shapes" Chapter 3. American Elsevier Publiching Company, inc., New York, 1969

8. Bray, M. "Scattering of a monochromatic wave by a vertical circular cylinder" Masters thesis, Department of Civil Engineering, MIT 1969

9. Burke, J.E., Christensen, E.J. and Lyttle, S.B. "Scattering patterns for elliptic cylinders" J. of the Optical Society of America, vol.54, pp.1065-6, August 1964

10. Burke, J.E. and Twersky, V. "On scattering of waves by an elliptic cylinder and by a semielliptic protuberance on a ground plane" J. of the Optical Society of America, vol.54, no.6, June, 1964

11. Clemm, D.S. "Algorithm 352, characteristic Values and associated solutions of Mathieu's differential equation (s22)" Communications of the ACM, vol.12, no.7, July, 1969

12. Erdelyi, A. "Higher Transcendental Functions" Bateman Manuscript Project, California Institute of Technology, vol.3, 1955

13. Garrett, C.J.R. "Wave forces on a circular dock" J. of Fluid Mechanics, vol.46, part 1, April, 1970

14. Garrison, C.J., Rao, V.S. and Snider, R.H. "Wave interaction with large submerged objects" ASCE National Structural Engineering Meeting, Portland, Oregon, April 6-10, 1970. Metting preprint 1222

15. Goldstein, S. "Mathieu function" Transactions of the Cambridge Philosophical Society, vol.xx111, no.x1, pp.303-6, 1927

16. Harleman, D.R.F. and Shapiro, W.C. "Experimental and analytical studies of wave forces on offshore structures" part 1, results for vertical cylinders, Hydrodynamics Laboratory, MIT, Technical Report no.19, May, 1955

17. Havelock, T.H. "The pressure of water waves upon a fixed obstacle" Proc. Royal Society of London, A, vol.175, July 18, 1940

18. Ince, E.L. "Tables of the Elliptic-cylinder Functions" Proc. of the Royal Society of Edinburgh, 52, pp.355-433, 1931-32

19. Ippen, A. "Estuary and Coastal Hydrodynamics" McGraw-Hill New York, 1966

20. Keulegan, G.H. and Carpenter L.H. "Forces on cylinders and plates in an oscillating fluid" J. of Research of the National Bureau of Standards, vol.60, no.5, May 1958

21. Lamb, H. "Hydrodynamics" Dover Publications, new York, 6th edition, 1932

22. Lowan, A.N. "Tables Relating Mathieu Functions, Characteristic Values, Coefficients, and Joining Factors" U.S. Department of Commerce, National Bureau of Standards, Applied Mathematics Series 59. August, 1967

23. MacCamy, R.C. and Fuchs, R.A. "Wave forces on piles : A diffraction theory" Institute of Engineering Research, Waves Investigation Laboratory, Series 3, Issue 334, Berkeley, California, Febuary, 1952

24. McLachlan, N.W. "Theory and Application of Mathieu functions" Dover Publications, Inc., New York, 1964

25. Montefusco, Luigi, "The diffraction of a plane wave by an isolated breakwater" MECCANICA, J. of the Italian Association of theoretical and applied mechanics, vol. 3, no.3, September, 1968

26. Morison, J.R., Johnson J.W. and O'Brien, M.P. "Experimental Studies of Forces on Piles" Proc. Fourth Conf. on Coastal Eng., 1953

27. Morse, P.M. and Feshbach, H. "Methods of Theoretical Physics" New York, McGraw-Hill, Inc., 1953

28. Morse, P.M. and Ingard, K.U. "Theoretical Acoustics" McGraw-Hill, Inc., 1968

29. Morse, P.M. and Rubenstein, P.J. "The diffraction of waves by Ribbons and by Slits" Physical Review, vol.54, December 1, 1938

30. Newman, J.N. "The damping of an oscillating ellipsoid near a free surface" J. of Ship Research, vol.5, no.3, December, 1961

31. Newman, J.N. "The exciting forces on fixed bodies in waves " J. of Ship Research, vol.6, no.3, December, 1962

32. Rschevkin, S.N. "A course of lectures on the theory of sound" translated from the Russian by Blunn, M., The Macmillan Company, New York, 1963

33. Schlichting, H. "Boundary-layer theory" chapter 15, sixth edition, McGraw-Hill, Inc., 1968

34. Stoker, J.J. "Water waves" Institute of Mathematical Sciences, New York University, New York, 1958

35. Stratton, J.A., Morse, P.M., Chu, L.J., Little, J.D.C., Corbato, F.J., "Spheroidal wave functions" published jointly by the Technology Press of MIT and John Willey and Sons, Inc., New York, 1956

36. Yeh, C. "The diffraction of waves by a penetrable ribbon"
J. of Mathematical Physics, vol.4, no.1, January 1963

Most of the material here is taken from McLachlan [24], and is included here for the convenience of the reader. In appendices A and B, q is defined to be positive.

APPENDIX A. ELLIPTICAL COORDINATES SYSTEM

A-1 Elliptical Coordinates

The ellipse can be described by

$$\frac{x^2}{a^2} + \frac{y^2}{b^2} = 1$$

or

$$F : b^2x^2 + a^2y^2 - a^2b^2 = 0 \qquad (A.1)$$

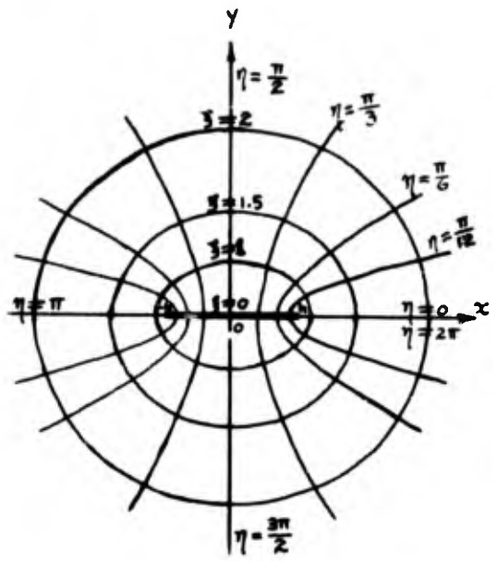

Fig. A.1 Orthogonally intersecting confocal ellipses and hyperbolas for elliptical coordinates.

The relationship between carterian coordinates (x,y) and elliptical coordinates (ξ,η) is

$$x = h\cosh\xi\cos\eta$$
$$y = h\sinh\xi\sin\eta$$

or (A.2)

$$x+iy = h\cosh(\xi+i\eta)$$

thus

$$\frac{x^2}{h^2\cosh^2\xi} + \frac{y^2}{h^2\sinh^2\xi} = 1 \qquad (A.3)$$

$$\frac{x^2}{h^2\cos^2\eta} - \frac{y^2}{h^2\sin^2\eta} = 1 \qquad (A.4)$$

(A.3) represents a family of confocal ellipses with semi-major axes $a=h\cosh\xi$, semi-minor axes $b=h\sinh\xi$, the common foci being the points $(\pm h,0)$. (A.4) represents a family of confocal hyperbolas with the same foci, as illustrated in Fig. (A.1). Evidently $h=(a^2-b^2)^{1/2}$.

When $\xi\to 0$ and finite h, then $a=h$, $b=0$. This is the limit case that a long elliptical cylinder degenerates to a ribbon of length 2h. If h is a constant, as $\xi\to\infty$, $a\to b\to r$; see (A.9), so that the confocal ellipses tend to become concentric circles. If $h\to 0$ in such a way that $\frac{h}{2}e^{\xi}\to r_o$ the ellipse becomes a circle of radius r_o. Now (A.4) may be written as $\frac{x^2}{\cos^2\eta}-\frac{y^2}{\sin^2\eta}=h^2$. As $h\to 0$, $y/x\to\pm\tan\eta$, so $\eta\to\theta$, the confocal hyperbolas ultimately become radii of the circle and make angles θ with x-axis.

A-2 Arc lengths ds_1, ds_2, and Radius vector r

The hyperbolic and elliptic arc lengths are respectively,

$$ds_1=\left[\left(\frac{\partial x}{\partial\xi}\right)^2+\left(\frac{\partial y}{\partial\xi}\right)^2\right]^{1/2}d\xi$$

$$ds_2=\left[\left(\frac{\partial x}{\partial\eta}\right)^2+\left(\frac{\partial y}{\partial\eta}\right)^2\right]^{1/2}d\eta \qquad (A.5)$$

Making use of (A.2), each bracketed member in (A.5) is

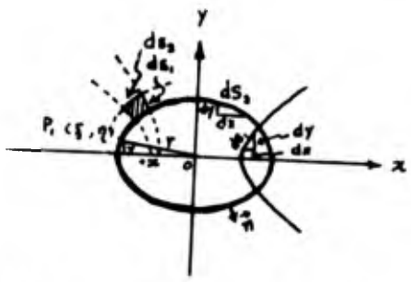

Fig. A.2 Hyperbolic (ds_1), elliptic (ds_2) arc length, radius vector and area ($ds_1 ds_2$) enclosed by two contiguous pairs of orthogonally intersecting confocal ellipses and hyperbolas.

$$l_1 = h(\cosh^2\xi \sin^2\eta + \sinh^2\xi \cos^2\eta)^{1/2}$$
$$= h(\cosh^2\xi - \cos^2\eta)^{1/2}$$
$$= \frac{h}{\sqrt{2}}(\cosh 2\xi - \cos 2\eta)^{1/2} \qquad (A.6)$$

we can also notice that ds_1 is along the direction of the normal ($\vec{n}$) to the ellipse. Hence (A.5) becomes

$$ds_1 = l_1 d\xi = dn$$
$$ds_2 = l_1 d\eta \qquad (A.7)$$

The distance of any point from the origin, expressed in elliptical coordinates, is

$$r = (x^2+y^2)^{\frac{1}{2}} = h(\cosh^2\xi \cos^2\eta + \sinh^2\xi \sin^2\eta)^{1/2}$$
$$= h(\cosh^2\xi - \sin^2\eta)^{\frac{1}{2}}$$
$$= \frac{h}{\sqrt{2}}(\cosh 2\xi + \cos 2\eta)^{\frac{1}{2}} \qquad (A.8)$$

when ξ is large enough and h constant, we have

$$l_1 \sim h\cosh\xi \sim h\sinh\xi \sim \tfrac{1}{2}he^{\xi} \sim r \qquad (A.9)$$

hence we may write

$$ds_1 \sim rd\xi \sim dr \quad ; \quad ds_2 \sim rd\eta \quad ; \quad ds_1 ds_2 \sim rdrd\eta \qquad (A.10)$$

which coincide with the expressions for cylindrical polar coordinates.

A-3 The Unit Outward Normal Vector to the Ellipse

The ellipse is described by (A.1), therefore the normal vector to the ellipse is

$$\nabla F = 2b^2 x\vec{i} + 2a^2 y\vec{j}$$

hence outward unit vector

$$\vec{n} = \frac{\nabla F}{|\nabla F|} = \frac{1}{l_1}(h\sinh\xi\cos\eta\vec{i} + h\cosh\xi\sin\eta\vec{j}) \qquad (A.11')$$

where l_1 is given in (A.6), and outward directional cosine of the normal to the ellipse with repect to x-, y-axes therefore is

$$(\cos(n,x),\ \cos(n,y)) = \left(\frac{h\sinh\xi\cos\eta}{l_1},\ \frac{h\cosh\xi\sin\eta}{l_1}\right) \qquad (A.11)$$

APPENDIX B. WAVE EQUATION IN ELLIPTICAL COORDINATES AND MATHIEU SOLUTIONS

The two dimensional wave equation in cartesian coordinates is given by

$$\frac{\partial^2\phi}{\partial x^2} + \frac{\partial^2\phi}{\partial y^2} + k_1^2\phi = 0 \qquad \text{(B.1)}$$

B-1 Transformation of equation (B.1) to elliptical coordinates (ξ,η).

By (A.2), write $z = x+iy = h\cosh(\xi+i\eta)$, $\bar{z} = x-iy = h\cosh(\xi-i\eta)$, then $z\bar{z} = x^2+y^2$, and

$$4\frac{\partial^2}{\partial z\partial\bar{z}} = \frac{\partial^2}{\partial x^2} + \frac{\partial^2}{\partial y^2} \qquad \text{(B.2)}$$

Putting $\zeta = \xi+i\eta$, $\bar{\zeta} = \xi-i\eta$, we get $z = h\cosh\zeta$, $\bar{z} = h\cosh\bar{\zeta}$, and $\zeta\bar{\zeta} = \xi^2+\eta^2$, thus

$$\frac{\partial\zeta}{\partial z} = \frac{1}{h\sinh\zeta}, \quad \frac{\partial\bar{\zeta}}{\partial\bar{z}} = \frac{1}{h\sinh\bar{\zeta}}, \quad 4\frac{\partial^2}{\partial\zeta\partial\bar{\zeta}} = \frac{\partial^2}{\partial\xi^2} + \frac{\partial^2}{\partial\eta^2}$$

$$\Rightarrow \frac{\partial}{\partial z} = \frac{1}{h\sinh\zeta}\frac{\partial}{\partial\zeta}, \qquad \frac{\partial}{\partial\bar{z}} = \frac{1}{h\sinh\bar{\zeta}}\frac{\partial}{\partial\bar{\zeta}}$$

$$\Rightarrow 4\frac{\partial^2}{\partial z\partial\bar{z}} = \frac{\partial^2}{\partial x^2} + \frac{\partial^2}{\partial y^2} = \frac{4}{h^2\sinh\zeta\sinh\bar{\zeta}}\frac{\partial^2}{\partial\zeta\partial\bar{\zeta}} =$$

$$= \frac{2}{h^2(\cosh 2\xi - \cos 2\eta)}\left(\frac{\partial^2}{\partial\xi^2} + \frac{\partial^2}{\partial\eta^2}\right) \qquad \text{(B.3)}$$

Applying (B.3) to (B.1) leads to the equation

$$\frac{\partial^2\phi}{\partial\xi^2} + \frac{\partial^2\phi}{\partial\eta^2} + 2k^2(\cosh 2\xi - \cos 2\eta)\phi = 0 \qquad \text{(B.4)}$$

with $k = \frac{k_1 h}{2}$. Then (B.4) is the two dimensional wave equation

expressed in elliptical coordinates.

B-2 Mathieu equations

By the method of separation of variables $\phi=X(\xi)Y(\eta)$, it follows that $X(\xi)$ and $Y(\eta)$ must satisfy respectively the equations :

$$\frac{d^2Y}{d\eta^2} + (a-2q\cos 2\eta)Y = 0 \qquad (B.5)$$

and

$$\frac{d^2X}{d\xi^2} - (a-2q\cosh 2\xi)X = 0 \quad , \qquad (B.6)$$

where

$$q = K^2 = \left(\frac{k_1 h}{2}\right)^2 \qquad (B.7)$$

representing the square of the ratio of body geometry length to the wave length ($\because k_1 h \sim \frac{h}{L}$), is an important physical parameter. "a" is the separation constant and is called the characteristic number of the Mathieu function.

(B.5) is known as Mathieu equation. We adopt, as the canonical form ,

$$\frac{d^2y}{dz^2} + (a-2q\cos 2z)y = 0 \qquad (B.8)$$

and corresponding to (B.6) we have

$$\frac{d^2y}{dz^2} - (a-2q\cosh 2z)y = 0 \qquad (B.9)$$

We note that (B.8) transforms into (B.9), and vice versa, if z is replaced by iz

B-3 Periodic solutions of Mathieu equation

Corresponding to a prescribed value of q and a separation constant "a" which is a function of q only and one of an infinite sequence of characteristic numbers, (B.8) has periodic solutions. (B.8) also has non-periodic solutions which, for physical reasons, are not of interest in this work. The corresponding solutions fall into four classes, according to their symmetry or anti-symmetry about $z=0$ and $z=\frac{\pi}{2}$. Using the notations of Ince[18,24], these functions are :

	the corresponding characteristic numbers	
$ce_{2n}(z,q) = \sum_{r=0}^{\infty} A_{2r}^{(2n)} \cos 2rz$	(a_{2n})	(B.10a,b, c,d)
$ce_{2n+1}(z,q) = \sum_{r=0}^{\infty} A_{2r+1}^{(2n+1)} \cos(2r+1)z$	(a_{2n+1})	
$se_{2n+1}(z,q) = \sum_{r=0}^{\infty} B_{2r+1}^{(2n+1)} \sin(2r+1)z$	(b_{2n+1})	
$se_{2n+2}(z,q) = \sum_{r=0}^{\infty} B_{2r+2}^{(2n+2)} \sin(2r+2)z$	(b_{2n+2})	

where $A^{(\ )}$, $B^{(\ )}$ are coefficients and are function of q only.

The normalization used by Ince is given by $\frac{1}{\pi}\int_0^{2\pi} y^2 dz = 1$, so that

$$2\left[A_0^{(2n)}\right]^2 + \sum_{r=1}^{\infty}\left[A_{2r}^{(2n)}\right]^2 = \sum_{r=0}^{\infty}\left[A_{2r+1}^{(2n+1)}\right]^2 = \sum_{r=0}^{\infty}\left[B_{2r+1}^{(2n+1)}\right]^2 = \sum_{r=0}^{\infty}\left[B_{2r+2}^{(2n+2)}\right]^2 = 1 \qquad \text{(B.11)}$$

B-4 Orthogonality of the periodic function ce_m , se_m

The orthogonality of $ce_m(z,q)$, $se_m(z,q)$ in the interval $[0,2\pi]$ for z is given here, the reader is referred to [ref. 24, p.22-25].

$$\int_0^{2\pi} ce_{2m+\alpha}(z,q)\,ce_{2n+\beta}(z,q)\,dz = \begin{cases} \pi & \text{if } m=n \;\&\; \alpha=\beta \\ 0 & \text{if } m\neq n \text{ or } \alpha\neq\beta \end{cases} \qquad (B.12a)$$

$$\int_0^{2\pi} ce_{2m+\alpha}(z,q)\,se_{2n+\beta}(z,q)\,dz = 0 \qquad (B.12b)$$

$$\int_0^{2\pi} se_{2m+\alpha}(z,q)\,se_{2n+\beta}(z,q)\,dz = \begin{cases} \pi & \text{if } m=n \;\&\; \alpha=\beta \\ 0 & \text{if } m\neq n \text{ or } \alpha\neq\beta \end{cases} \qquad (B.12c)$$

where α, β are defined to be 0 or 1 in corresponding to four classes of Mathieu functions.

Some integrations concerning ce_m , se_m which appear in this work are given below :

$$\begin{aligned} \int_0^{2\pi} ce_{2n+\alpha}(z,q)\cos sz\,dz &= \int_0^{2\pi}\Big[\sum_{j=0}^{\infty} A_{2j+\alpha}^{(2n+\alpha)}\cos(2j+\alpha)z\Big]\cos sz\,dz \\ &= \sum_{j=0}^{\infty} A_{2j+\alpha}^{(2n+\alpha)}\int_0^{2\pi}\cos(2j+\alpha)z\cos sz\,dz \\ &= \begin{cases} \pi A_1^{(2n+1)} & \text{if } \alpha=1 \\ 0 & \text{if } \alpha\neq 1 \end{cases} \qquad (B.13a) \end{aligned}$$

$$\begin{aligned} \int_0^{2\pi} se_{2n+\alpha}(z,q)\cos sz\,dz &= \int_0^{2\pi}\Big[\sum_{j=0}^{\infty} B_{2j+\alpha}^{(2n+\alpha)}\sin(2j+\alpha)z\Big]\cos sz\,dz \\ &= \sum_{j=0}^{\infty} B_{2j+\alpha}^{(2n+\alpha)}\int_0^{2\pi}\sin(2j+\alpha)z\cos sz\,dz \\ &= 0 \qquad (B.13b) \end{aligned}$$

$$\int_0^{2\pi} ce_{2n+\alpha}(z,q)\sin(2j+\beta)z\,dz = \int_0^{2\pi}\left[\sum_{i=0}^{\infty} A_{2i+\alpha}^{(2n+\alpha)}\cos(2i+\alpha)z\right]\sin(2j+\beta)z\,dz$$

$$= \sum_{i=0}^{\infty} A_{2i+\alpha}^{(2n+\alpha)} \int_0^{2\pi}\cos(2i+\alpha)z\sin(2j+\beta)z\,dz$$

$$= 0 \qquad \text{(B.14a)}$$

$$\int_0^{2\pi} se_{2n+\alpha}(z,q)\sin(2j+\beta)z\,dz = \int_0^{2\pi}\left[\sum_{i=0}^{\infty} B_{2i+\alpha}^{(2n+\alpha)}\sin(2i+\alpha)z\right]\sin(2j+\beta)z\,dz$$

$$= \sum_{i=0}^{\infty} B_{2i+\alpha}^{(2n+\alpha)} \int_0^{2\pi}\sin(2i+\alpha)z\sin(2j+\beta)z\,dz$$

$$= \begin{cases} \pi\, B_{2j+\beta}^{(2n+\beta)} & \text{if} \quad \alpha=\beta \\ 0 & \text{if} \quad \alpha\neq\beta \end{cases} \qquad \text{(B.14b)}$$

$$\int_{-\frac{\pi}{2}}^{\frac{\pi}{2}} ce_{2n}(z,q)\cos z\,dz = \int_{-\frac{\pi}{2}}^{\frac{\pi}{2}}\left[\sum_{j=0}^{\infty} A_{2j}^{(2n)}\cos 2jz\right]\cos z\,dz$$

$$= \sum_{j=0}^{\infty} A_{2j}^{(2n)} \int_{-\frac{\pi}{2}}^{\frac{\pi}{2}}\cos 2jz\cos z\,dz$$

$$= \sum_{j=0}^{\infty} A_{2j}^{(2n)}\left[\frac{\sin(2j-1)z}{2(2j-1)} + \frac{\sin(2j+1)z}{2(2j+1)}\right]$$

$$= \sum_{j=0}^{\infty} \frac{(-1)^{j+1}\,2A_{2j}^{(2n)}}{(2j-1)(2j+1)}$$

$$= 2A_0^{(2n)} + \sum_{j=1}^{\infty} \frac{(-1)^{j+1}\,2A_{2j}^{(2n)}}{4j^2-1} \qquad \text{(B.15a)}$$

$$\int_{-\frac{\pi}{2}}^{\frac{\pi}{2}} se_{2n+1}(z,q)\cos z\,dz = \int_{-\frac{\pi}{2}}^{\frac{\pi}{2}}\left[\sum_{j=0}^{\infty} B_{2j+1}^{(2n+1)}\sin(2j+1)z\right]\cos z\,dz$$

$$= \sum_{j=0}^{\infty} B_{2j+1}^{(2n+1)} \int_{-\frac{\pi}{2}}^{\frac{\pi}{2}}\sin(2j+1)z\cos z\,dz$$

$$= 0 \qquad \text{(B.15b)}$$

$$\int_{-\frac{\pi}{2}}^{\frac{\pi}{2}} ce_{2n}(z,q)\sin(2j+\beta)\,dz = \int_{-\frac{\pi}{2}}^{\frac{\pi}{2}}\left[\sum_{i=0}^{\infty} A_{2i}^{(2n)}\cos 2iz\right]\sin(2j+\beta)z\,dz$$

$$= \sum_{i=0}^{\infty} A_{2i}^{(2n)} \int_{-\frac{\pi}{2}}^{\frac{\pi}{2}}\cos 2iz\sin(2j+\beta)z\,dz = 0$$

(B.16a)

$$\int_{-\frac{\pi}{2}}^{\frac{\pi}{2}} se_{2n+1}(z,q)\sin z\,dz = \int_{-\frac{\pi}{2}}^{\frac{\pi}{2}} \left[\sum_{j=0}^{\infty} B_{2j+1}^{(2n+1)} \sin(2j+1)z\right] \sin z\,dz$$

$$= \sum_{j=0}^{\infty} B_{2j+1}^{(2n+1)} \int_{-\frac{\pi}{2}}^{\frac{\pi}{2}} \sin(2j+1)z \sin z\,dz$$

$$\underbrace{\left[\frac{z}{2} - \frac{\sin 2z}{4}\right]_{-\frac{\pi}{2}}^{\frac{\pi}{2}}}_{\text{if } j=0} \qquad \underbrace{\left[\frac{\sin 2jz}{4j} - \frac{\sin(2j+2)z}{2(2j+2)}\right]_{-\frac{\pi}{2}}^{\frac{\pi}{2}} = 0}_{\text{if } j\neq 0}$$

$$= \frac{\pi}{2} B_1^{(2n+1)}$$

(B.16b)

$$\int_{-\frac{\pi}{2}}^{\frac{\pi}{2}} se_{2n+1}(z,q)\sin 2z\,dz = \int_{-\frac{\pi}{2}}^{\frac{\pi}{2}} \left[\sum_{j=0}^{\infty} B_{2j+1}^{(2n+1)} \sin(2j+1)z\right] \sin 2z\,dz$$

$$= \sum_{j=0}^{\infty} B_{2j+1}^{(2n+1)} \int_{-\frac{\pi}{2}}^{\frac{\pi}{2}} \sin(2j+1)z \sin 2z\,dz$$

$$= \sum_{j=0}^{\infty} B_{2j+1}^{(2n+1)} \left[\frac{\sin(2j-1)z}{2(2j-1)} - \frac{\sin(2j+3)z}{2(2j+3)}\right]_{-\pi/2}^{\pi/2}$$

$$= \sum_{j=0}^{\infty} B_{2j+1}^{(2n+1)} \left[\frac{\sin(j-\frac{1}{2})\pi}{2j-1} - \frac{\sin(j+2-\frac{1}{2})\pi}{2j+3}\right]$$

$$= \sum_{j=0}^{\infty} B_{2j+1}^{(2n+1)} \left[\frac{(-1)^{j+1}}{2j-1} - \frac{(-1)^{j+1}}{2j+3}\right]$$

$$= \sum_{j=0}^{\infty} \frac{(-1)^{j+1} 2B_{2j+1}^{(2n+1)}}{(2j-1)(2j+3)}$$

(B.16c)

since,

$$2\int_{-\frac{\pi}{2}}^{\frac{\pi}{2}} ce_{2n}(\eta,q)ce_{2m}(\eta,q)d\eta = \int_{-\frac{\pi}{2}}^{\frac{\pi}{2}} ce_{2n}(\eta,q)ce_{2m}(\eta,q)d\eta + \int_{-\frac{\pi}{2}}^{\frac{\pi}{2}} ce_{2n}(\eta,q)ce_{2m}(\eta,q)d\eta$$

$$= \int_{-\frac{\pi}{2}}^{\frac{\pi}{2}} ce_{2n}(\eta,q)ce_{2m}(\eta,q)d\eta - \int_{\frac{3\pi}{2}}^{\frac{\pi}{2}} ce_{2n}(\pi-\eta,q)ce_{2m}(\pi-\eta,q)d\eta$$

$$= \int_{-\frac{\pi}{2}}^{\frac{\pi}{2}} ce_{2n}(\eta,q)ce_{2m}(\eta,q)d\eta + \int_{\frac{\pi}{2}}^{\frac{3\pi}{2}} ce_{2n}(\eta,q)ce_{2m}(\eta,q)d\eta$$

$$= \int_{-\frac{\pi}{2}}^{\frac{3\pi}{2}} = \int_{0}^{2\pi} ce_{2n}(\eta,q)ce_{2m}(\eta,q)d = \begin{cases} 0 & m \neq n \\ \pi & m = n \end{cases}$$

$$\Rightarrow \quad \int_{-\frac{\pi}{2}}^{\frac{\pi}{2}} ce_{2n}(\eta,q)ce_{2m}(\eta,q)d\eta = \begin{cases} 0 & m \neq n \\ \frac{\pi}{2} & m = n \end{cases} \qquad \text{(B.16'a)}$$

For the same reason

$$\int_{-\frac{\pi}{2}}^{\frac{\pi}{2}} se_{2m+1}(\eta,q)ce_{2m}(\eta,q)d\eta = 0 \qquad \text{(B.16'b)}$$

$$\int_{-\frac{\pi}{2}}^{\frac{\pi}{2}} se_{2n+1}(\eta,q)se_{2m+1}(\eta,q)d\eta = \begin{cases} 0 & m \neq n \\ \frac{\pi}{2} & m = n \end{cases} \qquad \text{(B.16'c)}$$

B-5 Reduction formulae of Mathieu functions

From equations (B-10a,b,c,d) , we can find the following relationships :

$$\begin{aligned} ce_{2n}(z,q) &= ce_{2n}(\pi-z,q) = ce_{2n}(\pi+z,q) = ce_{2n}(-z,q) \\ ce_{2n+1}(z,q) &= -ce_{2n+1}(\pi-z,q) = -ce_{2n+1}(\pi+z,q) = ce_{2n+1}(-z,q) \\ se_{2n+1}(z,q) &= se_{2n+1}(\pi-z,q) = -se_{2n+1}(\pi+z,q) = -se_{2n+1}(-z,q) \\ se_{2n+2}(z,q) &= -se_{2n+2}(\pi-z,q) = se_{2n+2}(\pi+z,q) = -se_{2n+2}(-z,q) \end{aligned} \qquad \text{(B.17)}$$

B-6 Modified Mathieu functions

(i) First solution of (B.9) ; Modified Mathieu function of the first kind.

Since (B.8) is transformed into (B.9) by writing iz for z , the solution of (B.9) can be obtained just by writing iz for z in equations (B.10a,b,cd). Other expressions in terms of Bessel functions have also been developed

$$Ce_{2n}(z,q) = ce_{2n}(iz,q) = \sum_{r=0}^{\infty} A_{2r}^{(2n)} \cosh 2rz$$

$$= \frac{ce_{2n}(\frac{\pi}{2},q)}{A_0^{(2n)}} \sum_{r=0}^{\infty} (-1)^r A_{2r}^{(2n)} J_{2r}(2k\cosh hz)$$

$$= \frac{ce_{2n}(0,q)}{A_0^{(2n)}} \sum_{r=0}^{\infty} A_{2r}^{(2n)} J_{2r}(2k\sinh hz)$$

$$= \frac{ce_{2n}(0,q)ce_{2n}(\frac{\pi}{2},q)}{[A_0^{(2n)}]^2} \sum_{r=0}^{\infty} (-1)^r A_{2r}^{(2n)} J_r(ke^{-z}) J_r(ke^{z})$$

$$Ce_{2n+1}(z,q) = ce_{2n+1}(iz,q) = \sum_{r=0}^{\infty} A_{2r+1}^{(2n+1)} \cosh(2r+1)z$$

$$= -\frac{ce'_{2n+1}(\frac{\pi}{2},q)}{kA_1^{(2n+1)}} \sum_{r=0}^{\infty} (-1)^r A_{2r+1}^{(2n+1)} J_{2r+1}(2k\cosh hz)$$

$$= \frac{ce_{2n+1}(0,q)}{kA_1^{(2n+1)}} \coth z \sum_{r=0}^{\infty} (2r+1) A_{2r+1}^{(2n+1)} J_{2r+1}(2k\sinh hz)$$

$$= \frac{ce_{2n+1}(0,q)ce'_{2n+1}(\frac{\pi}{2},q)}{k[A_1^{(2n+1)}]^2} \sum_{r=0}^{\infty} (-1)^r A_{2r+1}^{(2n+1)} \cdot$$

$$\cdot \left[J_r(ke^{-z}) J_{r+1}(ke^{z}) + J_{r+1}(ke^{-z}) J_r(ke^{z}) \right]$$

$$Se_{2n+1}(z,q) = -ise_{2n+1}(iz,q) = \sum_{r=0}^{\infty} B_{2r+1}^{(2n+1)} \sinh(2r+1)z$$

$$= \frac{se_{2n+1}(\frac{\pi}{2},q)}{kB_1^{(2n+1)}} \tanh z \sum_{r=0}^{\infty} (-1)^r (2r+1) B_{2r+1}^{(2n+1)} J_{2r+1}(2k\cosh hz)$$

$$= \frac{se'_{2n+1}(0,q)}{kB_1^{(2n+1)}} \sum_{r=0}^{\infty} B_{2r+1}^{(2n+1)} J_{2r+1}(2k\sinh hz)$$

$$= \frac{se'_{2n+1}(0,q)se_{2n+1}(\frac{\pi}{2},q)}{k[B_1^{(2n+1)}]^2} \sum_{r=0}^{\infty} (-1)^r B_{2r+1}^{(2n+1)} \cdot$$

$$\cdot \left[J_r(ke^{-z}) J_{r+1}(ke^{z}) - J_{r+1}(ke^{-z}) J_r(ke^{z}) \right]$$

$$Se_{2n+2}(z,q) = -ise_{2n+2}(iz,q) = \sum_{r=0}^{\infty} B_{2r+2}^{(2n+2)} \sinh(2r+2)z$$

$$= -\frac{se'_{2n+2}(\frac{\pi}{2},q)}{k^2 B_2^{(2n+2)}} \tanh z \sum_{r=0}^{\infty} (-1)^r (2r+2) B_{2r+2}^{(2n+2)} J_{2r+2}(2k\cosh hz)$$

$$= \frac{se'_{2n+1}(0,q)}{k^2 B_2^{(2n+1)}} \cot hz \sum_{r=0}^{\infty} (2r+2) B_{2r+2}^{(2n+1)} J_{2r+2}(2k\sinh z)$$

$$= -\frac{se'_{2n+1}(0,q)\, se'_{2n+1}(\frac{\pi}{2},q)}{k^2 \left[B_2^{(2n+1)}\right]^2} \sum_{r=0}^{\infty} (-1)^r B_{2r+2}^{(2n+1)} \cdot$$

$$\cdot \left[J_r(ke^{-z}) J_{r+2}(ke^{z}) - J_{r+2}(ke^{-z}) J_r(ke^{z}) \right]$$

(B.18a,b,c,d)

where primes denote derivatives with respect to z. The series involving Bessel functions converge absolutely and uniformly for all finite value of z. The rate of convergence of those involving products of Bessel functions increases with increasing z.

(2) Second solution of (B.9)

Since the Bessel functions J and Y satisfy the same differential equations and recurrence formula, and by virtue of (B.9) , (B.18a,b,c,d) , we have as the solution of (B.9)

$$Fey_{2n}(z,q) = \frac{ce_{2n}(\frac{\pi}{2},q)}{A_0^{(2n)}} \sum_{r=0}^{\infty} (-1)^r A_{2r}^{(2n)} Y_{2r}(2k\cosh z) \quad , |\cosh z| > 1$$

$$= \frac{ce_{2n}(0,q)}{A_0^{(2n)}} \sum_{r=0}^{\infty} A_{2r}^{(2n)} Y_{2r}(2k\sinh z) \quad , |\sinh z| > 1 \, , \, Re\{z\} > 0$$

$$= \frac{ce_{2n}(0,q)\, ce_{2n}(\frac{\pi}{2},q)}{\left[A_0^{(2n)}\right]^2} \sum_{r=0}^{\infty} (-1)^r A_{2r}^{(2n)} J_r(ke^{-z}) Y_r(ke^{z})$$

$$Fey_{2n+1}(z,q) = -\frac{ce'_{2n+1}(\frac{\pi}{2},q)}{kA_1^{(2n+1)}} \sum_{r=0}^{\infty} (-1)^r A_{2r+1}^{(2n+1)} Y_{2r+1}(2k\cosh z) \quad , |\cosh z| > 1$$

$$= \frac{ce'_{2n+1}(0,q)}{kA_1^{(2n+1)}} \cot hz \sum_{r=0}^{\infty} (2r+1) A_{2r+1}^{(2n+1)} Y_{2r+1}(2k\sinh z)$$

$$= \frac{ce'_{2n+1}(0,q)\, ce'_{2n+1}(\frac{\pi}{2},q)}{k\left[A_1^{(2n+1)}\right]^2} \sum_{r=0}^{\infty} (-1)^r A_{2r+1}^{(2n+1)} \cdot \quad , |\sinh z| > 1 \, , \, Re\{z\} > 0$$

$$\cdot\left[J_r(ke^{-z})Y_{r+1}(ke^{z}) + J_{r+1}(ke^{-z})Y_r(ke^{z})\right.$$

$$Gey_{2n+1}(z,q) = \frac{se_{2n+1}(\frac{\pi}{2},q)}{kB_1^{(2n+1)}}\tanh z \sum_{r=0}^{\infty}(-1)^r(2r+1)B_{2r+1}^{(2n+1)}Y_{2r+1}(2k\cosh z)$$

$$= \frac{se'_{2n+1}(0,q)}{kB_1^{(2n+1)}} \sum_{r=0}^{\infty} B_{2r+1}^{(2n+1)}Y_{2r+1}(2k\sinh z) \qquad , |\cosh z| > 1$$

$$= \frac{se'_{2n+1}(0,q)se_{2n+1}(\frac{\pi}{2},q)}{k\left[B_1^{(2n+1)}\right]^2} \sum_{r=0}^{\infty}(-1)^r B_{2r+1}^{(2n+1)} . \qquad , |\sinh z| > 1 \ , \ Re\{z\} > 1$$

$$\cdot\left[J_r(ke^{-z})Y_{r+1}(ke^{z}) - J_{r+1}(ke^{-z})Y_r(ke^{z})\right]$$

$$Gey_{2n+2}(z,q) = -\frac{se'_{2n+2}(0,q)}{k^2B_2^{(2n+2)}}\tanh z \sum_{r=0}^{\infty}(-1)^r(2r+2)B_{2r+2}^{(2n+2)}Y_{2r+2}(2k\cosh z)$$

$$= \frac{se'_{2n+2}(0,q)}{k^2B_2^{(2n+2)}}\coth z \sum_{r=0}^{\infty}(2r+2)B_{2r+2}^{(2n+2)}Y_{2r+2}(2k\sinh z) \qquad , |\cosh z| > 1$$

$$= -\frac{se'_{2n+2}(0,q)se'_{2n+2}(\frac{\pi}{2},q)}{kB_2^{(2n+2)}} \sum_{r=0}^{\infty}(-1)^r B_{2r+2}^{(2n+2)} . \qquad , |\sinh z| > 1 \ , \ Re\{z\} > 0$$

$$\cdot\left[J_r(ke^{-z})Y_{r+2}(ke^{z}) - J_{r+2}(ke^{-z})Y_r(ke^{z})\right]$$

(B.19a,b,c,d)

(B.19a,b,c,d) are obtained from (B.13a,b,c,d) by putting $Y(ke^{z})$ instead of $J(ke^{z})$.

(3) Combination solution (third kind) of (B.9)

Anologous to the relationship between the Bessel functions and Hankel functions (ref. 24 p.250), we can define

$$Me_m^{(1),(2)}(z,q) = Ce_m(z,q) + i\ Fey_m(z,q) \qquad (a_m)$$

(B.20a,b)

$$Ne_m^{(1),(2)}(z,q) = Se_m(z,q) + i\ Gey_m(z,q) \qquad (b_m)$$

These are used to represent incoming and outgoing waves in problems pertraining to an elliptic cylinder.

B-7 Notations of Blanch for the solutions of (B.9)

The notation of the solutions of (B.9) given by Blanch are $Mc_m^{(i)}(z,q)$ and $Ms_m^{(i)}(z,q)$ i=1,2,3,4, and are called the radial Mathieu functions of first, second, third and fourth kinds which correspond respectively to $Ce_m(z,q)$ and $Se_m(z,q)$, $Fey_m(z,q)$ and $Gey_m(z,q)$, and $Me_m^{(i)}(z,q)$ and $Ne_m^{(i)}(z,q)$, i=1,2. Since the most recent and comprehensive tables and computer programs were published by Blanch and Clemm, we use their notations here, The relationships are

$$\left.\begin{matrix} Ce_{2n}(z,q) \\ Fey_{2n}(z,q) \end{matrix}\right\} = \frac{ce_{2n}(\frac{\pi}{2},q)ce_{2n}(0,q)}{(-1)^n A_0^{(2n)}} \left\{\begin{matrix} Mc_{2n}^{(1)}(z,q) \\ Mc_{2n}^{(2)}(z,q) \end{matrix}\right.$$

$$\left.\begin{matrix} Ce_{2n+1}(z,q) \\ Fey_{2n+1}(z,q) \end{matrix}\right\} = \frac{ce'_{2n+1}(\frac{\pi}{2},q)ce_{2n+1}(0,q)}{(-1)^{n+1} q^{\frac{1}{2}} A_1^{(2n+1)}} \left\{\begin{matrix} Mc_{2n+1}^{(1)}(z,q) \\ Mc_{2n+1}^{(2)}(z,q) \end{matrix}\right.$$

$$\left.\begin{matrix} Se_{2n+1}(z,q) \\ Gey_{2n+1}(z,q) \end{matrix}\right\} = \frac{se_{2n+1}(\frac{\pi}{2},q)se'_{2n+1}(0,q)}{(-1)^n q^{\frac{1}{2}} B_1^{(2n+1)}} \left\{\begin{matrix} Ms_{2n+1}^{(1)}(z,q) \\ Ms_{2n+1}^{(2)}(z,q) \end{matrix}\right. \qquad \text{(B.21a,b,c,d)}$$

$$\left.\begin{matrix} Se_{2n+2}(z,q) \\ Gey_{2n+2}(z,q) \end{matrix}\right\} = \frac{se'_{2n+2}(\frac{\pi}{2},q)se'_{2n+2}(0,q)}{(-1)^{n+1} q\ B_2^{(2n+2)}} \left\{\begin{matrix} Ms_{2n+2}^{(1)}(z,q) \\ Ms_{2n+2}^{(2)}(z,q) \end{matrix}\right.$$

and

$$Mc_m^{(3),(4)}(z,q) = Mc_m^{(1)}(z,q) + i\ Mc_m^{(2)}(z,q)$$

$$Ms_m^{(3),(4)}(z,q) = Ms_m^{(1)}(z,q) + i\ Ms_m^{(2)}(z,q) \qquad \text{(B.22)}$$

B-8 Wronskians

The Wronskians of the two independent solution of (B.9) are

$$W\left[Mc_m^{(1)}(z,q)\ ,\ Mc_m^{(2)}(z,q)\right] =$$

$$= Mc_m^{(1)}(z,q)Mc_m^{(2)\prime}(z,q) - Mc_m^{(2)}(z,q)Mc_m^{(1)\prime}(z,q) = \frac{2}{\pi}$$

or

$$W\left[Mc_m^{(1)}(z,q)\ ,\ Mc_m^{(3)}(z,q)\right] =$$

$$= Mc_m^{(1)}(z,q)Mc_m^{(3)\prime}(z,q) - Mc_m^{(3)}(z,q)Mc_m^{(1)\prime}(z,q) = \frac{2i}{\pi}$$

(B.23a,b)

where the prime indicates the derivatives with respect to z.

Similarly, $Mc_m^{(\cdot)}$ can be replaced by $Ms_m^{(\cdot)}$ throughout (B.23a, b).

B-9 Approximations for small q, $q \to 0$

(1) Mathieu functions

When the fundamental ellipse tends to a circle or the wavelength is sufficiently large, $q = \frac{1}{4}k_1^2h^2 \longrightarrow 0$. then

$$\left.\begin{matrix} A_n^{(m)} \\ B_n^{(m)} \end{matrix}\right\} \longrightarrow \delta_{mn} \quad (m\neq 0)$$

$$\left.\begin{matrix} A_0^{(0)} \\ ce_0(\eta,q) \end{matrix}\right\} \longrightarrow \frac{1}{\sqrt{2}}$$

(B.24)

$$ce_n(\eta,q) \longrightarrow \cos n\eta = \cos n\theta$$

$$se_n(\eta,q) \longrightarrow \sin n\eta = \sin n\theta$$

(r,θ) are the cylindrical polar coordinates.

(2) Radial Mathieu functions

As ξ and $r \to \infty$, $q \to 0$. From (A.9) ; $r \to h\cosh\xi$, we have the following degenerate cases

$$\left.\begin{matrix} Mc_m^{(1)}(\xi,q) \\ Ms_m^{(1)}(\xi,q) \end{matrix}\right\} \longrightarrow J_m(k_1 r),$$

$$\left.\begin{matrix} Mc_m^{(2)}(\xi,q) \\ Ms_m^{(2)}(\xi,q) \end{matrix}\right\} \longrightarrow Y_m(k_1 r)$$

$$\left.\begin{matrix} Mc_m^{(3)}(\xi,q) \\ Ms_m^{(3)}(\xi,q) \end{matrix}\right\} \longrightarrow H_m^{(1)}(k_1 r) \sim \sqrt{\frac{2}{\pi k_1 r}}\, e^{i(k_1 r - \frac{m\pi}{2} - \frac{1}{4}\pi)}$$

$$\left.\begin{matrix} Mc_m^{(1)'}(\xi,q) \\ Ms_m^{(1)'}(\xi,q) \end{matrix}\right\} \longrightarrow k_1 r J_m'(k_1 r)$$

$$\left.\begin{matrix} Mc_m^{(2)'}(\xi,q) \\ Ms_m^{(2)'}(\xi,q) \end{matrix}\right\} \longrightarrow k_1 r Y_m'(k_1 r) \qquad \text{(B.25)}$$

B-10 Mathieu solutions for $-q < 0$

The following equations are taken from (ref. 1 P.738—739). The reader is also referred to the (ref. 24)

(i) The Characteristic numbers

$$a_{2r}(-q) = a_{2r}(q) \quad ; \quad b_{2r}(-q) = b_{2r}(q)$$
$$a_{2r+1}(-q) = b_{2r+1}(q) \quad ; \quad b_{2r+1}(-q) = a_{2r+1}(q) \tag{B.26}$$

(2) The Periodic Mathieu functions

$$ce_{2r}(z,-q) = (-1)^r ce_{2r}(\tfrac{\pi}{2}-z,q)$$
$$ce_{2r+1}(z,-q) = (-1)^r se_{2r+1}(\tfrac{\pi}{2}-z,q)$$
$$se_{2r+1}(z,-q) = (-1)^r ce_{2r+1}(\tfrac{\pi}{2}-z,q) \tag{B.27}$$
$$se_{2r+2}(z,-q) = (-1)^r se_{2r+2}(\tfrac{\pi}{2}-z,q)$$

(3) The coefficients associated with periodic Mathieu function

$$A_{2r}^{(2n)}(-q) = (-1)^{r-n} A_{2r}^{(2n)}(q) \quad ; \quad B_{2r}^{(2n)}(-q) = (-1)^{r-n} B_{2r}^{(2n)}(q)$$
$$A_{2r+1}^{(2n+1)}(-q) = (-1)^{r-n} B_{2r+1}^{(2n+1)}(q) \quad ; \quad B_{2r+1}^{(2n+1)}(-q) = (-1)^{r-n} A_{2r+1}^{(2n+1)}(q) \tag{B.28}$$

(4) The Modified Mathieu functions of third kind

Since $-q < 0$ corresponds to imaginary value ik_1 ($q = \frac{1}{4}k_1^2h^2$). We can use $-q$, ik_1 instead of q, k_1 respectively in (B.18)—(B.25) to obtain the Mathieu solutions with $-q$. Therefore, as $\xi \to \infty$, from (B.25), we have

$$\left.\begin{matrix} Mc_m^{(3)}(\xi,-q) \\ Ms_m^{(3)}(\xi,-q) \end{matrix}\right\} \longrightarrow H_m^{(1)}(ik_1r) = \frac{2}{i\pi} e^{-i\frac{n\pi}{2}} K_n(k_1r) \tag{B.29}$$

The reader is also referred to [ref. 24 p.251, p.369, p.163] for details.

B-11 Detailed calculation of Total Scattering Cross Section

From equation (3.20)

$$\sigma(\eta) = \frac{4}{\pi q_1^{\frac{1}{2}} \cosh \xi_0} \cdot$$

$$\cdot \left| \sum_{n=0}^{\infty} \left[\frac{Mc_{2n}^{(1)'}(\xi_0, q_1)}{Mc_{2n}^{(3)'}(\xi_0, q_1)} ce_{2n}(\eta, q_1) ce_{2n}(\theta_2, q_1) + \frac{Mc_{2n+1}^{(1)'}(\xi_0, q_1)}{Mc_{2n+1}^{(3)'}(\xi_0, q_1)} ce_{2n+1}(\eta, q_1) ce_{2n+1}(\theta_2, q_1) \right.\right.$$

$$\left.\left. + \frac{Ms_{2n+1}^{(1)'}(\xi_0, q_1)}{Ms_{2n+1}^{(3)'}(\xi_0, q_1)} se_{2n+1}(\eta, q_1) se_{2n+1}(\theta_2, q_1) + \frac{Ms_{2n+2}^{(1)'}(\xi_0, q_1)}{Ms_{2n+2}^{(3)'}(\xi_0, q_1)} se_{2n+2}(\eta, q_1) se_{2n+2}(\theta_2, q_1) \right] \right|$$

$$= \frac{4}{\pi q_1^{\frac{1}{2}} \cosh \xi_0} \left| \sum_{n=0}^{\infty} \left[\frac{Mc_{2n}^{(1)'}(\xi_0, q_1)}{Mc_{2n}^{(2)'}(\xi_0, q_1) + i Mc_{2n}^{(3)'}(\xi_0, q_1)} ce_{2n}(\eta, q_1) ce_{2n}(\theta_2, q_1) + \right.\right.$$

$$+ \frac{Mc_{2n+1}^{(1)'}(\xi_0, q_1)}{Mc_{2n+1}^{(2)'}(\xi_0, q_1) + i Mc_{2n+1}^{(3)'}(\xi_0, q_1)} ce_{2n+1}(\eta, q_1) ce_{2n+1}(\theta_2, q_1) +$$

$$+ \frac{Ms_{2n+1}^{(1)'}(\xi_0, q_1)}{Ms_{2n+1}^{(2)'}(\xi_0, q_1) + i Ms_{2n+1}^{(3)'}(\xi_0, q_1)} se_{2n+1}(\eta, q_1) se_{2n+1}(\theta_2, q_1) +$$

$$\left.\left. + \frac{Ms_{2n+2}^{(1)'}(\xi_0, q_1)}{Ms_{2n+2}^{(2)'}(\xi_0, q_1) + i Ms_{2n+2}^{(3)'}(\xi_0, q_1)} se_{2n+2}(\eta, q_1) se_{2n+2}(\theta_2, q_1) \right] \right|$$

$$= \frac{4}{\pi q_1^{\frac{1}{2}} \cosh \xi_0} \cdot$$

$$\cdot \left\{ \left[\sum_{n=0}^{\infty} \left(\frac{Mc_{2n}^{(1)'^2}(\xi_0, q_1)}{Mc_{2n}^{(1)'^2}(\xi_0, q_1) + Mc_{2n}^{(2)'^2}(\xi_0, q_1)} ce_{2n}(\eta, q_1) ce_{2n}(\theta_2, q_1) + \right.\right.\right.$$

$$+ \frac{Mc_{2n+1}^{(1)'^2}(\xi_0, q_1)}{Mc_{2n+1}^{(1)'^2}(\xi_0, q_1) + Mc_{2n+1}^{(2)'^2}(\xi_0, q_1)} ce_{2n+1}(\eta, q_1) ce_{2n+1}(\theta_2, q_1) +$$

$$+ \frac{Ms_{2n+1}^{(1)'^2}(\xi_0, q_1)}{Ms_{2n+1}^{(1)'^2}(\xi_0, q_1) + Ms_{2n+1}^{(2)'^2}(\xi_0, q_1)} se_{2n+1}(\eta, q_1) se_{2n+1}(\theta_2, q_1) +$$

$$\left.\left.\left. + \frac{Ms_{2n+2}^{(1)'^2}(\xi_0, q_1)}{Ms_{2n+2}^{(1)'^2}(\xi_0, q_1) + Ms_{2n+2}^{(2)'^2}(\xi_0, q_1)} se_{2n+2}(\eta, q_1) se_{2n+2}(\theta_2, q_1) \right) \right]^2 +$$

$$+ \left[\sum_{n=0}^{\infty} \left(\frac{Mc_{2n}^{(1)'}(\xi_0, q_1) Mc_{2n}^{(2)'}(\xi_0, q_1)}{Mc_{2n}^{(1)'^2}(\xi_0, q_1) + Mc_{2n}^{(2)'^2}(\xi_0, q_1)} ce_{2n}(\eta, q_1) ce_{2n}(\theta_2, q_1) + \right.\right.$$

$$+ \frac{Mc_{2n+1}^{(1)'}(\xi_0, q_1) Mc_{2n+1}^{(2)'}(\xi_0, q_1)}{Mc_{2n+1}^{(1)'^2}(\xi_0, q_1) + Mc_{2n+1}^{(2)'^2}(\xi_0, q_1)} ce_{2n+1}(\eta, q_1) ce_{2n+1}(\theta_2, q_1) +$$

$$+\frac{Ms^{(1)\prime}_{2m+1}(\xi_o,q_1)\,Ms^{(2)\prime}_{2m+1}(\xi_o,q_1)}{Ms^{(1)\prime}_{2m+1}(\xi_o,q_1)+Ms^{(2)\prime}_{2m+1}(\xi_o,q_1)}\,se_{2m+1}(\eta,q_1)se_{2m+1}(\theta_I,q_1)+$$

$$+\frac{Ms^{(1)\prime}_{2m+2}(\xi_o,q_1)\,Ms^{(2)\prime}_{2m+2}(\xi_o,q_1)}{Ms^{(1)\prime}_{2m+2}(\xi_o,q_1)+Ms^{(2)\prime}_{2m+2}(\xi_o,q_1)}\,se_{2m+2}(\eta,q_1)se_{2m+2}(\theta_I,q_1)\Big)^2\Big]\Big\}$$

$$=\frac{4}{\pi q_1^{\frac{1}{2}}\cosh\xi_o}\cdot$$

$$\cdot\Big\{\sum_{n=0}^{\infty}\Big[\frac{Mc^{(1)\prime 2}_{2n}(\xi_o,q_1)}{Mc^{(1)\prime}_{2n}(\xi_o,q_1)+Mc^{(2)\prime}_{2n}(\xi_o,q_1)}\,ce^2_{2n}(\theta_I,q_1)ce^2_{2n}(\eta,q_1)+$$

$$+\frac{Mc^{(1)\prime 2}_{2m+1}(\xi_o,q_1)}{Mc^{(1)\prime}_{2m+1}(\xi_o,q_1)+Mc^{(2)\prime}_{2m+1}(\xi_o,q_1)}\,ce^2_{2m+1}(\theta_I,q_1)ce^2_{2m+1}(\eta,q_1)+$$

$$+\frac{Ms^{(1)\prime 2}_{2m+1}(\xi_o,q_1)}{Ms^{(1)\prime}_{2m+1}(\xi_o,q_1)+Ms^{(2)\prime}_{2m+1}(\xi_o,q_1)}\,se^2_{2m+1}(\theta_I,q_1)se^2_{2m+1}(\eta,q_1)+$$

$$+\frac{Ms^{(1)\prime 2}_{2m+2}(\xi_o,q_1)}{Ms^{(1)\prime}_{2m+2}(\xi_o,q_1)+Ms^{(2)\prime}_{2m+2}(\xi_o,q_1)}\,se^2_{2m+2}(\theta_I,q_1)se^2_{2m+2}(\eta,q_1)\Big]+$$

$$+\big[\text{cross terms; } ce_m(\eta,q_1)se_m(\eta,q_1),\ ce_{2i}(\eta,q_1)\cdot$$

$$\cdot ce_{2j+1}(\eta,q_1),\ se_{2i}(\eta,q_1)se_{2j+1}(\eta,q_1)\big]\Big\}$$

(B.30)

Using the orthogonality of ce_m , se_m functions in the interval $[0\ ,\ 2\pi]$, equations (B.12a,b,c). Hence, we have

$$Q=\int_0^{2\pi}\sigma(\eta)d\eta$$

$$=\frac{4}{q_1^{\frac{1}{2}}\cosh\xi_o}\Big\{\sum_{n=0}^{\infty}\Big[\frac{Mc^{(1)\prime 2}_{2n}(\xi_o,q_1)}{Mc^{(1)\prime 2}_{2n}(\xi_o,q_1)+Mc^{(2)\prime 2}_{2n}(\xi_o,q_1)}\,ce^2_{2n}(\theta_I,q_1)+$$

$$+\frac{Mc^{(1)\prime 2}_{2m+1}(\xi_o,q_1)}{Mc^{(1)\prime 2}_{2m+1}(\xi_o,q_1)+Mc^{(2)\prime 2}_{2m+1}(\xi_o,q_1)}\,ce^2_{2m+1}(\theta_I,q_1)+$$

$$+\frac{Ms^{(1)\prime 2}_{2m+1}(\xi_o,q_1)}{Ms^{(1)\prime 2}_{2m+1}(\xi_o,q_1)+Ms^{(2)\prime 2}_{2m+1}(\xi_o,q_1)}\,se^2_{2m+1}(\theta_I,q_1)+$$

$$+\frac{Ms^{(1)\prime 2}_{2m+2}(\xi_o,q_1)}{Ms^{(1)\prime 2}_{2m+1}(\xi_o,q_1)+Ms^{(2)\prime 2}_{2m+1}(\xi_o,q_1)}\,se^2_{2m+2}(\theta_I,q_1)\Big]\Big\}$$

(B.31a)

or

$$= \frac{4}{q_1^2 \cosh\xi_0} \sum_{n=0}^{\infty} \left\{ \left| \frac{Mc_{2n}^{(1)\prime}(\xi_0, q_1)}{Mc_{2n}^{(3)\prime}(\xi_0, q_1)} \, ce_{2n}(\theta_2, q_1) \right|^2 + \right.$$

$$+ \left| \frac{Mc_{2n+1}^{(1)\prime}(\xi_0, q_1)}{Mc_{2n+1}^{(3)\prime}(\xi_0, q_1)} \, ce_{2n+1}(\theta_2, q_1) \right|^2 +$$

$$+ \left| \frac{Ms_{2n+1}^{(1)\prime}(\xi_0, q_1)}{Ms_{2n+1}^{(3)\prime}(\xi_0, q_1)} \, se_{2n+1}(\theta_2, q_1) \right|^2 +$$

$$\left. + \left| \frac{Ms_{2n+2}^{(1)\prime}(\xi_0, q_1)}{Ms_{2n+2}^{(3)\prime}(\xi_0, q_1)} \, se_{2n+2}(\theta_2, q_1) \right|^2 \right\} \qquad \text{(B.31b)}$$

APPENDIX C. SCATTERING AND RADIATION OF WATER WAVES BY A CIRCULAR CYLINDER

The scattering and radiation of gravity wave by a circular cylinder are summarized here for the sake of comparison with the results of elliptic cylinder.

(1) Scattering problem

MacCamy and Fuchs (1952) have worked out this problem . The reader may be referred to their paper for details.

The velocity potential of the incident wave of amplitude a_I , travelling in the x-direction, can be written as

$$\begin{aligned}\Phi_I(r,\theta,z,t) &= \phi_I(r,\theta,z)\, e^{-i\omega t} \\ &= \frac{ga_I}{\omega}\frac{\cosh k_1(d+z)}{\cosh k_1 d}\, e^{ik_1 x} e^{-i\omega t} \\ &= \frac{ga_I}{\omega}\frac{\cosh k_1(d+z)}{\cosh k_1 d}\, e^{ik_1 r\cos\theta} e^{-i\omega t} \\ &= \frac{ga_I}{\omega}\frac{\cosh k_1(d+z)}{\cosh k_1 d} e^{-i\omega t} \sum_{n=0}^{\infty} \epsilon_n i^n J_n(k_1 r)\cos n\theta\end{aligned} \tag{C.1}$$

where $\epsilon_0 = 1$, $\epsilon_n = 2$ ($n \geq 1$).

The total velocity potential at any point in the water domain is

$$\begin{aligned}\Phi &= \Phi_I + \Phi_S \\ &= \frac{ga_I}{\omega}\frac{\cosh k_1(z+d)}{\cosh k_1 d} e^{-i\omega t} \sum_{n=0}^{\infty} \epsilon_n i^n \left[J_n(k_1 r) - \frac{J_n'(k_1 r_0)}{H_n^{(1)\prime}(k_1 r_0)} H_n^{(1)}(k_1 r) \right] \cos n\theta\end{aligned}$$

(C.2)

From Bernoulli's equation, The pressure is

$$P = -\rho\frac{\partial\Phi}{\partial t}$$

$$= iga_I\rho\left(\frac{\cosh k_1(z+d)}{\cosh kd}\right)e^{-i\omega t}\sum_{n=0}^{\infty}\epsilon_n i^n\left[J_n(kr) - \frac{J_n'(kr_0)}{H_n^{(1)'}(kr_0)}H_n^{(1)}(kr)\right]\cdot$$

$$\cdot\cos n\theta \qquad (C.3)$$

Hence, the x-, y-component forces and moments about x-, y-, z-axis are

$$F_x = -\int_S P\cos\theta\Big|_{r=r_0} dS = -\int_{-d}^{0} dz \int_0^{2\pi} P\cos\theta a d\theta$$

$$= (2a_I\rho g)(2ad)\left(\frac{\tanh kd}{kd}\right)e^{-i\omega t}C_x \qquad (C.4)$$

where

$$C_x = \frac{i}{k_1 r_0 H_1^{(1)'}(kr_0)} \qquad (C.4a)$$

and

$$M_y = -\int_S (z+d)P\cos\theta\, dS = -a\int_{-d}^{0} dz \int_0^{2\pi} (z+d)P\cos\theta\, d\theta$$

$$= F_x d C_{kxy} \qquad (C.5)$$

where C_{kxy} is defined in (3.13a).

and

$$F_y = M_z = M_x = 0 \qquad (C.6)$$

The elevation of the scattered waves at far field is

$$\zeta_S = -\frac{1}{g}\frac{\partial\Phi_s}{\partial t}$$

$$= ia_I e^{-i\omega t} \sum_{n=0}^{\infty} \epsilon_n i^n \frac{J_n'(k_1 r_0)}{H_n^{(1)\prime}(k_1 r_0)} H_n^{(1)}(k_1 r) \cos n\theta$$

since $H_n^{(1)}(k_1 r) \sim \sqrt{\frac{2}{\pi k_1 r}} e^{i(k_1 r - \frac{2n+1}{4}\pi)}$

$$\zeta_s = a_I A(\theta) \sqrt{\frac{k_1 r}{k_1 r}}\, e^{i(k_1 r - \omega t)}$$

where $A(\theta)$ is the scattering amplitude. Hence

$$A(\theta) = i\sqrt{\frac{2}{\pi k_1 r_0}} e^{-i\frac{\pi}{4}} \sum_{n=0}^{\infty} \epsilon_n \frac{J_n'(k_1 r_0)}{H_n^{(1)\prime}(k_1 r_0)} \cos n\theta$$

$$= \sqrt{\frac{2}{\pi k_1 r_0}}\, e^{i\frac{\pi}{4}} \sum_{n=0}^{\infty} \epsilon_n \frac{J_n'(k_1 r_0)}{H_n^{(1)\prime}(k_1 r_0)} \cos n\theta \qquad (C.7)$$

Therefore the differential scattering cross section is

$$\sigma(\theta) = \left| A(\theta) \right|^2 = \frac{2}{\pi k_1 r_0} \left| \sum_{n=0}^{\infty} \epsilon_n \frac{J_n'(k_1 r_0)}{H_n^{(1)\prime}(k_1 r_0)} \cos n\theta \right|^2 \qquad (C.8)$$

$$= \frac{2}{\pi k_1 r_0} \left\{ \left[\sum_{n=0}^{\infty} \epsilon_n \frac{J_n'^2(k_1 r_0)}{J_n'^2(k_1 r_0) + Y_n'^2(k_1 r_0)} \cos n\theta \right]^2 + \right.$$

$$\left. + \left[\sum_{n=0}^{\infty} \epsilon_n \frac{J_n'(k_1 r_0)\, Y_n'(k_1 r_0)}{J_n'^2(k_1 r_0) + Y_n'^2(k_1 r_0)} \cos n\theta \right]^2 \right\} \qquad (C.8a)$$

$$= \frac{2}{\pi k_1 r_0} \left\{ \left[\sum_{n=0}^{\infty} \epsilon_n^2 \frac{J_n'^2(k_1 r_0)}{J_n'^2(k_1 r_0) + Y_n'^2(k_1 r_0)} \cos^2 n\theta \right] + \right.$$

$$\left. + \underbrace{\left[\text{terms with } \cos j\theta \right]}_{\text{no contribution after integration } \theta \text{ from } 0 \text{ to } 2\pi.} \right\}$$

and the total cross section area is

$$Q = \int_0^{2\pi} \sigma(\theta) d\theta$$

$$= \frac{2}{K_1 r_0} \left[\frac{2J_0'^2(k_1 r_0)}{J_0'^2(k_1 r_0) + Y_0'^2(k_1 r_0)} + \sum_{n=1}^{\infty} \epsilon_n^2 \frac{J_n'^2(k_1 r_0)}{J_n'^2(k_1 r_0) + Y_n'^2(k_1 r_0)} \right] \qquad (C.9)$$

or

$$= \frac{8}{k_1 r}\left[\frac{1}{2}\left|\frac{J_0'(k_1 r_0)}{H_0^{(2)'}(k_1 r_0)}\right|^2 + \sum_{n=1}^{\infty}\left|\frac{J_n'(k_1 r_0)}{H_n^{(2)'}(k_1 r_0)}\right|^2\right] \qquad (C.9a)$$

(2) Radiation problem

The total spatial velocity of any point on the circular cylinder is given by (5.1). Now we are dealing with circular cylinder coordinates : $x = r\cos\theta$, $y = r\sin\theta$. Hence (5.1) gives

$$\begin{aligned} U_x &= V_x + (z+d)\Omega_y - r\sin\theta\,\Omega_z \\ U_y &= V_y + r\cos\theta\,\Omega_z - (z+d)\Omega_x \\ U_z &= \quad r\sin\theta\,\Omega_x - r\cos\theta\,\Omega_y \end{aligned} \qquad (C.10)$$

Making use of the boundary condition on the normal velocity at mean position of the solid rigid wall $r=r_0$, with the unit outward normal vector to the circle $\vec{n} = (\cos\theta , \sin\theta)$, (2.3) leads to

$$\begin{aligned} \left.\frac{\partial \phi_R}{\partial r}\right|_{r=r_0} &= \vec{U}\cdot\vec{n} \\ &= \left[V_x + (z+d)\Omega_y\right]\cos\theta + \left[V_y - (z+d)\Omega_x\right]\sin\theta \end{aligned} \qquad (c.11)$$

where ϕ_R is defined as the spatial part of velocity potential of the fluid. (C.11) is the boundary condition of the fluid on the body.

The solution of Laplace equation : $\nabla^2\phi_R = 0$, with boundary condition at bottom and at free surface : $\left.\frac{\partial \phi_R}{\partial z}\right|_{z=-d} = 0$

and $\frac{\partial \phi_R}{\partial z} - \frac{\omega^2}{g}\phi_R = 0\Big|_{z=0}$, and the radiation condition at large distances is

$$\phi_R = \sum_{n=0}^{\infty}\sum_{m=1}^{\infty} c_n^{(m)} \cosh k_m(z+d)\, H_n^{(1)}(k_m r)\cos n\theta \qquad (C.12)$$

where $c_n^{(m)}$ are constant coefficients to be determined through the boundary condition on the body wall : (C.11). We recall k_1 is real and k_n is imaginary $(n \geq 2)$.

Substituting (C.12) into (C.11)

$$\left.\frac{\partial \phi_R}{\partial r}\right|_{r=r_o} = \sum_{n=0}^{\infty}\sum_{m=1}^{\infty} c_n^{(m)} k_m \cosh k_m(z+d) H_n^{(1)\prime}(k_m r)\cos n\theta$$

$$= \left[V_x + (z+d)\Omega_y\right]\cos\theta + \left[V_y - (z+d)\Omega_x\right]\sin\theta \qquad (C.13)$$

Multipling $\cosh k_m(z+d)$ and $\cos n\theta$ in both sides of (C.13) and integrating z from -d to 0, and θ from 0 to 2π. By orthogonality of $\cosh k_m(z+d)$: (2.5) and of $\cos n\theta$, $\sin n\theta$, we obtain,

$$c_n^{(m)} = 0 \qquad n \neq 1$$

$$c_1 = \frac{\int_{-d}^{0}\left[V_x + (z+d)\Omega_y\right]\cosh k_m(z+d)\,dz}{N_{k_m} k_m H_1^{(1)\prime}(k_m r_o)}$$

$$= \frac{V_x\left(\frac{\sinh k_m d}{k_m d}\right)d + \Omega_y\left(\frac{\sinh k_m d}{k_m d}\right)\left(1 - \frac{\coth k_m d}{k_m d} + \frac{\operatorname{csch} k_m d}{k_m d}\right)d^2}{N_{k_m} k_m H_1^{(1)\prime}(k_m r_o)} \qquad (C.14)$$

Using the definition of (3.13a) : $C_{k_m xy} = 1 - \frac{\coth k_m d}{k_m d} + \frac{\operatorname{csch} k_m d}{k_m d}$, we have,

$$\phi_R = \sum_{m=1}^{\infty}\left[\frac{(\frac{\sinh k_m d}{k_m d})(V_x d+\Omega_y d^2 C_{k_m xy})}{N_{k_m} k_m H_1^{(1)\prime}(k_m r_o)}\right]\cosh k_m(z+d)H_1^{(1)}(k_m r)\cos\theta \tag{C.15}$$

We recall that k_m's ($m \geq 2$) are imaginary, and $K_n(x)=i\frac{1}{2}e^{i\frac{n\pi}{2}} \cdot H_n^{(1)}(ix)$. Thus in the far field $H_1^{(1)}(k_m r)\sim K_1(-ik_m r)\sim 0$ for $m \geq 2$, and they do not contribute to the radiated wave potential,

$$\phi_{R_\infty}\sim \frac{(\frac{\sinh k_1 d}{k_1 d})(V_x d+\Omega_y d^2 C_{k_1 xy})}{N_{k_1} k_1}\cosh k_1(z+d)\frac{H_1^{(1)}(k_1 r)}{H_1^{(1)\prime}(k_1 r_o)}\cos\theta$$

since $H_1^{(1)}(k_1 r)\sim\sqrt{\frac{2}{\pi k_1 r}}\, e^{i(k_1 r-\frac{3\pi}{4})}$

$$\sim \frac{(\frac{\sinh k_1 d}{k_1 d})(V_x d+\Omega_y d^2 C_{k_1 xy})}{N_{k_1} k_1 H_1^{(1)\prime}(k_1 r_o)}\cosh k_1(z+d)\frac{2}{\pi k_1 r}e^{i(k_1 r-\frac{3\pi}{4})}\cdot$$

$$\cdot\cos\theta \tag{C.16}$$

Now the radiation damping coefficients: (5.21) and (5.22). By differentiation,

$$\frac{\partial \Phi_{R_\infty}}{\partial t} = -\omega(\frac{(\frac{\sinh k_1 d}{k_1 d})(V_x d+\Omega_y d^2 C_{k_1 xy})}{N_{k_1} k_1 H_1^{(1)\prime}(k_1 r_o)}\cosh k_1(z+d)\cdot$$

$$\cdot\sqrt{\frac{2}{\pi k_1 r}}\, e^{i(k_1 r-\frac{\pi}{4}-\omega t)}\cos\theta$$

$$\frac{\partial \Phi_{R_\infty}}{\partial r} = (\frac{(\frac{\sinh k_1 d}{k_1 d})(V_x d+\Omega_y d^2 C_{k_1 xy})}{N_{k_1} k_1 H_1^{(1)\prime}(k_1 r_o)})\cosh k_1(z+d)\cdot$$

$$\cdot\sqrt{\frac{2k_1}{\pi r}}\, e^{i(k_1 r-\frac{\pi}{4}-\omega t)}\cos\theta$$

hence the average rate of energy flux across a control volume at infinity is

$$\frac{d\bar{E}}{dt} = \frac{1}{T}\int_0^T \left[\rho \int_{S_\infty} \mathrm{Re}\left\{\frac{\partial \Phi_0}{\partial t}\right\} \mathrm{Re}\left\{\frac{\partial \Phi_0}{\partial r}\right\} dS\right] dt$$

$$= -(\rho\omega)\left[\frac{\left(\frac{\sinh k_1 d}{k_1 d}\right)(V_x d + \Omega_y d^2 C_{k_1 xy})}{k_1}\right]^2 \left[\frac{1}{N_{k_1}}\right]\left[\frac{1}{J_1'^2(k_1 r_0) + Y_1'^2(k_1 r_0)}\right]$$

and (5.21) gives the damping coefficient

$$B = -\frac{2}{|U|^2}\frac{d\bar{E}}{dt}$$

$$= (2\rho\omega)\left\{\frac{\left(\frac{\sinh k_1 d}{k_1 d}\right)(V_x d + \Omega_y d^2 C_{k_1 xy})}{k_1}\right\}^2 \left(\frac{1}{N_{k_1}}\right)\left(\frac{1}{J_1'^2(k_1 r_0) + Y_1'^2(k_1 r_0)}\right) \tag{C.17}$$

The damping coefficient for the surge mode ; $V_x = 1$, $V_y = \Omega_x = \Omega_y = \Omega_z = 0$ is

$$B_1 = (2\rho\omega)\left(\frac{\sinh kd}{kd}\right)^2 (\pi d)^2 \left(\frac{1}{N_{k_1}}\right)\left[\frac{1}{(k_1 r_0 J_1'(k_1 r_0))^2 + (k_1 r_0 Y_1'(k_1 r_0))^2}\right] \tag{C.18}$$

The damping coefficient for the pitch mode ; $\Omega_y = 1$, others=0 is ,

$$B_5 = (2\rho\omega)\left[\left(\frac{\sinh kd}{kd}\right) C_{k_1 xy}\, d\right]^2 \left[\pi r_0^2\right]^2 \left[\frac{1}{N_{k_1}}\right] \cdot$$

$$\cdot \left[\frac{1}{(k_1 r_0 J_1'(k_1 r_0))^2 + (k_1 r_0 Y_1'(k_1 r_0))^2}\right] \tag{C.19}$$

all the damping coefficients of other modes vanish :

$$B_2 = B_3 = B_4 = B_6 = 0 .$$

We note that in the limit $\zeta \to \infty$, $h \to 0$ and $h\cosh\zeta \sim h\sinh\zeta \sim \frac{1}{2}he^{\zeta} \sim r_0$, the formalas in chapter 3 , 5 , reduce to the corresponding formulas in this appendix. If the same incident

wave and conditions are given, as the elliptical cylinder reduces to a circular cylinder.